UCSF
UC San Francisco Electronic Theses and Dissertations

Title
Tax-2

Permalink
https://escholarship.org/uc/item/3165d1d0

Author
Coburn, Cara Marie

Publication Date
1996

Peer reviewed|Thesis/dissertation

eScholarship.org Powered by the California Digital Library
University of California

tax-2: a putative cyclic nucleotide-gated channel required for sensory neuron function and development in C. elegans

by

Cara Marie Coburn

DISSERTATION

Submitted in partial satisfaction of the requirements for the degree of

DOCTOR OF PHILOSOPHY

in

Biochemistry

in the

GRADUATE DIVISION

of the

UNIVERSITY OF CALIFORNIA

San Francisco

Cori Bargmann Aug 6 1996

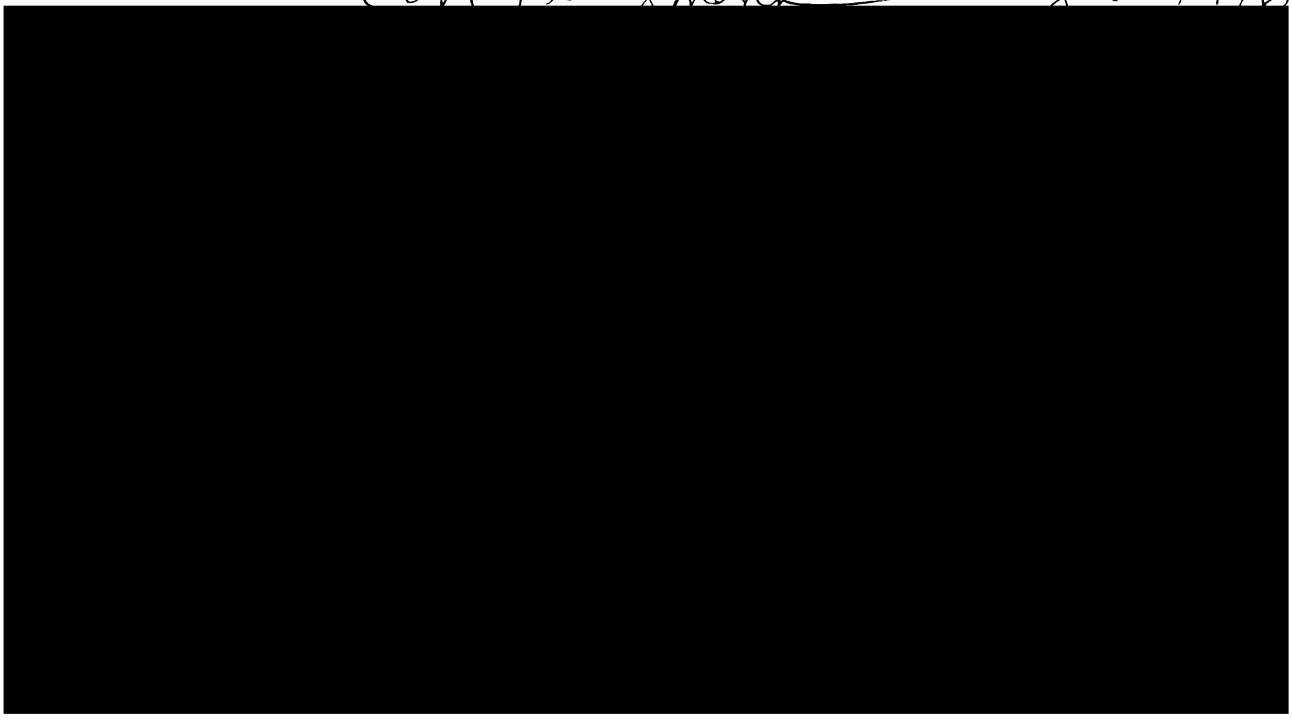

Acknowledgements

I thank my parents Phyllis Schnell and Ron Coburn for providing support, humor, interest and enthusiasm throughout my graduate studies. My sister Cynthia Coburn and her "friend" Nathan MacBrien helped me lighten up by sharing cheerful and sustaining companionship, conversation, advice, symphony tickets, and many skiing, camping and skating breaks. I also thank my Coburn and Pennypacker grandparents for their support and interest, and for always being more excited about my graduate career than I was.

My thesis committee, Cynthia Kenyon, Marc Tessier-Lavigne and Lily Jan, provided a lot of time, interest, encouragement and advice, and actually made my thesis committee meetings kind of fun. My graduate career would not been as pleasant without the assistance of Sue Adams and the Biochemistry office, who expertly administrated everything!

I thank all of the members of the Bargmann lab, especially my various baymates over the years, for providing entertainment, extraordinary amounts of gossip, mystery novels, 5$ loans over and over again, occasional ABBA dance-a-thons, heated discussions of current events as disparate as 90210, existential semantics, and the OJ trial, summaries of seminars that I forgot to attend, and of course, lots of scientific advice and discussions. Kate Wesseling, Shannon Grantner and Liqin Tong deserve special thanks and cheers for a LOT of help with DNA sequencing. I also thank Caroline Murphy and members of the Martin and Tessier-Lavigne labs for sharing lunchtime conversations, the latest CDs, and science talk.

Finally, I thank my advisor, Cori Bargmann. I feel fortunate to have been a member of Cori's lab, for it is difficult for me to imagine a better advisor for me. Cori gave me a lot of space to plan my project and pursue different ideas while simultaneously being tremendously available for advice, conversations and guidance (as well as occasional laser ablations, coffee nibs and opera sing-alongs). Her interest and enthusiasm for my project helped keep me going even when things weren't working so well, and her interest in science in general has always been inspiring.

tax-2:* A predicted cyclic nucleotide-gated channel required for normal sensory development and function in *C. elegans

Cara M. Coburn

Cori Bargmann

Cori Bargmann
Associate Professor

Abstract:

The *C. elegans* gene, *tax-2*, is required for some forms of olfaction, for chemosensation of salts, and for thermosensation. We show here that *tax-2* encodes a predicted subunit of a cyclic nucleotide-gated channel, indicating that a role of this channel in sensory function has been conserved from nematodes to vertebrates. *tax-2* is also required for normal axon outgrowth of some sensory axons, showing that the channel also functions in sensory neuron development. Consistent with this proposed dual function, the Tax-2 protein is expressed both in sensory cilia and in sensory axons.

We also discovered that *tax-2* and the similar *tax-4* gene play a role in dauer larva formation, a developmental process controlled by sensory stimuli and four classes of sensory neurons. Depending on the genetic background, cyclic nucleotide-gated channel function can either stimulate or inhibit dauer larva formation. In addition, the dauer formation mutants *daf-11* and *daf-21* have sensory axon guidance defects that are similar to those of *tax-2*, indicating that these genes may act in a similar process as *tax-2*. Surprisingly, although the chemosensory neurons are of embryonic origin, temperature-shift experiments showed that the *tax-2* and *daf-11* gene products are required continuously until the adult stage to preserve normal axon morphology. These results reveal an unexpected plasticity that allows axons to be remodeled long after functional connections have been established.

Table of Contents

Introduction 1

Chapter One: A putative cyclic nucleotide-gated channel required for sensory development and function in C. elegans 28

Chapter Two: Multiple developmental functions of a cyclic nucleotide-gated channel in C. elegans sensory neurons 66

Chapter Three: A genetic screen to identify more *tax*-2-like mutants 99

Chapter Four: Conclusions and future directions 119

Bibliography 135

Appendix A: A *tax*-2 homolog identified by the C. elegans genome sequencing project is expressed in the amphid sensory neurons 158

Appendix B: *tax*-2 has genetic interactions with other mutants that affect amphid and phasmid axon structure 164

List of Tables

Introduction

Table I-1: Comparison of properties of native and cloned CNG channels 24

Table I-2: Alignment of the predicted pore region of CNG channel α and β subunits 27

Chapter One

Table 1-1: *tax-2* and *tax-4* mutant animals have behavioral defects that are similar to the loss of some amphid neuron functions 56

Chapter Two

Table 2-1: Percent dauer and L4 segregants at 15°C from single broods from *tax-2/unc-13lin-11*;group II *daf-c* and *tax-4/dpy-17unc-32;* group II *daf-c* animals 91

Chapter Three

Table 3-1: The first *daf-11* suppressor screen identified 7 classes of suppressors, based on amphid and phasmid sensory neuron structure 115

Table 3-2: Benzaldehyde chemotaxis behavior of *suppressor; daf-11* strains identified in the second *daf-11* suppressor screen 117

Table 3-3: Characterization of suppressors re-isolated as single mutants based on their amphid axon phenotype 118

List of Figures

Introduction

Figure I-1: A cartoon of a generic CNG channel subunit 26

Chapter One

Figure 1-1: Responses of *tax-2* mutants to volatile odorants 57

Figure 1-2: Localization and sequence analysis of *tax-2* 58

Figure 1-3:*tax-2* protein is expressed in sensory neurons and is localized to both the sensory cilia and the axons 61

Figure 1-4: Developmental defects of *tax-2* and *tax-4* mutants visualized by DiO staining 62

Figure 1-5: Chemotaxis and axon guidance defects of *tax-2; tax-4* double mutants 64

Figure 1-6*tax-4* over-expression rescues *tax-2* mutant phenotypes 65

Chapter Two

Figure 2-1: Percent dauer-constitutivity of *tax-2, tax-4, daf-11* and *daf-21* single mutants and double mutant combinations 92

Figure 2-2: Percent dauer recovery of *tax-2, tax-4, daf-11* and *daf-21* single mutants and double mutant combinations 93

Figure 2-3: Developmental defects of *daf-11* and *daf-21* mutants visualized by DiO staining 94

Figure 2-4: Percent defective amphid axons in *tax-2, tax-4, daf-11* and *daf-21* single mutants and double mutants combinations 95

Figure 2-5: *tax-2(ks31ts)* is temperature-sensitive for chemotaxis and axon guidance defects 96

Figure 2-6: *tax-2* is continuously required for normal axon structure and benzaldehyde chemotaxis and *daf-11* is continuously required for normal axon structure 97

Chapter 4

Figure 4-1: Models of *tax-2*, *tax-4* and *daf-11* interaction 133

Appendices

Figure A-1: Sequence comparisons of the predicted transmembrane and cyclic nucleotide-binding domains of the predicted amino acid sequences of F38E11.8, the *tax-2* cDNA and the predicted amino acid sequence of TAX-4 163

Figure B-1: Percent normal phasmid axons in double mutants combinations between *tax-2* and other genes required for normal phasmid axon development 167

Introduction

Overview

During sensory transduction, external stimuli modify the electrical activity of sensory neurons. In the vertebrate visual and olfactory systems, sensory receptors regulate second messenger pathways that modulate cyclic nucleotide-gated ion channels in the sensory neurons (Fesenko et al., 1979; Nakamura and Gold, 1987; Sklar et al., 1986; Stryer, 1991). In the olfactory neuron, odorant receptors, acting through G_{olf}, activate adenylyl cyclase, which generates cAMP and opens a cAMP-activated cation-selective channel (Firestein and Zufall, 1994). This leads to depolarization of the olfactory neuron and the generation of an action potential. In the rod photoreceptor neuron, photoactivated rhodopsin activates $G_{transducin}$, which activates a phosphodiesterase. Phosphodiesterase activity catalyzes a decrease in the cGMP level, which results in the closure of the cGMP-activated conductance. This results in hyperpolarization of the photoreceptor, leading to a decrese in neurotransmitter release (Yau and Baylor, 1989). Phototransduction in the cone photoreceptor neurons is similar, although the channel is encoded by a distinct gene (Bonigk et al., 1993).

The cyclic-nucleotide-gated (CNG) channels are directly activated by cAMP and cGMP binding at varying efficiencies, depending on the channel. Multiple nucleotides bind cooperatively to open the channel, providing a sensitive link between cytosolic cNTP concentration and channel opening (Zagotta and Siegelbaum, 1996). Activation of the CNG channels is only weakly voltage sensitive, in contrast with distantly related K^+ channels which are activated by both voltage and cyclic nucleotide binding (Bruggemann et al., 1993). CNG channel activity can be modulated by changes in neuronal physiology; the apparent ligand sensitivity is modulated by Ca^{2+} (Kramer and Siegelbaum, 1992), Ca^{2+}-calmodulin (Chen and Yau, 1994; Hsu

and Molday, 1993), phosphorylation (Gordon et al., 1992), diacylglycerol analogues (Gordon et al., 1995), nitric oxide (Broillet and Firestein, 1996)and transition metal divalent cations (Gordon and Zagotta, 1995). This may provide a mechanism for integrating multiple physiological stimuli.

The CNG channels display a non-specific cation conductance, allowing mostly Na^+, Ca^{2+} and Mg^{2+} to pass (Frings et al., 1995). Ca^{2+} entry plays several roles in CNG channel function. In olfactory neurons, odorant-induced channel opening leads to Ca^{2+} entry, which contributes to adaptation (Zufall et al., 1994). In addition, Ca^{2+} can trigger a Ca^{2+}-gated Cl^- channel, which can amplify the electrical response to odorant (Kleene, 1993; Lowe and Gold, 1993). In the rod photoreceptors, light response results in a reduction in Ca^{2+}, which leads to adaptation (Kountalos and Yau, 1996). CNG channels show a strong voltage-sensitive block which is caused by Ca^{2+} and Mg^{2+} ions; because Ca^{2+} and Mg^{2+} permeation is so slow, the divalent cations effectively block the conductance of monovalent cations. Thus, at physiological conditions, the CNG conductance is very small (Yau and Baylor, 1989; Zufall et al., 1994). This enhances signal-to-noise contrast, permitting the detection of relatively small changes. For example, the rod channel responds to one photon (Baylor et al., 1979).

In *C. elegans*, a putative CNG channel is required for both sensory neuron function and sensory neuron development (This thesis ; Komatsu et al., pers. comm.). Cyclic nucleotide-gated channels are well-situated to regulate other processes, such as axon guidance, outgrowth and synaptic function, by virtue of their ability to integrate multiple extracellular and intracellular signals. Activation of the vertebrate cyclic nucleotide-gated channel leads both to depolarization of the neurons and to substantial calcium entry (Frings et al., 1995) and cAMP and cGMP levels can be regulated

by G protein-coupled receptors, by ligand-activated transmembrane guanylyl cyclases, or by gases such as nitric oxide. The role of channels in development will be considered briefly at the end of the chapter.

Molecular Cloning

The first CNG channel was cloned from bovine rod (Kaupp et al., 1989), and homologs from rod photoreceptors (Dhallen et al., 1992), cone photoreceptors (Bonigk et al., 1993) and olfactory neurons (Dhallan et al., 1990; Goulding et al., 1992) of many species were soon identified based on sequence homology. Two subunits of the olfactory and rod CNG channels have been cloned; the α (or first) subunit) and the β (or second subunit) (Bradley et al., 1994; Chen et al., 1993; Korschen et al., 1995; Liman and Buck, 1994). The human rod α and β subunits can be co-immunoprecipitated from transfected HEK cell, indicating that the subunits associate in vivo (Chen et al., 1994). The α and β channels are highly similar to each other, and, although they are gated by a cyclic nucleotide ligand, show substantial structural and sequence homology to the voltage-gated K^+ channel family (Jan and Jan, 1992). Based on this homology, the CNG channels are proposed to have six hydrophobic transmembrane domains (S1-S6), cytoplasmic amino- and carboxy-terminal tails, a S4 voltage sensor-like domain and a pore-forming (P) region between S5 and S6. The carboxy terminus contains a 120 amino acid cyclic nucleotide binding domain which is similar to those found in other cyclic nucleotide binding proteins (Figure 1). The proposed membrane topology has been partially confirmed by gene fusion (Henn et al., 1995) and antibody experiments (Molday et al., 1991; Wohlfart et al., 1992).

Based on the Hill coefficient of cyclic-nucleotide binding and the structural homology with voltage-gated K^+ channels, it was proposed that the

channel consistedof four subunits. Recently, Liu et al. expressed α subunits from two CNG channels with different conductance properties and recorded conductances consistant with tetrameric channels formed from two copies of each different α subunit (Liu et al., 1996). Interestingly, the order of subunit assembly also affected channel conductance properties.

When the cloned rod α channel is expressed in a heterologous system, a functional channel forms; however, these channels differ from the native channels in several ways. The cloned rod channel shows different kinetics and conductance properties, loss of Ca^{2+}-calmodulin modulation, and decreased sensitivity to the cation channel blocker cis-diltiazen (Kaupp et al., 1989). The β subunits do not form functional channels as homomultimers, but when β and α are co-expressed, CNG channels are produced that more closely resemble the native channel: the characteristic flickery conductance, Ca^{2+}-calmodulin modulation, and cis-diltiazem sensitivity are restored (Chen et al., 1994; Chen et al., 1993)(Table I-1and below). Interestingly, there are three alternatively spliced forms of the rod β subunit which differ in the length of the highly-charged amino-terminal tail; the short form and the longest form behave similarly when reconstituted with the α subunit indicating that the large charged amino-terminus is unnecessary for β function under these conditions (Korschen et al., 1995).

Like the rod channel, the cloned olfactory channels show altered kinetics and conductance properties, drastically altered cyclic nucleotide preferences, and altered sensitivity to cyclic nucleotides when the α subunit is expressed alone in heterologous systems (Dhallan et al., 1990; Goulding et al., 1992) The rat olfactory β subunit does not form functional channels as a homomultimer, however, when the olfactory α and β subunits are co-expressed, the channel formed shows kinetic and ligand activation properties

that are more similar to the native channel (Bradley et al., 1994; Liman and Buck, 1994)(see below). Interestingly, Liman and Buck observed the conductance of an α and β heteromultimeric channel displayed current desensitization, which is not seen in the native channel (Liman and Buck, 1994). However, in a similar paper, Bradley et al. did not observe this desensitization (Bradley et al., 1994). The difference could be due to differences in their expression systems (Xenopus vs. HEK cells).

Functional analysis

The CNG were originally thought to consist of homomultimeric α subunits, hence all of the available structural information regards the α subunit only. While some of the structural characterization of α subunit homomutimeric channels may prove relevant to the function of α and β subunit heteromultimeric channels, it should be noted that no structure-function analysis has been performed in the α and β context. This is an important point, since the β subunits, at the very least, modulate channel behavior, and the order of subunit assembly can change channel characteristics, .

Channel permeation and block

Sequence comparisons between CNG channels and the voltage-gated K^+ channels showed that CNG channels had a region that was highly homologous to the K^+ channel pore region. The 20 amino acids of the K^+ channel pore (or P-region) form a beta-hairpin in the membrane, determine the ionic permeation and probably form the narrowest region of the channel pore. The adjacent S5 and S6 regions also contribute to ion permeation, and are thought to make up the channel vestibule (Catterall, 1995). Consistent with this homology, the normally non-inactivating rat olfactory and bovine

rod CNG channel will actually bind the Shaker K^+ channel inactivation peptide in the pore region and inactivate (Kramer et al., 1994). Despite the P-region homology, K^+ and CNG channels show very different permeation properties, especially with regard to ion selectivity and divalent cation block; K^+ channels are highly selective for K^+ ions and are not blocked by divalent cations. Heginbotham et al. analysed the P-region structural differences which contributed to the permeation differences. They identified two conserved residues that were present in K^+ channels but deleted from CNG channels (Heginbotham et al., 1992). When these residues were deleted from the *Shaker* K^+ channel, the mutant channels displayed ion selectivities and a divalent cation block similar to that of the CNG channels.

Goulding et al. demonstrated that the P-region forms the pore of the CNG channels by constructing chimeras between the bovine rod and the catfish olfactory α subunits, which possess different single ion conductances and monovalent ion preferences (Goulding et al., 1993). In these experiments, the P-region was sufficient to determine the permeation properties. Since the P-region also determined the apparent pore diameter of the chimeric channels, it was proposed to form the selectivity filter. In CNG channels, pore diameter is apparently the major determinant of ion selectivity, as opposed to K^+, Na^+ and Ca^{2+} channels where specific ion binding is also important (Catterall, 1995).

Sun et al. probed the position of P-region residues in the open and closed states of the bovine rod channel α subunit by determining the assessibility of 11 cysteine-substituted P residues to small, charged sulfhydryl-specific modifying reagents applied to the inside or outside of membrane patches (Sun et al., 1996). Residues that are modified in the open and closed states may define residues forming the channel selectivity filter and the gate

that keeps the channel from passing ions in the closed state, respectively. They identified seven accessible residues; three were accessible from only the inside of the patch, three were state dependent (showing an effect only when the channel was closed), three residues were modified from either the inside or outside when the channel was closed, and two were accessible under all condition. Interestingly, some residues were modified in both the open and closed states, suggesting that they are accessible in both processes. The authors proposed that the pore consists of a thin iris which forms the gate in the closed state and the selectivity filter in the open state. It is important to note, however, that the effects of modification were investigated in α homomultimeric channels in which all subunits carried the cysteine substitution. It is unknown if all subunits in a multimeric channel are symmetric, providing equal access to the cysteines in all four subunits. Furthermore, the β subunit may have a structural effect on the P-region.

Root and MacKinnon identified a glutamate residue in the bovine rod α subunit P-region which bound external divalent cations, mediated the voltage-sensitive cation block and influenced the conduction of monovalent cations (Root and MacKinnon, 1993). Mutating the glutamate residue to a neutral residue (Gly or Asn) eliminated the external Mg^{2+} blockage and increased the outward rectification of the channel in the absence of external divalents while conservative substitutions (Glu to Asp) had no effect. Eismann et al. confirmed these results and also demonstrated that mutation of other charged residues in the bovine rod P-region had no effect on divalent cation blockage (Eismann et al., 1994). The glutamate residue is conserved in all rod and olfactory channel α subunits, but not in the β subunits (Figure 3). Interestingly, in their natural context, both the bovine rod (Korschen et al., 1995) and rat olfactory (Bradley et al., 1994) α and β heteromultimeric

channels display less external rectification due to cation block and increased outward rectification in the absence of divalent cations than is seen with wild-type α channels in heterologous systems Thus the native channel is similar to the mutated α channels (Gly or Asn) described above. In the rod channel, this effect could be explained by the presence of a neutral residue (G) replacing the glutamate residue in the β subunit. However, the olfactory β subunit has a conservative substitution (Asp) in the glutamate position, suggesting that other residues may contribute to the observed effects.

The same conserved glutamate residue is responsible for external proton block in the catfish olfactory α-subunit homomultimeric channel (Root and MacKinnon, 1994). Three conductance states of the channel were identified which corresponded to zero, one, or two protons bound, suggesting that each channel has two sites which can interact with either protons or cations. These subconductance states disappeared when glycine replaced the glutamate residue. It is not known whether these subconductance states are physiologically relevant.

Ligand specificity

The native olfactory and rod CNG channels have different cyclic nucleotide specificities, despite the homology of the predicted cyclic nucleotide binding regions (over 80% identical). The olfactory channel has similar affinities for cAMP and cGMP while the rod channel has a 20-50 fold higher affinity for cGMP than cAMP (Yau and Baylor, 1989; Zufall et al., 1994)(Table 1). While the maximal currents produced by cAMP and cGMP activation are similar in the olfactory channel, the maximal response to cAMP is only a fraction of the maximal response to cGMP in the rod channel. Teleologically, the different preferences of the olfactory and rod channels could reflect the different physiological roles of cAMP and cGMP in olfaction

and vision, although based on this argument, it is unclear why the olfactory channel is equally responsive to cAMP and cGMP.

The cyclic nucleotide responses of the cloned rod α subunit alone, α and β heteromultimers and native channels are similar (Chen et al., 1993; Kaupp et al., 1989), but the cyclic nucleotide responses of the cloned olfactory CNG channels are different from those observed in native channels (Table 1). Like the native catfish channel, the expressed catfish α subunit responds to equally well to cGMP and cAMP and both nucleotides evoke a similar maximum conductance. However, the cloned channel is about 15-20 times less sensitive to cyclic nucleotides (Goulding et al., 1992). When the rat α subunit is expressed alone, channels are formed in which the cAMP response is 25-40 times less sensitive than that for cGMP. The maximal activated conductance is similar for the two nucleotide, as is observed in the native channel (Dhallan et al., 1990). Addition of the rat olfactory channel β subunit increases the cAMP sensitivity substantially, although it is still 3 times less sensitive than the native channel (Bradley et al., 1994; Liman and Buck, 1994).

Several groups have investigated the molecular basis for cyclic nucleotide selectivity. The 120 amino acid predicted cyclic nucleotide binding site (Figure 1) is homologous to the binding sites of other cyclic nucleotide-binding proteins, including the bacterial catabolite activator protein (CAP) transcription factor. The crystal structure of the cAMP-binding site of CAP (Weber and Steitz, 1987) showed that the site consists of a amino-terminal α helix (A) followed by an eight-stranded antiparallel β-roll, followed by two α helixes (B and C). Critical residues which contact bound cyclic nucleotides or occur at turns between adjacent β-strands are conserved between CAP and the CNG channels. Based on this sequence homology, the rod cGMP-binding site was modeled (Kumar and Webr, 1992).

Because cAMP and cGMP differ only in the purine ring, the C-helix, which makes hydrogen bonds with the purine ring of the cyclic nucleotide, seemed to be a likely site of selectivity. Goulding et al. constructed chimeras between the fish olfactory and the bovine rod CNG channels and found that replacing the olfactory C-helix with the rod C-helix resulted in a channel that was selectively activated by cGMP (Goulding et al., 1994). Conversely, replacing the rod C-helix with the olfactory C-helix produced a channel that was equally activated by cAMP and cGMP. In the CAP C-helix, threonine-127 hydrogen-bonds with a critical amino group on the purine ring (Weber and Steitz, 1987); Varnum and Zagotta found that the homologous residue in the bovine rod α channel, Asp-604, is important for selective cGMP activation (Varnum et al., 1995). If Asp-604 was replaced by a neutral polar residue (glutamine, as in the fish olf channel) or a nonpolar residue (methionine, as in the rat olfactory b subunit), the nucleotide selectivity was significantly altered at saturating nucleotide concentrations. Since these substitutions affected the maximal channel current response more than the ligand affinity, Asp-604 may serve a stabilizing role once cGMP has already bound. Altenhofen et al. examined the role of a conserved threonine in the bovine rod α subunit β-strand region (T-560); the homologous residue in CAP hydrogen bonds with the cyclic nucleotide purine ring (Altenhofen et al., 1991). Mutating the residue to alanine resulted in decreased cGMP affinity, however, this mutation is unlikely to be physiologically relevant since all cloned CNG channels have a threonine in this position.

Allosteric changes during gating

The rod and olfactory channels have very different free energies of allosteric channel opening; it is energetically much more favorable to open the olfactory channel (Gordon and Zagotta, 1995; Goulding et al., 1994). It is

not understood how ligand binding is coupled to channel opening;, however, several regions of the channel have been implicated. Experiments in which the amino termini of the rod and olfactory α subunit CNG channels were swapped demonstrated that the amino terminus is important. When the rod amino terminus was replaced with the olfactory amino terminus, the resulting channel was more easily opened, and vice-versa (Gordon and Zagotta, 1995; Goulding et al., 1994). When a larger portion of the amino terminus was swapped (amino terminus through the S2-S3 linker), a stronger effect was observed. The authors hypothesized that the amino terminus may mediate subunit-subunit interactions important for allosteric changes during gating (Goulding et al., 1994).

Low concentrations of Ni^{2+} potentiate the native rod channel (Karpen et al., 1993) and inhibit the rat olfactory α subunit (Gordon and Zagotta, 1995). Gordon and Zagotta identified the histidine residues that mediate these effects; when the channels are aligned, the histidines are three residues apart in the putative "vestibule" of the channel pore (Gordon and Zagotta, 1995; Gordon and Zagotta, 1995). Ni^{2+} appeared to bind and stabilize the open state of the rod channel, while it bound and stabilized the closed state of the olfactory channel. These experiments are consistent with a model in which the region between S6 and the ligand binding region undergoes allosteric changes associated with channel gating. Interestingly, potentiation of a model heteromultimeric rod channel requires that the histidine residue are located in adjacent subunits (Gordon and Zagotta, 1995). Direct sulfhydryl modification of a cysteine residue in the same region by nitric oxide can directly activate native salamander olfactory CNG channels (Broillet and Firestein, 1996). This activation is independent of ligand and very long-lasting. While it is unclear if this modification by NO is physiologically

relevant, it suggests that conformational changes in this region of the protein are directly or indirectly required for channel gating.

Channel modulation

Ca^{2+}-calmodulin decreases the apparent cyclic nucleotide affinity of the olfactory and rod CNG channels (Chen and Yau, 1994; Hsu and Molday, 1993)and it was proposed that Ca^{2+}-calmodulin may interfere with channel gating (Liu et al., 1994). Ca^{2+}-calmodulin binds to a specific site in the amino terminus of the olfactory α subunit (Liu et al., 1994) and to the rod β subunit (Chen et al., 1994). In addition to Ca^{2+}-calmodulin, other calcium-binding protein may bind and inhibit CNG channels (Gordon et al., 1995). Protein phosphatases and diacylglycerol analogs also modulate the apparent ligand affinity of native salamander rod CNG channels, although it is not known if these effect are physiologically relevent (Gordon et al., 1992; Gordon et al., 1995).

CNG channel diversity

Expression and cloning experiments demonstrated that the rod, cone and olfactory CNG are also expressed in non-sensory neurons and in non-neuronal tissues, where their function is not understood. The α subunit of the rod CNG channel is also expressed in kidney (Biel et al., 1994) and retinal ganglion cells (Ahmad et al., 1994), while the cone channel is found in the testes, kidney, and heart (Biel et al., 1994; Weyand et al., 1994). The olfactory α and β subunits of the channel are expressed in other brain neurons and the β subunit is also found in the vomeronasal organ (Berghard and Buck, 1996; Bradley et al., 1994; El-Husseini et al., 1995). In addition, a cyclic nucleotide-gated cation conductance was described in the hippocampus, though the channel has not been molecularly characterized (Leiders-Zufall et al., 1995).

The CNG channels also function in non-ciliary cellular compartments; Ca^{2+} entry through the cone CNG channel mediates exocytosis in the cone inner segment (Rieke and Schwartz, 1994) and rod CNG channels are found at low densities in the rod inner segment (Watanabe and Matthews, 1988).

CNG channel homologues have also been identified in non-vertebrate sensory systems. A Drosophila homologue is expressed in antennal and eye neurons (Baumann et al., 1994) while a Na^+ current in mollusc neurons is gated by cyclic nucleotides (Sudlow et al., 1993). In addition, related CNG K^+ channels function in marine echinoderm sperm chemotaxis (Cook and Babcock, 1993), mollusc photoreceptor neurons (Gomez and Nasi, 1995), and lobster olfactory neurons (Hatt and Ache, 1994). Interestingly, lobster olfactory neurons have IP3-responsive channels as well as CNG channel, indicating that two transduction pathways could function in these sensory neurons.

Role of channels in development

Ion channels play a role in many aspects of neuronal development, including differentiation, neurite outgrowth *in vitro*, synapse elaboration, and activity-dependent refinement of neuronal connections. This section will briefly consider several aspects of ion channel function in neuronal development. This topic is also extensively reviewed (Goodman and Shatz, 1993; Neeley and Nicholls, 1995; Shatz, 1990).

***weaver* and granule cell differentiation**

The mouse *weaver* (*wv*) gene is required for differentiation and neuronal survival of cerebellar granule cells and other neurons (Hess, 1996). *wv* encodes the GIRK2 K^+ channel, a member of the class of inwardly-rectifying K^+ channels that are gated by G protein subunits. The *wv* mutation is a

missense mutation which alters a conserved residue in the pore region (Patil et al., 1995). Electrophysiological experiments demonstrated that this change results in constitutively active channels with altered ion selectivity; instead of conducting K^+, the *wv* mutant channels conducted high levels of $Na^+$when expressed as homomultimers in *Xenopus* oocytes. Consistent with this observation, blocking the aberrant Na^+ conductance pharmacologically rescued the granule cell differentiation defect *in vitro* (Kofuji et al., 1996). However, *wv* mutant channels are likely to function as heteromultimer with other GIRK channels and mixing experiments where *wv* GIRK2 subunits were expressed with GIRK1 subunits in oocytes produced a highly reduced K^+ current (Slesinger et al., 1996). Although it is unclear exactly how *wv* mutant channels disrupt neuronal differentiation and survival, depolarization due to unregulated Na^+ influx and disrupted K^+ efflux may play a role.

Neurite outgrowth *in vitro*

The role of ion channels in neurite outgrowth has been examined in several *in vitro* systems and two interesting effects have been reported. 5-HT application inhibits outgrowth of the identified B19 neurons in the snail, *Heliosoma*, by causing membrane depolarization and subsequent activation of voltage-sensitive Ca^{2+} channels (Kater and Mills, 1991). This effect was mimicked by triggering action potentials with current pulses or adding Ca^{2+} ionophores, suggesting that Ca^{2+} is necessary. It was blocked by inhibiting membrane depolarization by application of the inhibitory neurotransmitter, acetylcholine, or by hyperpolarizing the membrane. Thus, in this *in vitro* system, control of membrane potential by ion channels regulates neurite outgrowth. While the targets of the B19 neurons produce 5-HT, it is not clear if this effect is physiologically relevant. Further experiments in the same system showed that both increased and decreased Ca^{2+} levels can inhibit

neuronal outgrowth, indicating that precise control of Ca^{2+} concentration is important (Mattson and Kater, 1987). In a different *in vitro* system, the L1 cell adhesion molecule stimulates voltage-gated Ca^{2+} channel-dependent neurite growth of PC12 cells and cerebellar neurons. This effect depended on extracellular Ca^{2+} and could be blocked by L-type and N-type channel blockers (Williams et al., 1992).

Cultured frog neurons and mouse neuroblastoma cells will extend neurites in the direction of an imposed electric field (galvanotaxis); several groups demonstrated that this effect resulted from Ca^{2+} channel activation and subsequent Ca^{2+} influx (Bedlack et al., 1992; McCaig, 1989). In fact, localized electrical fields applied to growth cones cause localized Ca^{2+} influx and filopodial "protrusion" in the direction of the electrical field; these effects are also blocked by Ca^{2+} channel blockers and the absence of extracellular Ca^{2+}. Thus, ion channel activity might control growth cone turning in these system.

Development at the neuromuscular junction

Studies of motor neuron development in Drosophila took advantage of mutants in which motor neuron electrical activity is increased or decreased. Budnik et al. (1990) found increased branching of motor neurons and extra synaptic sites in an *ether a go-go (eag) Shaker(Sh)* double mutant strain. These mutations affect potassium channels and increase electrical exitability. *no action potential (nap-ts)*, a mutations which reduces electrical activity by affecting Na^{+} channels, suppressed the effects of the *eag Sh* double mutant. *nap-ts* alone showed only a slight reduction in nerve branching (Budnick et al., 1990). Interestingly, the *dunce (dnc)* mutation which increases cAMP levels in the motoneurons also showed increased branches and synaptic site, implicating the cAMP cascade in mediating activity-dependent

changes in the neuromuscular junction. The *dnc* phenotype was enhaced by the potassium channel mutations; *dnc eag* or *dnc Sh* double mutant combinations displayed a stronger phenotype than the *dnc* single mutant (Zhong et al., 1992).

Jarecki and Keshishian (1995) examined motoneuron morphology in mutants that reduce neural activity by affecting Na^+ channel function or expression . They observed extensive neuronal sprouting and the formation of ectopic endings on inappropriate target motoneurons. This phenotype contrasts with the more elaborate but appropriately innervating synapses of the hyperexcitable mutants (described above). The authors hypothesize that neuronal activity is required to maintain the correct pattern of connections through development (Jarecki and Keshishian, 1995).

Development of the visual system

While activity-independent mechanisms are used to establish the crude initial connections during development of the visual system, neuronal activity is required to remodel and restrict the axon arborizations to create the correct pattern of connections. In mammals, axons project from the lateral geniculate nucleus (LGN) to area 4 of the visual cortex (Shatz, 1996; Shatz, 1990). Initially, axons representing both eyes are completely intermixed, however, over time the terminals segregate into discrete eye-specific patches known as ocular dominance columns. This remodeling involves both the retraction of axons from inappropriate areas and the elaboration of short branches and synapses in the correct areas. Early studies showed that neural activity was required for ocular dominance column formation; monocular eye closure during the period of column formation caused an expansion of the area occupied by open-eye axons at the expense of the area occupied by closed-eye axons (Shatz, 1996; Shatz, 1990).

Many experiments have subsequently shown that activity-dependent competition between LGN axons drives ocular dominance column formation. Tetrodotoxin (TTX, which blocks voltage-gated Na^+ channels) treatment of both eyes inhibits the formation of ocular dominance columns (Stryker and Harris, 1986). However, when electrodes were implanted in the optic nerves of TTX-treated eyes and both nerves were asynchronously stimulated, ocular dominance columns formed. Synchronous stimulation did not cause column formation, indicating that the pattern of activity is important in axon refinement within the cortex (Stryker and Strickland, 1984). While there is evidence linking post-synaptic activation of NMDA receptors to column formation in an amphibian model system (Constantine-Paton et al., 1990), it is not clear if NMDA receptors play a similar role in mammalian visual development. Blockade of NMDA receptors by APV infusion in the visual cortex prevented ocular dominance column formation, however, this experiment was difficult to interpret because NMDA is required for normal synaptic transmission (Kleinschmidt et al., 1987); it is difficult to distinguish elimination of activity by APV block of normal synaptic transmission from inhibition of plasticity by NMDA receptor blockade. Neuronal activity is also required for proper segregation of retinal ganglion cell axons into eye-specific layers in the lateral geniculate nucleus (Shatz, 1996) and related processes occur in the somatosensory cortex (Fox et al., 1996).

C. elegans

The nematode, *C. elegans*, is an attractive model system for integrating neuronal, behavioral, genetic and molecular approaches to sensory neuron function and development. Its nervous system is simple, consisting of only

302 neurons in the adult hermaphrodite (White et al., 1986). In addition, development is extremely stereotyped in C. elegans, and the cell lineage and predicted neuronal connections of every neuron have been described (Sulston and Horvitz, 1977; Sulston et al., 1983). The *C. elegans* nervous system generates many behaviors, and in several cases, the sensory neurons regulating these behaviors have been defined (Bargmann, 1993). This information has been used to characterize genes that affect these neurons.

The work described in this thesis concerns the development and function of several neurons required for chemosensory and thermosensory behavior in *C. elegans*. The worm chemotaxes to several salts, biotin, cAMP, several amino acids, and more than 50 volatile compounds (Bargmann et al., 1993; Bargmann and Horvitz, 1991; Ward, 1973; Dusenbery, 1974). High osmotic strength and some volatile chemicals repel the worm (Bargmann et al., 1990; Troemel et al., 1995). In addition, *C. elegans*' development is regulated by chemical signals. In the presence of high concentrations of a pheromone, the worm arrests in a specialized developmental stage called the dauer larva (Riddle, 1988). Food and temperature modulate dauer formation, and recovery from the dauer stage is regulated by food availability. Finally, worms show a thermotaxis behavior; they will migrate across a thermal gradient to the temperature at which they were raised (Hedgecock and Russell, 1975).

When this thesis was begun, the neurons required for volatile and water-soluble chemotaxis, chemical avoidance, thermosensation, and normal regulation of dauer formation and recovery had been defined by laser ablation experiments. All of these neurons were amphid sensory neurons that had ciliated ending exposed or continuous with the outside environment . Two pairs of neurons recognized chemical repellents (ASH, ADL)(Bargmann et al.,

1990; Troemel et al., 1995), five pairs of neurons recognized water-soluble attractants (ASE, ADF, ASG, ASI, ASK) (Bargmann and Horvitz, 1991), two pairs of neurons recognized volatile attractants (AWC, AWA)(Bargmann et al., 1993)and one pair of neurons detected temperature (AFD) (Mori and Ohshima, 1995). Three pairs of neurons that sensed water-soluble attractants also regulated a developmental decision between two alternative larval states: the third-stage larva that will develop to a fertile adult, and the arrested dauer larva (ADF, ASG, ASI) (Bargmann and Horvitz, 1991). The ASJ neurons had two distinct functions in dauer development; they promoted dauer formation in the presence of dauer pheromone and promoted dauer recovery in the absence of phermone and the presence of food (Bargmann and Horvitz, 1991; Shackwitz and Thomas, pers. comm.).

Chemosensory and thermosensory mutants had been identified by screening for animals that failed to respond to water-soluble attractants (*che* and *tax* mutants) , volatile odorants (*odr* mutants), or temperature (*ttx* mutants) or that failed to avoid high osmotic strength (*osm* mutants) (Bargmann et al., 1993; Culotti and Russell, 1978; Dusenbery et al., 1975; Hedgecock and Russell, 1975; Lewis and Hodgkin, 1977; Mori and Ohshima, 1995). While a few of the *odr* and *ttx* mutants had extremely specific behavioral phenotypes, consistent with the gene affecting one sensory neuron, most of the *che, tax, odr, osm* and *ttx* mutants had pleiotropic behavioral defects indicating that the genes affected the function of several sensory neurons. Similarly, other mutants that were first identified by their effect of dauer formation had chemosensory and thermosensory defects (*daf* mutants) (Bargmann et al., 1993; Riddle et al., 1981; Vowels and Thomas, 1992).

While there was no molecular information available at the start of this thesis, the cloning and expression pattern of several genes were reported in the last couple of years and provided insight into the molecular basis of olfactory signal transduction in *C. elegans*. The mechanisms of aqueous chemotaxis and thermotaxis remained mysterious. Olfactory recognition in *C. elegans* appears to be initiated by interactions between odorants and G protein-coupled receptors. The *odr-10* gene encodes a seven transmembrane domain receptor that is required for the response to the volatile odorant diacetyl, and a tagged Odr-10 protein is localized to the sensory cilia of the AWA chemosensory neurons (Sengupta et al., 1996). Its genetic and molecular properties suggest that the Odr-10 gene product is a diacetyl receptor, although it has not been demonstrated to bind to odorant. Several different families of predicted G protein-coupled receptors could encode additional *C. elegans* chemoreceptors. There are at least forty candidate receptor genes in six gene families (the *sra, srb, srd, sre, srg,* and *sro* genes) that appear to be expressed predominantly in chemosensory neurons (Troemel et al., 1995), as well as at least eighty other *odr-10*-like genes (E. Troemel, J. Chou, and C. Bargmann, unpublished). The *odr-3* gene encodes a $G\alpha i/G\alpha o$-like G protein subunit, which may mediate signal transduction downstream of G protein-coupled receptors. *odr-3* is required for all forms of volatile chemotaxis, consistent with its expression in both the AWA and AWC sensory neurons (K. Roiayaie, G. Crump, and C. Bargmann, unpublished). Finally, the *osm-9* gene encodes a predicted protein with homology to Ca^{2+} channels, which is required for normal function of the AWA olfactory neuron and for the function of amphid neurons that sense water-soluble repellents. *osm-9* is expressed in the AWA neurons, consistent with its role

in AWA chemosensory function (H. Colbert, and C. Bargmann, unpublished).

This thesis describes the genetic and molecular characterization of *tax-2*, a predicted cyclic nucleotide-gated channel required for sensory neuron function and development. In Chapter One, we describe phenotypic characterization of *tax-2* mutants, cloning of the *tax-2* gene, and the similarity *tax-2* to *tax-4*, another *C. elegans* predicted cyclic nucleotide-gated channel. Both *tax-2* and *tax-4* are required for the forms of olfaction mediated by the AWC neuron, indicating that similar CNG channels could function in both vertebrate and worm olfaction. The *tax-2* and *tax-4* CNG channels are also required for normal salt chemosensation and thermosensation; a role for CNG channels in salt taste and thermotransduction has not been previously described. Finally, in a novel function of CNG channels, *tax-2* and *tax-4* are required for normal axon outgrowth of some sensory neurons. A tagged Tax-2 protein is expressed in both the cilia and the axons of the affected sensory neurons, consistent with the possibility that *tax-2* could independently function in both locations. Expression patterns, genetic analysis, and over-expression experiments suggest that *tax-2* and *tax-4* may be acting together in these processes. In Chapter Two, the function of *tax-2* and *tax-4* in the *C. elegans* dauer developmental pathway is discussed. *tax-2* and *tax-4* are expressed in some of the amphid neurons that regulate the pheromone-controlled developmental decison, and genetic analysis indicates that *tax-2* and *tax-4* function to both promote and prevent dauer-formation depending on the genetic background. In addition, *tax-2* and *tax-4* each suppress the dauer-constitutivity of the *daf-11* guanylyl cyclase mutant. The *daf-11* guanylyl cyclase mutant has similar behavioral and axon outgrowth defects to those of *tax-2* and *tax-4*, providing evidence that these genes act in similar

processes. Furthermore, temperature-shift experiments show that the *tax-2* and *daf-11* gene products are continuously required for normal neuron function and axon morphology, even though the sensory neurons develop embryonically. These results demonstrate a novel late-acting developmental plasticity of neuronal structure. In Chapter Three, preliminary results of a genetic screen to identify more *tax-2*-like mutants are described. 56 genetic suppressors of the *daf-11* dauer-constitutive phenotype that resembled the *tax-2;daf-11* double mutant strain were isolated. Three classes of suppressors were characterized, including 5 new *tax-2* and *tax-4* alleles and an interesting novel mutant, *ky95*.

Table I-1: Comparison of properties of native and cloned CNG channels. Adapted from Zagotta and Siegelbaum (1996).

Channel	Composition	Conductance (g)	$K_{1/2}$ (mM) cAMP	cGMP	Ca^{2+}-calmodulin modulation?	References
rat olfactory	native	12-15	4	1.8	yes	(Frings et al., 1992)
	α subunit	35	55	2	yes	(Dhallan et al., 1990)
	α + β	19	14-16	4	ND	(Bradley et al., 1994; Liman and Buck, 1994)
fish olfactory	native	44	3.4	2.5	ND	(Goulding et al., 1992)
	α subunit	55	42	40	ND	(Goulding et al., 1992)
bovine rod	native	6	---	165	yes	(Yau and Baylor, 1989)
	α subunit	20	2000	60	no	(Kaupp et al., 1989)
	α + β	30; flickery	2100	40	yes	(Korschen et al., 1995)
human rod	α subunit	25-30	---	60	ND	(Dhallen et al., 1992)
	α + β	flickery	---	60	ND	(Chen et al., 1993)

Table I-2: Alignment of the predicted pore region of CNG channel α and β subunits.

hRCNC1	Y	V	Y	S	L	Y	W	S	T	L	T	L	T	T	I	G	**E**	T	P	P	P
rOCNC1	Y	I	Y	C	L	Y	W	S	T	L	T	L	T	T	I	G	**E**	T	P	P	P
fOCNC	Y	V	Y	C	F	Y	W	S	T	L	T	L	T	T	I	G	**E**	M	P	P	P
hRCNC2	Y	I	R	C	Y	Y	F	A	V	K	T	L	I	T	I	G	G	L	P	D	P
rOCNC2	Y	L	Y	S	F	Y	F	S	T	L	I	L	T	T	V	G	D	T	P	L	P
TAX-4	Y	V	Y	S	F	Y	W	S	T	L	I	L	T	T	I	G	**E**	V	P	S	P
TAX-2	Y	I	R	C	F	Y	F	T	A	A	V	A	T	S	T	G	N	N	P	A	P

Highly conserved residues are boxed and the glutamate residue that binds divalent cations is indicated in bold type. Abbreviations are as follows: hR, human rod; rO, rat olfactory; fO, fish olfactory; 1, alpha subunit; 2, beta subunit

Figure legend

Figure I-1: A cartoon of a generic CNG channel subunit. S1-S6 refer to transmembrane domains. Labelled regions and residues indicate information gleaned from studies of rod and olfactory channels. Adapted from Zimmerman (1995).

Figure I-1

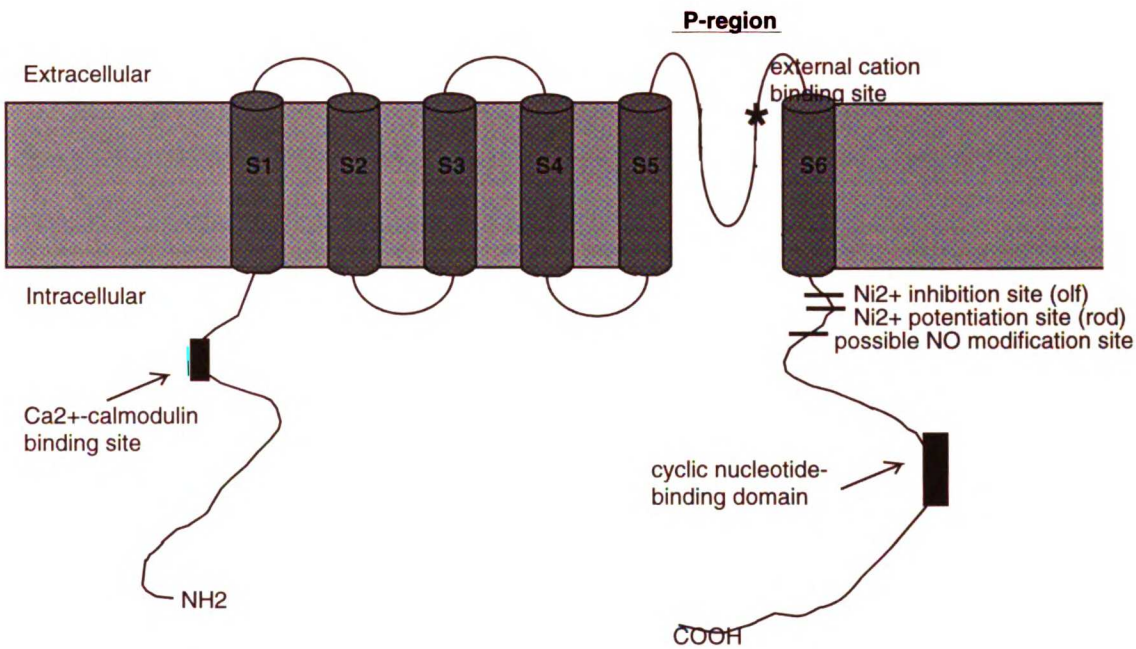
P-region
Extracellular
external cation
binding site
S1
S2
S3
S4
S5
S6
Intracellular
Ni2+ inhibition site (olf)
Ni2+ potentiation site (rod)
possible NO modification site
Ca2+-calmodulin
binding site
cyclic nucleotide-
binding domain
NH2
COOH

Chapter One

A putative cyclic nucleotide-gated channel required for sensory development and function in C. elegans

Summary

In vertebrate visual and olfactory systems, a cyclic nucleotide-gated channel couples receptor activation to electrical activity of the sensory neurons. The C. elegans *tax-2* gene is required for some forms of olfaction, for chemosensation of salts, and for thermosensation. We show here that *tax-2* encodes a predicted subunit of a cyclic nucleotide-gated channel that is expressed in olfactory, gustatory, and thermosensory neurons, implicating this channel in multiple sensory modalities. Some sensory neurons display axon outgrowth defects in *tax-2* mutants. Thus, the channel has an unexpected role in sensory neuron development in addition to its role in sensory transduction. Consistent with this proposed dual function, the Tax-2 protein is expressed both in sensory cilia and in sensory axons.

Introduction

Sensory neurons respond to the environment by transducing external stimuli into patterned electrical activity. In both vertebrate visual and olfactory neurons, sensory receptor proteins initiate this process by regulating second messengers that open cyclic nucleotide-gated ion channels. In photoreceptors, light-activated rhodopsin stimulates cGMP hydrolysis to reduce channel activity; in olfactory neurons, odorants induce cAMP production to stimulate channel activity (Fesenko et al., 1985; Nakamura and Gold, 1987; Sklar et al., 1986; Stryer, 1991). Although they are regulated by different nucleotides, the genes that encode vertebrate visual and olfactory cyclic nucleotide-gated channels are highly similar to one another (Kaupp et al., 1989).(Dhallan et al., 1990).

The cyclic nucleotide-gated channels are distantly related to the Shaker class of voltage-gated potassium channels, but they are gated by an intracellular ligand (cAMP or cGMP) instead of membrane potential. Cyclic nucleotide binding to an intracellular domain of the channel allows nonspecific cation entry and neuronal depolarization (Goulding et al., 1994). Each channel is composed of related alpha and beta subunits that assemble to form a heteromeric channel protein (Bradley et al., 1994; Korschen et al., 1995; Liman and Buck, 1994).

Although the prominence of cyclic nucleotide-gated channels in sensory transduction is well-established, questions about their function remain. First, other types of odor-activated channels have been reported in olfactory neurons, and the relative importance of each channel in signal transduction is unknown (Dubin and Dionne, 1994; Kleene, 1993; Lowe and Gold, 1993). Second, it is not known whether the cyclic nucleotide-gated channels in sensory neurons act only in sensory transduction, or if they participate in other aspects of neuronal function. Third, these channels are expressed in other neuronal and non-neuronal cell types, but their function in these cell types is not understood (Ahmad et al., 1994; Biel et al., 1994; el-Husseini et al., 1995; Weyand et al., 1994).

In C. elegans, genetic analysis can be used to probe chemosensory transduction *in vivo*. The C. elegans nervous system contains thirty two chemosensory neurons, which can be divided into fourteen types based on morphology (Ward et al., 1975; Ware et al., 1975; White et al., 1986). Laser killing experiments have demonstrated chemosensory functions for ten types of neurons in the major chemosensory organ, the amphid (Bargmann et al., 1993; Bargmann and Horvitz, 1991; Bargmann and Horvitz, 1991; Kaplan and Horvitz, 1993; Troemel et al., 1995). Different amphid neurons can detect

water-soluble attractants, volatile attractants, pheromones, and chemical repellents. The amphid also contains one type of neuron that detects temperature (Mori and Ohshima, 1995). Screens for chemotaxis mutants in C. elegans have identified mutations in various *odr*, *che* and *tax* genes (Bargmann et al., 1993; Dusenbery et al., 1975; Lewis and Hodgkin, 1977). Some of these mutants have defects in many chemosensory neurons, while others have defects that are limited to one or a few chemosensory responses.

Olfactory recognition in C. elegans appears to be initiated by interactions between odorants and G protein-coupled receptors. Genetic and molecular analysis suggests that a seven transmembrane domain protein encoded by the *odr-10* gene is a diacetyl receptor, although it has not been demonstrated to bind to odorant (Sengupta et al., 1996). *odr-10* is required for the response to the volatile odorant diacetyl, and a tagged Odr-10 protein is localized to the sensory cilia of the neurons that detect diacetyl. Several different families of predicted G protein-coupled receptors could encode additional C. elegans chemoreceptors. There are at least forty candidate receptor genes in six gene families (the *sra*, *srb*, *srd*, *sre*, *srg*, and *sro* genes) that appear to be expressed predominantly in chemosensory neurons (Troemel et al., 1995), as well as at least eighty other *odr-10*-like genes (E. Troemel, J. Chou, and C.I.B., unpublished). Each individual chemosensory neuron appears to express several different candidate chemosensory receptor genes (Troemel et al., 1995); correspondingly, laser killing experiments and behavioral studies indicate that each chemosensory neuron detects several chemical stimuli (Colbert and Bargmann, 1995; Ward, 1973).

The second messenger pathways that are used by C. elegans sensory neurons are not known. While the *odr-10* mutant phenotype is extremely selective, as is expected of a receptor, we expected that the genes that act in

sensory transduction might affect multiple sensory responses. We describe here the characterization of the *tax-2* gene, which affects chemotaxis to attractive compounds, avoidance of repulsive compounds, and thermotaxis (Bargmann et al., 1993; Dusenbery et al., 1975). *tax-2* encodes a predicted beta subunit of a cyclic nucleotide-gated channel. A cyclic nucleotide-gated channel alpha subunit that might function with *tax-2* is encoded by the *tax-4* gene (Komatsu et al., pers. comm.); *tax-4* affects the same behavioral responses as does *tax-2*. *tax-2* is expressed in the subset of sensory neurons whose function is defective in the mutants, and its protein product is localized both to the sensory cilia and to the axons.

In addition to their apparent sensory function, both *tax-2* and *tax-4* have an unexpected role in sensory axon guidance. In *tax-2* and *tax-4* mutants, sensory axons invade regions from which they are normally excluded, suggesting that channel activity inhibits or limits axon outgrowth of sensory neurons.

Results

tax-2 encodes a cyclic nucleotide-gated channel subunit required for multiple sensory functions

Seven *tax-2* mutant alleles have been isolated based on defects in chemotaxis, thermotaxis, and dauer larva formation ((Dusenbery et al., 1975), and Coburn et al., in prep.). These mutants were compared to one another in various behavioral assays. All alleles were defective in chemotaxis to water-soluble attractants and in thermotaxis ((Dusenbery et al., 1975), Coburn et al., in prep., and data not shown); these defects imply a loss of function of the ASE, ASK, and AFD sensory neurons (Table 1-1). In addition, six of the seven mutants were defective in chemotaxis to a subset of volatile odorants (Figure

1-1). *p671, p691, ks10, ks15, ks31* and *ky139* were defective for chemotaxis to benzaldehyde and isoamyl alcohol, but proficient in chemotaxis to diacetyl, pyrazine, and trimethylthiazole. These chemotaxis defects are characteristic of animals that lack the function of the AWC olfactory neurons, but maintain function of the AWA olfactory neurons (Bargmann et al., 1993)(Table 1-1). By contrast, animals mutant for the *tax-2* allele *p694* were normal for chemotaxis to all volatile odorants.

Negative chemotaxis responses to volatile repellents including 1-octanol and 2-nonanone were also defective in *tax-2(p671), tax-2(p691)* and *tax-2(ks31)* mutants; the cells required for these responses are unknown. However, the mutants responded normally to water-soluble repellents, indicating that the ASH sensory neurons functioned normally. Movement, fertility, and development appeared normal, though the mutants were often slightly smaller than wild-type animals and had slightly slowed development.

These results indicate that most *tax-2* alleles affect a common set of sensory functions, while the weak allele *p694* only affects a subset of those functions. All of the *tax-2* mutants are recessive and fail to complement one another. In addition, the phenotype of *tax-2(p691)* is not enhanced in a *tax-2(p691)*/deletion heterozygote (data not shown). Taken together, these results are consistent with the mutations causing a loss of *tax-2* gene function.

tax-2 was cloned by genetically mapping the gene to the interval between *unc-29* and *lin-11*, and testing cosmid clones from that interval for their ability to complement the *tax-2* mutant phenotype in transgenic worms. The cosmid T18D4 or a 6.5 kb HindIII fragment of that cosmid rescued the benzaldehyde chemotaxis defect of *tax-2* mutants (Figure 1-2a). cDNA clones from this region were identified by screening a mixed-stage library and by

reverse transcriptase-polymerase chain reaction amplification of *tax-2* clones from total mRNA. The genomic sequence and the sequence of cDNA clones representing the entire *tax-2* coding regions were determined.

tax-2 encoded a predicted protein of 800 amino acids with substantial structural and sequence similarity to the cyclic nucleotide-gated channels from vertebrate photoreceptors and olfactory neurons (Figure 1-2b). The overall structure consists of a non-conserved amino terminal region, a central region that includes 6 potential membrane-spanning domains, and a carboxy-terminal cyclic nucleotide-binding domain (Henn et al., 1995). Based on the presence of an asparagine residue at position 662, *tax-2* would be predicted to interact more strongly with cGMP than with cAMP (Varnum et al., 1995). *tax-2* was most similar to the beta subunit of the human rod channel, with which it shared 40% amino acid identity over the transmembrane domains and cyclic nucleotide binding domain. *tax-2* and the beta subunit of the rod channel were more similar to one another than either was to any other member of the channel family (Figure 1-2c).

To confirm the identification of the *tax-2* gene, the coding regions of the mutant alleles were sequenced. The weak allele *tax-2(p694)* was a deletion of the first exon and about 1.8 kb of upstream sequences (Figure 1-2a,b). Four of the other mutations were missense mutations in the potential membrane-spanning regions of *tax-2* (Figure 1-2b), including three mutations found within the predicted pore region. *tax-2(p691)* led to the substitution of a serine for a proline residue at position 426, *tax-2(ky139)* led to the substitution of a cysteine for an arginine residue at position 410, and *tax-2(ks31)* led to the substitution of an isoleucine for a threonine residue at position 427. *tax-2(p671)* was a missense mutation in the first membrane-spanning domain, leading to the substitution of an arginine for a cysteine at position 229. The

presence of these mutations at conserved positions suggests that the predicted pore region and membrane-spanning domains are essential for normal *tax-2* function, consistent with the prediction that it acts as part of a channel.

The *tax-4* gene encodes a predicted subunit of a cyclic nucleotide-gated channel that is most similar to the alpha subunits of the vertebrate rod and olfactory channels (Komatsu et al., pers. comm.). The phenotypes and expression patterns of *tax-2* and *tax-4* mutants are similar, suggesting that these two genes function in the same sensory neurons (see below).

tax-2 is expressed in thermosensory neurons and a subset of chemosensory neurons

To ask whether *tax-2* functioned within the sensory neurons or in the interneurons that mediate chemosensory behaviors, the expression of *tax-2* was examined. Fusions of *tax-2* to the green fluorescent protein (GFP) revealed expression of GFP in eleven classes of sensory neurons (Figure 1-3). *tax-2::GFP* expression was observed in all four types of neurons that were affected in *tax-2* mutants, including neurons required for thermotaxis, water-soluble chemotaxis, and volatile chemotaxis (AFD, ASE, ASK, and AWC). It was not expressed in sensory neurons whose function was intact in *tax-2* mutants, or in any non-sensory cell type.

The expression pattern suggests that *tax-2* acts cell-autonomously in the sensory cells whose function is compromised in these mutants. Support for this model is provided by analysis of the *tax-2* deletion mutation *p694*, which lacks the first exon and the upstream region of *tax-2*. A *tax-2Δ::GFP* fusion with a similar deletion was expressed in only seven classes of sensory neurons. The deleted fusion gene was expressed in the AWC neurons, whose function is normal in *p694* mutants, but not in the AFD or ASE neurons, whose function was disrupted by the *p694* deletion (Figure 1-3b). This

correlation is consistent with a direct requirement for *tax-2* expression within the affected sensory cell types.

Comparison of three *tax-2::GFP* fusion genes revealed two distinct regions that regulated *tax-2::GFP* expression in different neurons (Figures 2a, 3). An upstream element was required for expression in four cell types (ADE, AFD, ASE, BAG), while a region in the first intron was required for consistent expression in ASG, ASJ, ASK, and AWB. Either the upstream region or the first intron was sufficient for expression in ASI, AWC, and PQR.

To confirm these observations, two *tax-2* genomic clones were tested for rescue of different *tax-2* phenotypes (Figure 1-2a). Only a clone that included the upstream element rescued Cl- chemotaxis, consistent with the observation that the upstream element was required for ASE expression. However, a clone that lacked the first exon and upstream sequences could fully rescue benzaldehyde chemotaxis, consistent with the AWC expression of a similar *tax-2::GFP* fusion gene.

Interestingly, these results also indicate that the normal amino terminus of *tax-2* is not required for its olfactory function in AWC, since the first coding exon is deleted in *tax-2(p694)* and in the shorter *tax-2* rescuing fragment. The truncated *tax-2(p694)* protein might initiate at methionine 138 of *tax-2*, upstream of the first transmembrane domain. A short version of the rod beta channel that lacks much of its non-conserved amino terminus retains normal channel function when expressed in Xenopus oocytes (Korschen et al., 1995).

tax-2 and _tax-4_ affect axon outgrowth of some sensory neurons

All of the known defects in *tax-2* and *tax-4* mutants can be ascribed to defective function of the amphid chemosensory neurons. The amphids are a bilaterally symmetric pair of sensory organs in the head that each contain

twelve sensory neurons; the phasmid organs of the tail each contain two sensory neurons (Ward et al., 1975; Ware et al., 1975). The sensory neurons are bipolar neurons, with one axon, or presynaptic process, and one dendrite, which terminates in the sensory cilia (Figures 3,4). The axons of the amphid neurons extend to a central neuropil called the nerve ring, in which they synapse onto various target neurons. The phasmid axons synapse onto their targets in the ventral nerve cord neuropil.

Interestingly, defects in sensory axon development were observed in *tax-2* and *tax-4* mutants. The sensory neurons were examined using the dye DiO, which stains dendrites, cell bodies, and axons of six amphid neuron pairs and two phasmid neuron pairs (Herman and Hedgecock, 1990)(Figure 1-4a,d). The most common defect was the presence of one or more inappropriate posteriorly-directed amphid axons in the ventral nerve cord (Figure 1-4b). This defect was observed in 60%-90% of *tax-2* and *tax-4* mutant animals (Figure 1-4f). The process was assigned to the ASJ neurons by examining different subsets of axons with a set of GFP fusion genes (see Experimental Procedures).

In wild-type animals, the axons of the ASJ neurons terminate in the dorsal nerve ring. In *tax-2* and *tax-4* mutants, about 50% of the ASJ axons continued past their normal site of termination and extended into the ventral nerve cord. Furthermore, in 5% of *tax-2* and *tax-4* mutants, the initial outgrowth of the ASJ axon was posteriorly rather than ventrally directed (Figure 1-4c).

The six strong *tax-2* mutations showed comparable axon phenotypes, but the weak *tax-2* mutant *p694* did not display any ASJ developmental defects. In addition, both the full-length *tax-2* genomic clone and the clone with the deleted promoter rescued all ASJ developmental defects of *tax-*

2(p691) mutants. These results support the model that the phenotypes of *tax-2* are cell-autonomous in affected sensory neurons, since the *tax-2(p694)* deletion mutant should retain expression in ASJ (see above). Likewise, both *tax-2* clones that rescued the axon defects should be expressed in ASJ.

Defects were also observed in the ASE sensory neurons and the phasmid neurons. 45% of the ASE neurons in *tax-2(p691)* had both a normal axon and an extra process that extended posteriorly from the ASE cell body (data not shown). In 2-6% of the mutant animals (depending on the mutant allele) the phasmid processes failed to terminate at the proper position in the ventral nerve cord. Mutant phasmid axons could continue in the ventral nerve cord for up to twice their normal length (Figure 1-4d,e). However, many of the sensory neurons appeared to have normal axons in *tax-2* and *tax-4* mutants. In particular, the AWC, AFD and ASK axons were normal in the mutants, despite the compromised function of those sensory cell types (data not shown).

These results demonstrated that the cyclic nucleotide-gated channel affects both sensory function and outgrowth of some sensory cell axons. The timing of *tax-2* expression was consistent with functions in both development and transduction, since all *tax-2::GFP* fusion genes were expressed continuously from about mid-embryogenesis until the adult stage (data not shown). Transduction molecules should be found in the sensory cilia, while guidance molecules should act in the axon. To explore these possibilities further, the location of the Tax-2 protein was examined using an epitope-tagged protein. The *tax-2* rescuing fragment was fused to the green fluorescent protein at the 3' end of the *tax-2* coding region (Figure 1-2a). This Tax-2::GFP fusion gene fully rescued both the volatile chemotaxis defect and

the axon guidance defect of *tax-2* mutants, indicating that the protein was functional.

Strong Tax-2::GFP protein expression was observed both in the sensory cilia and in the axons of the chemosensory neurons (Figure 1-3c,d). Weaker fluorescence was visible in the dendrites and cell bodies. By contrast, unmodified GFP diffuses freely through the cell, and GFP-tagged *odr-10* or *sr* receptors are localized to the cilia and not the axons (Sengupta et al., 1996)(L. Tong, D. Tobin, and C.I.B., unpublished). In the axons, the Tax-2::GFP fusion protein was localized to the synapse-rich nerve ring and excluded from the amphid commissures, which lack synapses. The axon staining was visible as soon as Tax-2::GFP could be detected, but cilium staining was not visible until later in embryogenesis when cilia could be resolved (the pretzel stage).

***tax-2* and *tax-4* may function together in chemosensation and axon guidance**

The similar mutant phenotypes of *tax-2* and *tax-4* suggested that they might function together as subunits of a single channel. To determine whether the *tax-2* and *tax-4* mutants showed any genetic interaction or redundancy, axon morphology and chemotaxis were observed in *tax-2; tax-4* double mutants. In all cases, *tax-2; tax-4* double mutant strains had similar phenotypes to the *tax-2* and *tax-4* single mutants, and no new defects were apparent (Figure 1-5). In particular, the same subset of olfactory responses was abnormal, and there was no increase in the number of defective axons per animal compared to the single mutants. This result indicates that the channel subunits are not redundant with one another to any appreciable extent; rather, they seem to act in a single process.

To ask whether either gene could compensate for the absence of the other, we injected the *tax-4* genomic rescuing clone into *tax-2* mutants and vice versa. The transgenic animals generated in these experiments typically

contain hundreds of copies of the transgene, and express 10-20 times as much protein as is expressed from the endogenous gene ((Mello, 1991), A.V. Maricq and C.I.B, unpublished). We found that high expression of *tax-4* was able to rescue both the chemotaxis phenotype and the axon guidance phenotype of *tax-2* mutants (Figure 1-5). Thus, an alpha-like cyclic nucleotide-gated channel gene can bypass defects in a beta-like subunit when expressed at sufficiently high levels. The *tax-2* transgene did not ameliorate the *tax-4* mutant phenotype.

Discussion

A predicted cyclic nucleotide-gated channel acts in olfaction, salt sensation, and thermosensation

Cyclic nucleotide-gated channels are the major transduction channel in vertebrate olfactory neurons (Firestein et al., 1991; Nakamura and Gold, 1987). Our results implicate similar channels in C. elegans olfaction. Genetic characterization of *tax-2* and *tax-4* indicates that these two putative channel genes are essential for normal olfaction, and the Tax-2 protein is localized to the cilia where sensory transduction occurs. These observations suggest that similar channels are used in vertebrate and invertebrate olfaction. A Drosophila cyclic nucleotide-gated channel is expressed in the antennae, which contain fly olfactory neurons (Baumann et al., 1994); although its function is unknown, its localization is consistent with a role in olfaction.

While the AWC olfactory neurons require *tax-2* and *tax-4* function, the AWA olfactory neurons neither require nor express these two genes. Thus, different olfactory channels may operate in different olfactory cell types.

Interestingly, our results also implicate cyclic nucleotide-gated channels in salt taste and thermosensation. *tax-2* and *tax-4* mutants are defective in their ability to sense both Na^+ ions and Cl^- ions, and *tax-2* is expressed in the neurons that detect these ions (ASE)(Bargmann and Horvitz, 1991). In vertebrate salt sensation, an amiloride-sensitive sodium channel accounts for some but not all aspects of salt taste (Avenet and Lindemann, 1988), but the other components of this process are unknown. *tax-2* and *tax-4* mutants are also defective in thermotaxis, and *tax-2* is expressed in the AFD thermosensory neurons, suggesting that the channel acts in thermosensation (Mori and Ohshima, 1995). Little is known about thermotransduction; these results suggest that this sensory modality and many others share a common type of channel.

The signalling pathways from the receptor proteins to the channel in C. elegans are unknown. By sequence, the channel appears most likely to be cGMP-activated, suggesting that it could respond to a phosphodiesterase cascade like that used in vertebrate vision (Stryer, 1991). However, further electrophysiological and genetic characterization of olfaction in C. elegans is needed to elucidate these pathways.

The Tax-2 and Tax-4 proteins have similar functions and appear to be expressed mostly in the same sensory neurons (Komatsu et al., pers. comm.), suggesting that they might contribute to a single heteromeric channel. *tax-2* and *tax-4* mutants have similar behavioral and developmental defects, and *tax-2 tax-4* double mutants are indistinguishable from the single mutants. Since molecular analysis is consistent with the existing alleles being loss of function alleles (particularly *tax-2(p694)* and *tax-4(p678))*, both subunits of the proposed C. elegans channel may be required for its function or proper regulation *in vivo*. Nonetheless, high levels of *tax-4* expression bypass the

requirement for *tax-2*, suggesting that the alpha-like *tax-4* subunit can either function alone to a limited extent or provide some *tax-2* function. Similarly, while most vertebrate cyclic nucleotide-gated channels are probably heteromeric *in vivo*, the alpha subunits are capable of forming channels on their own when expressed at high levels (Dhallan et al., 1990; Kaupp et al., 1989). Beta subunits are required for the channels to show normal kinetics and nucleotide sensitivity (Bradley et al., 1994; Liman and Buck, 1994; Yao et al., 1995).

Axon guidance and termination are regulated by a cyclic nucleotide-gated channel

The *tax-2* and *tax-4* mutants reveal an unexpected function for the cyclic nucleotide-gated channel in the development of a few sensory neurons. C. elegans neurons have highly stereotyped axon morphologies in wild-type animals. In *tax-2* and *tax-4* mutants the ASJ neurons frequently grow well beyond their normal stopping point, while the ASE neurons have an extra process in an ectopic location. Since the mutant axons are more extensive than wild-type axons, the normal activity of the channel must inhibit or limit axon outgrowth in inappropriate regions.

Only a subset of the neurons whose sensory function is defective have abnormal axons in *tax-2* and *tax-4* mutants. In particular, the ASK, AWC, and AFD neurons, whose functions are essential for chemotaxis and thermotaxis, do not have any obvious developmental defects. The *tax-2* gene product is required during the adult stage for normal AWC olfactory behavior, consistent with a direct role of the channel in AWC olfaction (C.M.C. et al., in preparation). We suggest that the channel functions primarily in sensory transduction, but has additional developmental effects in some neurons.

tax-2 and *tax-4* might have a direct role in guidance, or they might act indirectly by regulating sensory neuron activity. Although activity-dependent processes have not been previously described in C. elegans neuronal development, they drive a late stage of axon refinement in other sensory systems (Shatz and Stryker, 1988). In contrast with the late time of action of neuronal activity in other systems, the ASJ axon in *tax-2* and *tax-4* mutants is sometimes misrouted from the first point that the axon leaves the cell body, at a time before normal sensory stimuli are present and before synapses are made. In addition, the presence of the Tax-2::GFP channel protein in the synaptic regions of sensory axons raises the possibility that the channel acts in axons during their development.

During olfaction, it is likely that signal transduction is initiated through binding of ligands to seven transmembrane receptors such as the *sr* genes and *odr-10*-like genes (Sengupta et al., 1996; Troemel et al., 1995). However, the known receptors of this family appear to be localized to the sensory cilia, far from the axons (Sengupta et al., 1996)(L. Tong, D. Tobin, and C.I.B., unpublished observations). If *tax-2* and *tax-4* act in the axons, relevant cGMP or cAMP levels might be regulated by other G protein-coupled receptors, by ligand-activated transmembrane guanylyl cyclases, or by gases such as nitric oxide.

Indirect evidence from other systems suggests that cyclic nucleotides could function during synapse formation. cGMP suppresses synapse formation at the vertebrate neuromuscular junction (Wang et al., 1995) and potentiates synaptic function in hippocampus and retina (Arancio et al., 1995; Rieke and Schwartz, 1994; Zhuo et al., 1994); cAMP levels modify axon morphology in Aplysia and Drosophila (Schacher et al., 1993; Zhong et al., 1992). Cyclic nucleotide-gated channels might contribute to these

developmental functions by allowing calcium entry into neuronal growth cones (Frings et al., 1995). Defects in synapse formation can lead to axonal defects in vertebrate neurons (Henderson et al., 1983); similar mechanisms might contribute to the axonal abnormalities in *tax-2* and *tax-4* mutants.

Ion channels are widely studied for their effects on neuronal function, but increasing evidence indicates that they play important roles in neuronal development. A G protein-regulated channel encoded by the mouse *weaver* gene acts in neuronal differentiation and survival (Patil et al., 1995). Mutations in several voltage-activated channels modify synaptic arbors of motor neurons in Drosophila (Budnik et al., 1990), and some *in vitro* models of neurite outgrowth depend on the activity of voltage-activated calcium channels (Williams et al., 1992). Our results show that a cyclic nucleotide-gated channel has both a behavioral function and a critical developmental function in axon outgrowth *in vivo*. We speculate that regulation of this bifunctional channel could coordinate sensory function and sensory connectivity throughout the animal's life.

Acknowledgments

We thank Ikue Mori for stimulating discussions and for sharing her data with us prior to publication, Wallace Marshall for generating the high magnification image of Tax-2::GFP protein, Didier Stainier, Lily Jan, Cynthia Kenyon, Marc Tessier-Lavigne, Jen Zallen, David Tobin and Noelle Dwyer for their comments on this manuscript, Kate Wesseling, Shannon Grantner and Liqin Tong for excellent technical support, Amy Kistler for isolating *ky89*, and Andrew Fire for the expression vectors. Some strains were provided by The Caenorhabditis Genetics Center. This work was supported by NIH grant

DC01393 and funds from the Lucille P. Markey Trust and the Searle Scholars Program. C.M.C. was supported by a predoctoral fellowship from the National Science Foundation. C.I.B. is an Assistant Investigator of the Howard Hughes Medical Institute.

Experimental Procedures

Strain and genetics.

Wild-type worms were C. elegans variety Bristol, strain N2. Worms were grown on plates, using standard methods (Brenner, 1974). The following strains were used in this work: PR691 *tax-2(p691)* I, PR671 *tax-2(p671)* I, PR694 *tax-2(p694)* I, CX139 *tax-2(ky139)* I, FK31 *tax-2(ks31)* I, FK10 *tax-2(ks10)* I, FK15 *tax-2(ks15)* I, PR678 *tax-4(p678)* III, and CX89 *tax-4(ky89)III.* Double mutant strains without additional marker mutations were constructed using standard genetic methods and verified by complementation testing.

Behavioral assays

Population chemotaxis assays were performed as described (Bargmann et al., 1993). Chemotaxis index was calculated as follows: CI= ($N_{attractant}$-$N_{counterattractant}$)/Total N. Osmotic avoidance assays were performed as described (Vowels and Thomas, 1994). Negative chemotaxis to 1-octanol and 2-nonanone was tested on square assay plates; in other respects, this population chemotaxis assay is similar to the positive chemotaxis assays (B.E. Kimmel and C.I.B., unpublished). Long-range negative chemotaxis is distinct from the acute reversal seen in response to a pulse of 1-octanol (Troemel et al., 1995).

DiO staining and GFP visualization of chemosensory neurons.

DiO staining was performed essentially as described (Herman and Hedgecock, 1990), except that animals were stained for 16-18 hours on a rotator in the presence of 1 microliter of concentrated *E. coli* per ml of M9 buffer. Stained animals were viewed by fluorescence microscopy using Zeiss long-pass FITC filters. An animal was scored as having defective amphids if any amphid neuron had abnormal axons (see Figure 1-3).

A set of GFP fusion genes were used to identify the affected DiO-staining neuron, and to visualize other sensory neurons (particularly AWC, AFD, ASE, and ASK). These included a *ceh-23::GFP* fusion gene, which stains AWC, AFD, ASE, ADF, ASG, ASH, and ADL neurons ((Wang, 1993) and J. Zallen and C.I.B., unpublished), *srd-1::GFP* (ASI) (Troemel et al., 1995), *M7::GFP* (ASI)(E. Troemel and C.I.B., unpublished), *C42::GFP* (AWB)(E. Troemel and C.I.B., unpublished), and *tax-2::GFP* fusion genes (see below) including *tax-2Δ::GFP* (AWB, AWC, ASG, ASI, ASJ, and occasionally ASK) and *tax-2p::GFP* (AWC, AFD, ASE, ASG, ADE, and BAG).

High-resolution three dimensional images of Tax-2::GFP protein in the cilia were acquired using wide-field fluorescence microscopy and refined by constrained iterative deconvolution (Hiraoka et al., 1990).

Molecular biology methods

Southern blots, subcloning and general DNA manipulations were carried out as described (Sambrook et al., 1989). Nested deletions for DNA sequencing were generated using Exonuclease III (New England Biolabs). Subclones were sequenced using the *fmol* sequencing system (Promega). Sequence analysis was performed using Geneworks (Intelligenetics). Sequence comparisons were carried out using the BLAST network service (Altschul, 1990) and

sequence alignments were produced using the CLUSTAL W program (Thompson et al., 1994).

Germline transformation

Germline transformation (Mello, 1991) was performed by coinjecting test DNA at a concentration of 10-40 ug/ml and marker DNA at a concentration of 60 ug/ml into the gonad of animals. For *tax-2* injections, the *tax-2(p691)* strain was injected with *glr-1::GFP* marker DNA (Maricq et al., 1995) and transgenic animals were recognized on the basis of neuronal GFP expression. For *tax-4* injections, a *tax-4; lin-15(n765ts)* strain was injected with JM23 *lin-15* marker DNA and transgenic animals were recognized by rescue of the *lin-15* multi-vulval phenotype at 20°C (Huang et al., 1994). Multiple independent lines were established from each injection.

Genomic localization of *tax-2*

tax-2 had been incorrectly mapped to chromosome II, but we found that *p691* was linked to chromosome I, between the two cloned genes *unc-29* and *lin-11;* from a strain of genotype *tax-2/unc-29 lin-11*, 3/15 Lin non-Unc recombinants segregated *tax-2* and 57/60 Unc non-Lin segregated *tax-2*. Cosmid clones from this interval were tested for their ability to complement the *tax-2* mutant phenotype in transgenic worms. The cosmid T18D4 rescued the *tax-2(p691)* benzaldehyde chemotaxis defect and the axon outgrowth phenotype, as did a 6.5 kb HindIII fragment of T18D4. The 6.5 kb fragment was sequenced on one strand, revealing one open reading frame. A frame-shift mutation was introduced into the 6.5 kb HindIII fragment by digesting with BsaB1 and inserting a linker with the sequence 5'-CCCCCGGGGG-3' (NewEngland BioLabs). This insertion added 8 amino acids after position 384 followed by a

stop codon at position 393, effectively deleting transmembrane domains 4 and 5, the presumed pore and cyclic nucleotide-binding regions and the COOH-terminus. This construct failed to rescue the *tax-2(p691)* mutant phenotypes. A genomic clone containing the entire coding region of *tax-2* plus 1.8 kb of upstream sequences was constructed by adding a 2.2 kb BglI-HindIII fragment 5' to the 6.5 Kb HindIII fragment.

Isolation and characterization of cDNAs

The 6.5 kb HindIII genomic fragment was used to screen approximately 1.1 X 10^6 plaques of a mixed-stage worm cDNA library (Barstead, 1989). Three positive clones were identified and DNA sequencing revealed that they were partial cDNAs beginning at amino acid positions 399, 492 and 527 and continuing to the 3' end. The sequences of the three clones were identical in overlapping regions. RT-PCR was used to isolate the remainder of the cDNA. Total worm RNA was prepared from mixed-stage N2 worms by LiCl precipitation (M. Finney, personal communication). First-strand cDNA was synthesized using an oligonucleotide in exon 8 and was used as a template for subsequent amplification using nested oligonucleotides. The conditions used for PCR were the following: 30s at 95°C, 1 min. at 52°C, and 2 minutes at 72°C for 30 or 35 cycles followed by 10 min. at 72°C. One band of 661 bp was detected and sequenced. In a second experiment, first-strand cDNA was synthesized an oligonucleotide in exon 4 and was used as a template for subsequent amplification using oligonucleotides that detect SL-1 and SL-2 *trans*-spliced mRNAs (Huang and Hirsh, 1989). Reactions were subjected to additional rounds of amplification using nested oligonucleotides. A 704 bp band was detected in samples amplified using SL-1. No bands were detected in reactions using SL-2. All cDNAs were sequenced on both strands.

Sequencing of *tax-2* alleles

Genomic DNA was isolated from *N2, tax-2(p694), tax-2(p671), tax-2(p691), tax-2(ks10), tax-2(ks15), tax-2(ks31)* and *tax-2(ky139)* worms as described (Klein, 1993). Fragments of *tax-2* genomic DNA were PCR-amplified using primers within introns and sequenced using ^{33}P end-labelled primers. At least one strand of the open reading frame of all fourteen exons, their splice junctions, and approximately 30 bp beyond the 3' and 5' ends of open reading frames were sequenced. The exons containing the mutations were sequenced on both strands. PCR and Southern blot analysis of N2 and *tax-2(p694)* genomic DNA revealed an approximately 2 kb deletion encompassing exon 1 and ~1.6 kb 5' of the *tax-2* coding region. To define the right break-point of the deletion, primers flanking this region were used to amplify and sequence the region from *tax-2(p694).*

***tax-2::GFP* expression**

Translational fusions between *tax-2* and GFP were constructed using expression vectors generously provided by A. Fire (A. Fire, S. Xu, J. Ahnn, and G. Seydoux, personal communication). The *tax-2* promoter construct was constructed by amplifying 1.8 kb of *tax-2* upstream sequence and the first three amino acids of *tax-2* from genomic DNA, using the Expand PCR kit (Boeringer Mannheim). The conditions used for PCR were the following: 30 sec. at 95°C, 1 min. at 52°C, and 2 min. at 72°C for 20 cycles, followed by 10 min. at 72°C. This fragment was digested with BamHI and SalI and ligated into the GFP expression vector pPD95.79 to make P[*tax-2p::GFP].* To make P[*tax-2::GFP],* the BglI-SalI genomic fragment containing ~1.8 kb of *tax-2* upstream sequences and 215 amino acids of *tax-2* protein was ligated into the

GFP expression vector pPD95.77. To make P[*tax-2Δ::GFP*], the HindIII-SalI genomic fragment containing part of intron 1 and 188 amino acids of *tax-2* coding region was ligated into pPD95.77. Constructs were co-injected with plasmid pJM23*(lin-15)* into the gonads of *lin-15(n765ts)* animals and *lin-15(+)* transformed progeny were viewed using fluorescence microscopy.

The GFP-tagged Tax-2 protein was constructed by ligating the 4.2 kb HindIII-BamHI genomic fragment into the GFP expression vector pPD95.75. This construct was injected into *lin-15(n765ts)* animals with pJM23 as described above. The Tax-2-GFP tagged gene was also injected into *tax-2(p691)* animals using *glr-1::GFP* co-injection marker, and GFP-positive transformed progeny were assayed for rescue of *tax-2* mutant phenotypes.

Expression of *tax-4* in *tax-2* mutants

The *tax-4* genomic rescuing clone pSF12 (Komatsu et al., accompanying manuscript) and co-injection marker *glr-1::GFP* were injected into *tax-2(p691)* mutant worms. The *tax-2* full-length genomic rescuing clone was injected into *tax-4(n678);lin-15(n765)* mutant worms with pJM23. Transgenic strains were identified by GFP fluorescence or rescue of the *lin-15* multi-vulval phenotype, respectively.

Generating the *tax-2(p691)* mutant allele

To ask whether *tax-2* mutations poison wild-type *tax-4* function, a clone bearing the *tax-2(p691)* mutant allele was injected into wild-type animals, so that the transgenic animals would express a large excess of defective beta subunit relative to normal beta subunit. These animals responded normally to odorants, and had normal sensory axons. Therefore,

the level of overexpression provided by the transgene was not sufficient to poison the function of the endogenous *tax-2* and *tax-4* genes.

PCR was used to amplify the full *tax-2* coding region and about 1.8 kb of upstream sequences from *tax-2(p691)* genomic DNA, using the Expand kit (Boehringer Mannheim). The conditions used for PCR were the following: 30s at 95°C, 1 min. at 54°C, and 8 minutes at 72°C for 30 or 35 cycles followed by 10 min. at 72°C. The 6.4 kb fragment was gel-purified using Gene Clean (Bio101) and injected into *lin-15(n765ts)* animals with pJM23. Transformed progeny were assayed for chemotaxis and axon outgrowth phenotypes.

Figure legends

Figure 1-1: Responses of *tax-2* Mutants to Volatile Odorants
Each data point represents the average of at least 8 independent assays using approximately 100-200 well-fed adult animals per assay (error bars equal the SEM). The dilution of odorants in ethanol were the following: 1:200 benzaldehyde, 1:100 isoamyl alcohol, 10 mg/ml pyrazine, 1:1000 diacetyl and 1:1000 2,4,5-trimethylthiazole.

Figure 1-2: Localization and Sequence Analysis of *tax-2*
(A) Localization of the *tax-2* gene on the physical map. Cosmid T18D4 and subclones were tested for rescue of the chemotaxis and amphid axon defects of *tax-2(p691)*. For each experiment, the number of independent transformed lines that rescued the *tax-2* mutant phenotype is given as a fraction of the total number of lines tested. Rescue was scored if a line had a chemotaxis index greater than or equal to 0.6, or had >50% normal amphid axon morphology. Inset diagram shows *tax-2* genomic organization with the

location of the *p694* deletion and the *p671*, *ky139*, *p691*, and *ks31* mutations indicated. Boxes depict exons. GFP expression plasmids are described in Experimental Procedures. An inverted triangle indicates the restriction site at which a frameshift mutation was created. Abbreviations: B, BamHI; Bg, BglII; Bs, BsaBI; H, HindIII; S, SalI.

(B) Predicted amino acid sequence of the *tax*-2 cDNA and sequence comparisons. The comparison between the predicted amino acid sequences of the *tax*-2 cDNA, the human rod cyclic nucleotide-gated channel beta subunit (hRCNC2) and the rat olfactory cyclic nucleotide-gated channel alpha subunit (rOCNC1) is shown. Identical residues are shaded. Amino acids are numbered beginning at the first methionine. Predicted transmembrane domains and the cyclic-nucleotide binding domain are underlined. The location of the *p694* deletion and the *p671*, *ky139*, *p691* and *ks31* mutations are indicated along with the predicted amino acid alterations. The predicted ATG used in the *p694* deletion mutant and in clone p[*tax-2Δ::GFP*] (Figure 1-2b) is marked by an asterisk.

(C) A rooted parsimonious tree of cyclic nucleotide-gated channel protein sequences from the first transmembrane domain through the cyclic nucleotide-binding site. Tree was calculated using the Phylogeny Inference Package of programs (Felsenfeld, 1989). Prefixes: h, human; r, rat; f, catfish.

Figure 1-3: *tax*-2 Protein is Expressed in Sensory Neurons and is Localized to Both the Sensory Cilia and the Axons

(A) GFP expression driven by the *tax-2::GFP* construct, which includes the upstream sequences and the first intron (see Figure 1-2b). Left-lateral view of a transgenic worm showing the GFP-expressing AWC, AFD, ASE, ASG, ASJ, ADE, and BAG neurons. The GFP-expressing ASK, ASI, and AWB neurons

are out of this plane of focus. A construct which contained only the upstream sequences drove GFP expression in the neurons AWC, AFD, ASE, ASI, ADE, BAG, and occasionally ASK (Data not shown). All constructs were expressed occasionally in the tail sensory neuron PQR. Anterior is to the left and dorsal is up.

(B) GFP expression driven by the *tax-2Δ::GFP* construct, which lacks the promoter and most of the first intron (mimicking the *tax-2(p694)* deletion; see Figure 1-2b). Left-lateral view of a transgenic worm showing the GFP-expressing neurons AWB, AWC, ASG, ASI, ASK, and ASJ. The positions of the sensory neurons are diagrammed at right. Anterior is to the left and dorsal is up.

(C) Localization of the Tax-2::GFP tagged protein. Left-lateral view of a transgenic animal expressing the GFP-tagged *tax-2* protein. Intense staining in the sensory cilia and axons is diagrammed in black while weaker staining in the dendrites and cell bodies is diagrammed in gray. Anterior is at left and dorsal is up.

(D) Higher magnification view of Tax-2::GFP in the sensory cilia. Dorsal view of the two bilaterally-symmetrical AWC sensory cilia showing expression of the tagged Tax-2 protein, generated by constrained iterative deconvolution. Other sensory cilia are out of the plane of focus. Anterior is at the top. Diagrammed dots indicate punctate staining in the dendrites. Scale bar = 5 um.

Figure 1-4: Developmental Defects of *tax-2* and *tax-4* Mutants Visualized By DiO Staining

(A) DiO staining of wild-type animal. Left-lateral view of one amphid showing DiO staining of dendrites, cell bodies and axons of 6 amphid

neurons. Positions of the staining neurons are diagrammed. The normal position of the neuron ASJ is marked. Some DiO staining is observed in the gut of the animal. In all cases, anterior is to the left and dorsal is up.
(B) DiO staining of a *tax-2* mutant animal. Left-lateral view of a DiO-stained *tax-2* mutant animal, showing an aberrant amphid neuron process projecting posteriorly from the nerve ring. *tax-4* animals have an identical phenotype.
(C) DiO staining of a *tax-2* mutant animal. Left-lateral view of a DiO-stained *tax-2* mutant animal, showing an aberrant process projecting laterally from the ASJ neuron into the posterior body region. *tax-4* animals have an identical phenotype.
(D) DiO staining of wild-type phasmid neurons. Left-lateral view of one phasmid sensory organ showing DiO staining of dendrites, cell bodies and axons of 2 phasmid sensory neurons. Positions of the staining neurons are diagrammed. The normal termination point of the phasmid axons is marked.
(E) DiO staining of *tax-2* mutant animals. Left-lateral view of a DiO-stained *tax-2* mutant phasmid. The normal termination point of the phasmid axon is indicated. The *tax-4* mutant phenotype is identical.
(F) Percent normal amphids in *tax-2* and *tax-4* mutants. For each point, 200-700 DiO-stained worms were viewed (error bars denote the 95% confidence level). An amphid was scored as defective if any amphid neuron had a defect.

Figure 1-5. Chemotaxis and Axon Guidance Defects of *tax-2; tax-4* Double Mutants
(A) Response of *tax-2; tax-4* double mutant combinations to volatile odorants. Each data point represents the average of 4-8 independent assays using approximately 100-200 animals per assay (error bars equal the SEM). The

dilution of odorants in ethanol were the following: 1:200 benzaldehyde, 1:100 isoamyl alcohol, 10 mg/ml pyrazine, 1:1000 diacetyl and 1:1000 2,4,5-trimethylthiazole.
(B) Amphid axon defects of *tax-2; tax-4* double mutants. Data points refer to the percentage of normal amphids (error bars denote the 95% confidence level). For each point, 200-700 DiO-stained worms were viewed. An amphid was scored as defective if any amphid neuron had a defect.

Figure 1-6: *tax-4* Overexpression Rescues *tax-2* Mutant Phenotypes
(A) Benzaldehyde chemotaxis of *tax-2(p691)* animals overexpressing *tax-4* genomic DNA. Each data point represents the average of 8-10 independent assays using approximately 100-200 animals per assay (error bars equal the SEM). *kyEx131, kyEx142, and kyEx143* are independent transgenic lines carrying extrachromosomal arrays of the *tax-4* rescuing clone and the co-injection marker. NaCl chemotaxis was also rescued in the transgenic strains (data not shown). Overexpression of p[*tax-2*] in *tax-4(p678)* did not rescue the *tax-4* chemotaxis phenotypes (data not shown).
(B) Amphid axon defects of *tax-2(p691)* animals overexpressing *tax-4* genomic DNA. Data points refer to the percentage of normal amphid axons (error bars equal the 95% confidence level). For each point, 200 DiO-stained worms were viewed. An amphid was scored as defective if any amphid neuron had a defect. Overexpression of the *tax-2* genomic DNA in *tax-4(p678)* did not rescue the *tax-4* amphid neuron defects (data not shown).

Table 1-1: *tax-2* and *tax-4* mutant animals have behavioral defects that are similar to the loss of some amphid neuron functions.

Amphid neuron	Known function	*tax-2/tax-4* phenotype	*tax-2(p694)* phenotype
AWA	Pyrazine, diacetyl, trimethy-thiazole chemotaxis[a]	+	+
AWC	Benzaldehyde, isoamyl alcohol, 2-butanone, trimethythiazole chemotaxis[a]	-	+
AFD	Thermotaxis[b]	-	-
ASE	Chemotaxis to water-soluble compounds (major role)[c]	- Axon morphology abnormal	-
ASG	Chemotaxis to water-soluble compounds (minor role); Regulation of dauer formation (minor role)[c,d]	unknown	unknown
ASH	Osmotic avoidance; Nose-touch avoidance[e]	+	+
ASJ	Regulation of dauer recovery[d]	Axon morphology abnormal	+
ASK	Lysine chemotaxis[c]	-	N.D.

The functions of some amphid sensory neurons determined by laser ablation experiments. N.D. = not determined.

[a]Bargmann et al. (1993)
[b]Mori and Oshima (1995)
[c] Bargmann and Horvitz (1991a)
[d]Bargmann and Horvitz (1991b)
[e]Kaplan and Horvitz (1993)

Figure 1-1

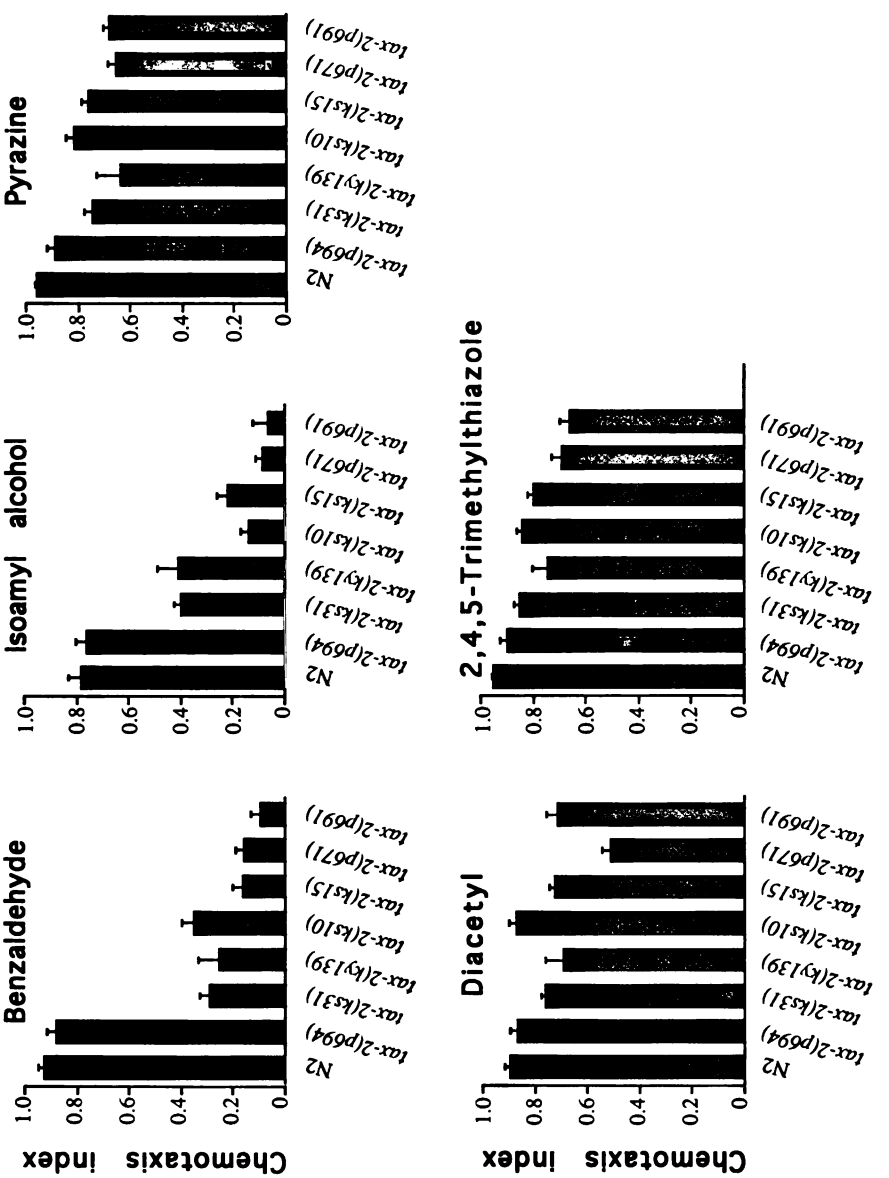
Chemotaxis index
Benzaldehyde
Isoamyl alcohol
Pyrazine
Diacetyl
2,4,5-Trimethylthiazole
1.0
0.8
0.6
0.4
0.2
0
N2
tax-2(p694)
tax-2(ks31)
tax-2(ky139)
tax-2(ks10)
tax-2(ks15)
tax-2(p671)
tax-2(p691)

Figure 1-2A

A.

clone		Rescue		
		Benzaldehyde chemotaxis	Chloride chemotaxis	Amphid axon morphology
cosmid T18D4	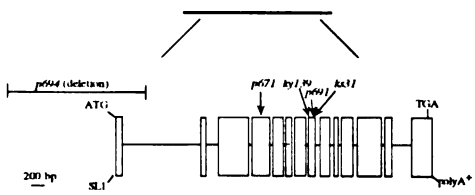	2/3	N.D.	2/3
p[*tax-2*]	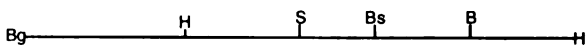	2/2	2/2	2/2
p[*tax-2p::GFP*]	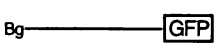			
p[*tax-2::GFP*]	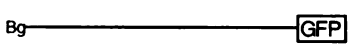			
p[*tax-2* Δ]	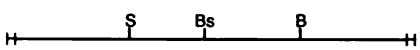	6/6	0/6	6/6
p[*tax-2* Δ*::GFP*]	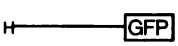			
		0/7	N.D.	N.D.
	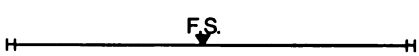	0/4	N.D.	N.D.
p[Tax-2::GFP]	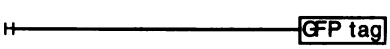	4/4	0/4	4/4
	no DNA injected	none	none	none
	glr-1::gfp marker DNA alone	0/10	N.D.	0/10

Figure 1-2b

p694 deletion
TAX-2
hRCNC2
rOCNC1
p671C→R
S1
S2
S3
S4
ky139R→C
S5
p691P→S ks31T→I
PORE
S6
CYCLIC NUCLEOTIDE BINDING REGION

Figure 1-2C

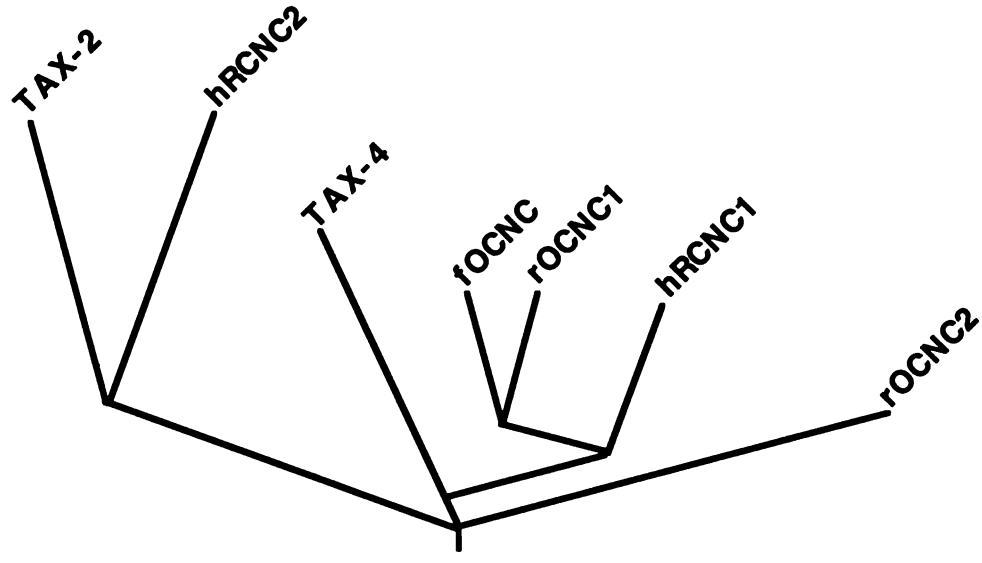

Figure 1-3

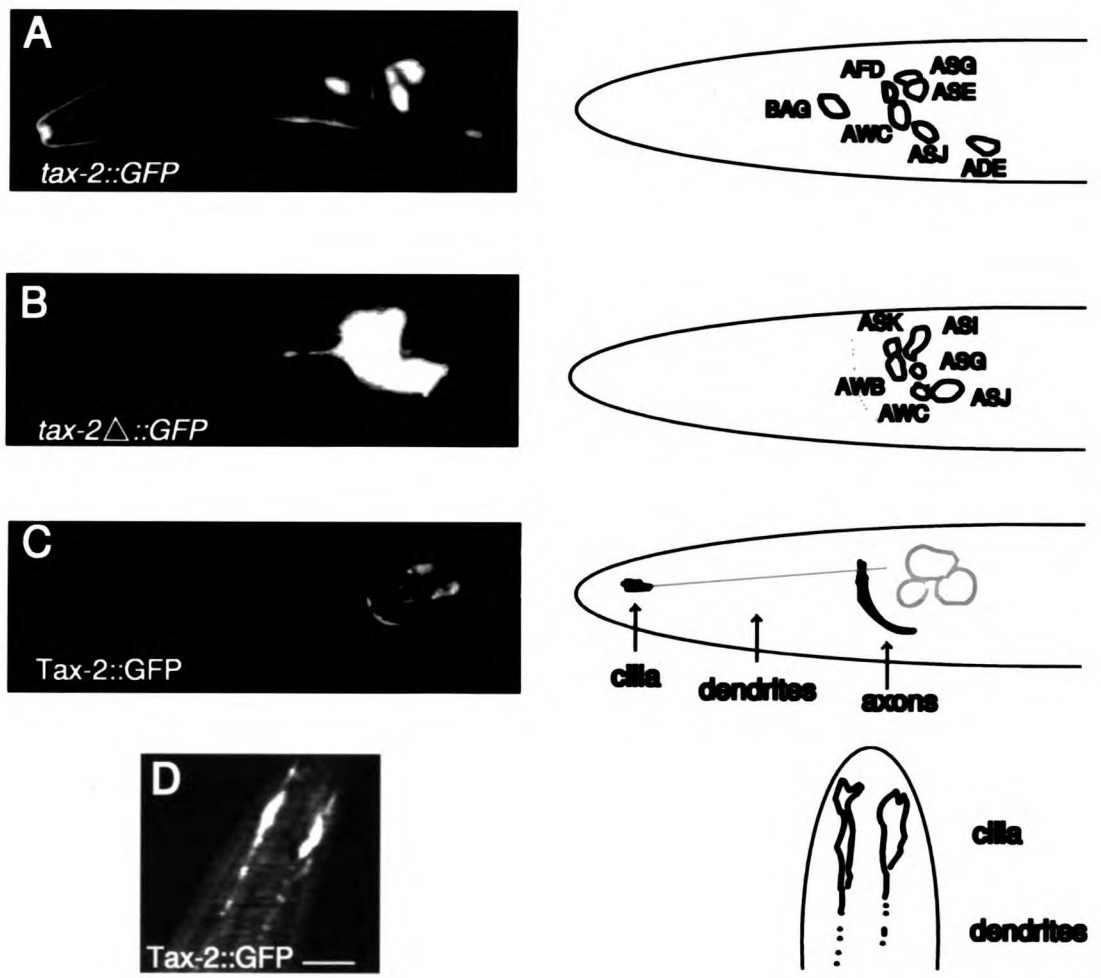
A
tax-2::GFP
AFD
ASG
ASE
BAG
AWC
ASJ
ADE
B
tax-2△::GFP
ASK
ASI
ASG
AWB
AWC
ASJ
C
Tax-2::GFP
cilia
dendrites
axons
D
Tax-2::GFP
cilia
dendrites

Figure 1-4

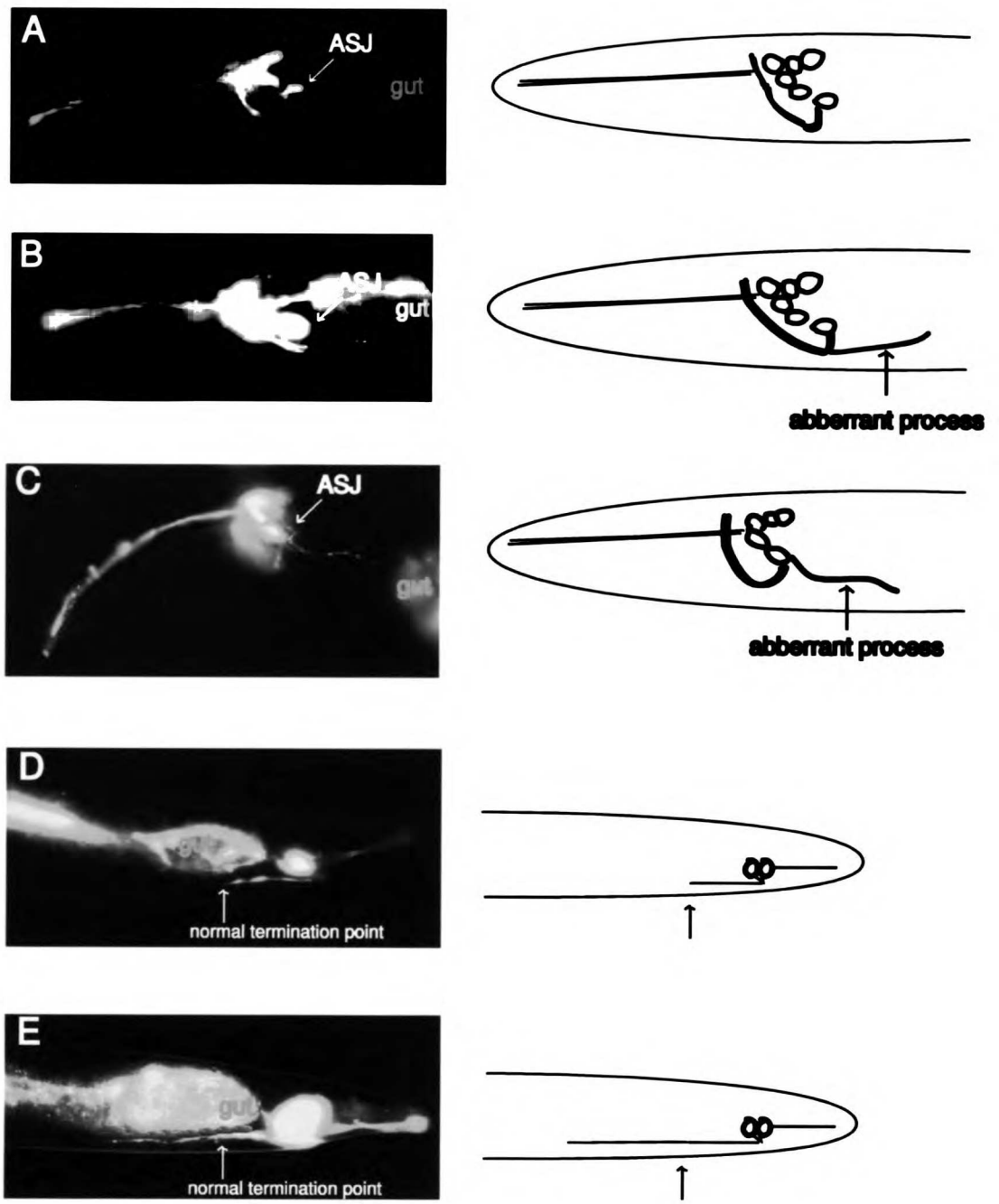
A
ASJ
gut
B
ASJ
gut
abberrant process
C
ASJ
gut
abberrant process
D
normal termination point
E
gut
normal termination point

Figure 1-4F

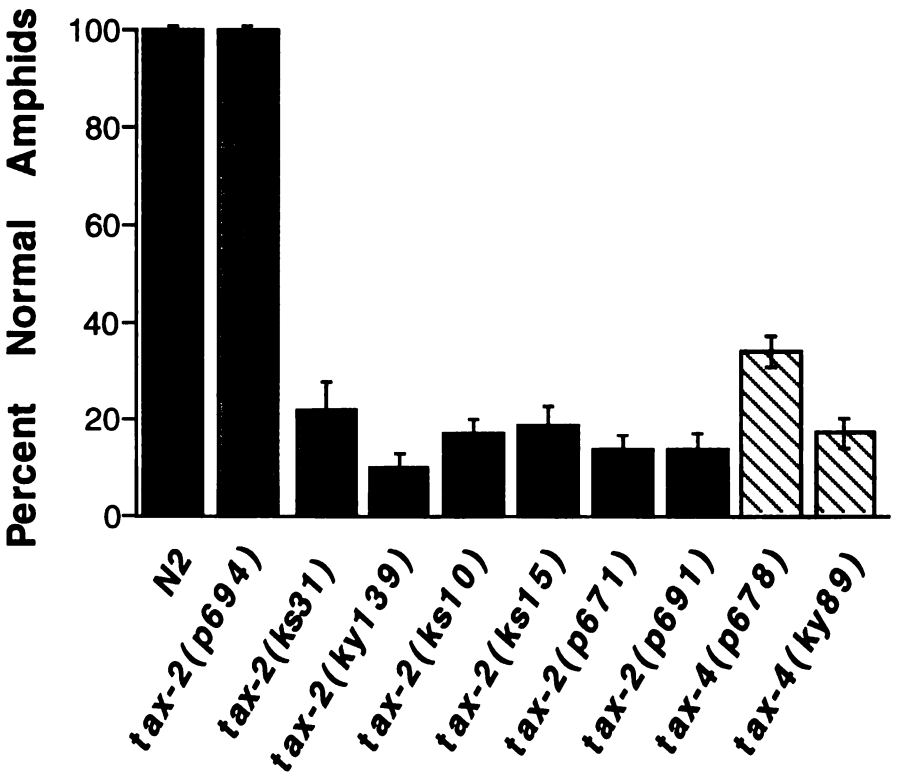
Percent Normal Amphids
100
80
60
40
20
0
N2
tax-2(p694)
tax-2(ks31)
tax-2(ky139)
tax-2(ks10)
tax-2(ks15)
tax-2(p671)
tax-2(p691)
tax-4(p678)
tax-4(ky89)

Figure 1-5

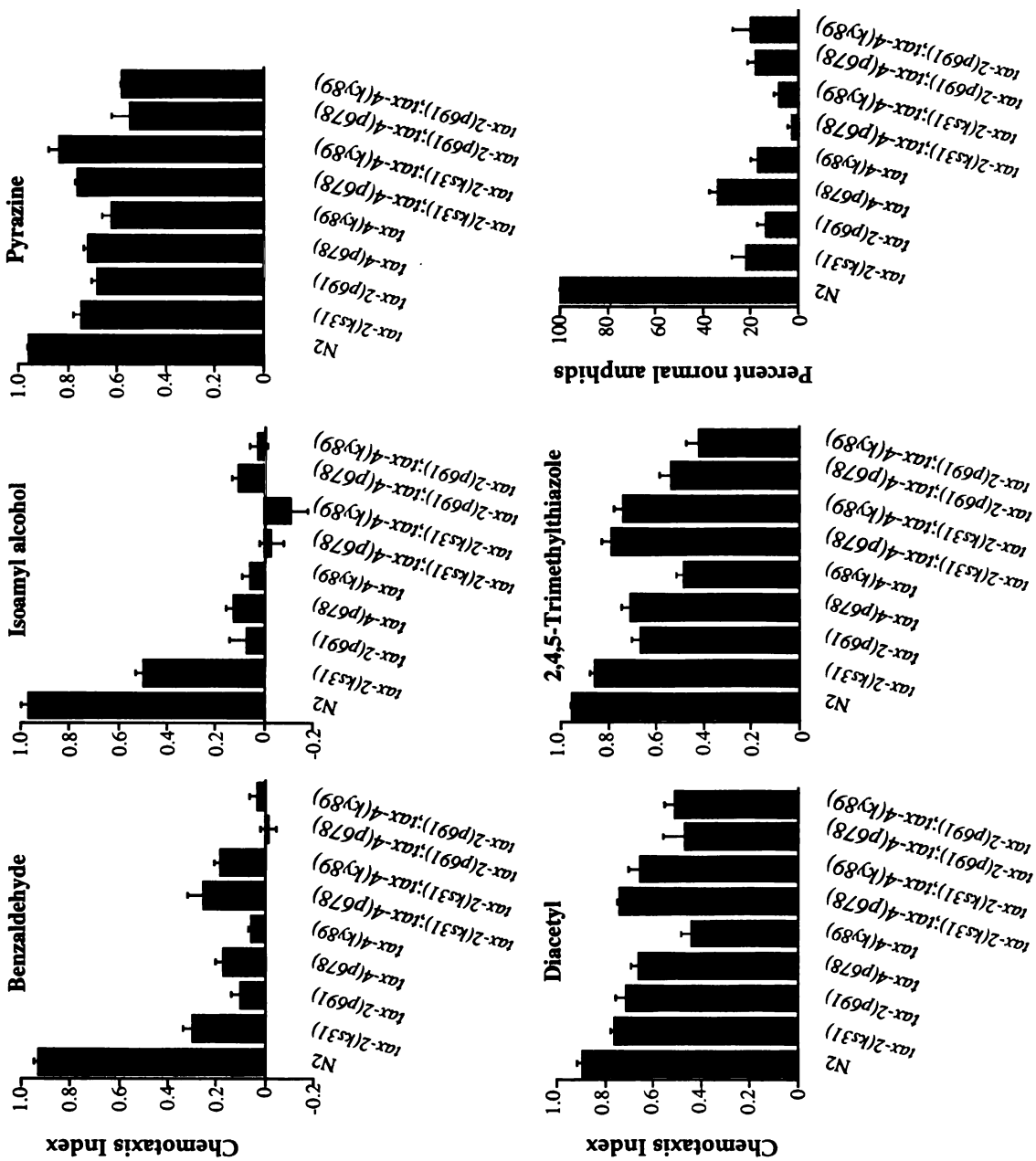
Chemotaxis Index
Benzaldehyde
Isoamyl alcohol
Pyrazine
Diacetyl
2,4,5-Trimethylthiazole
Percent normal amphids
N2
tax-2(ks31)
tax-2(p691)
tax-4(p678)
tax-4(ky89)
tax-2(ks31);tax-4(p678)
tax-2(ks31);tax-4(ky89)
tax-2(p691);tax-4(p678)
tax-2(p691);tax-4(ky89)

Figure 1-6

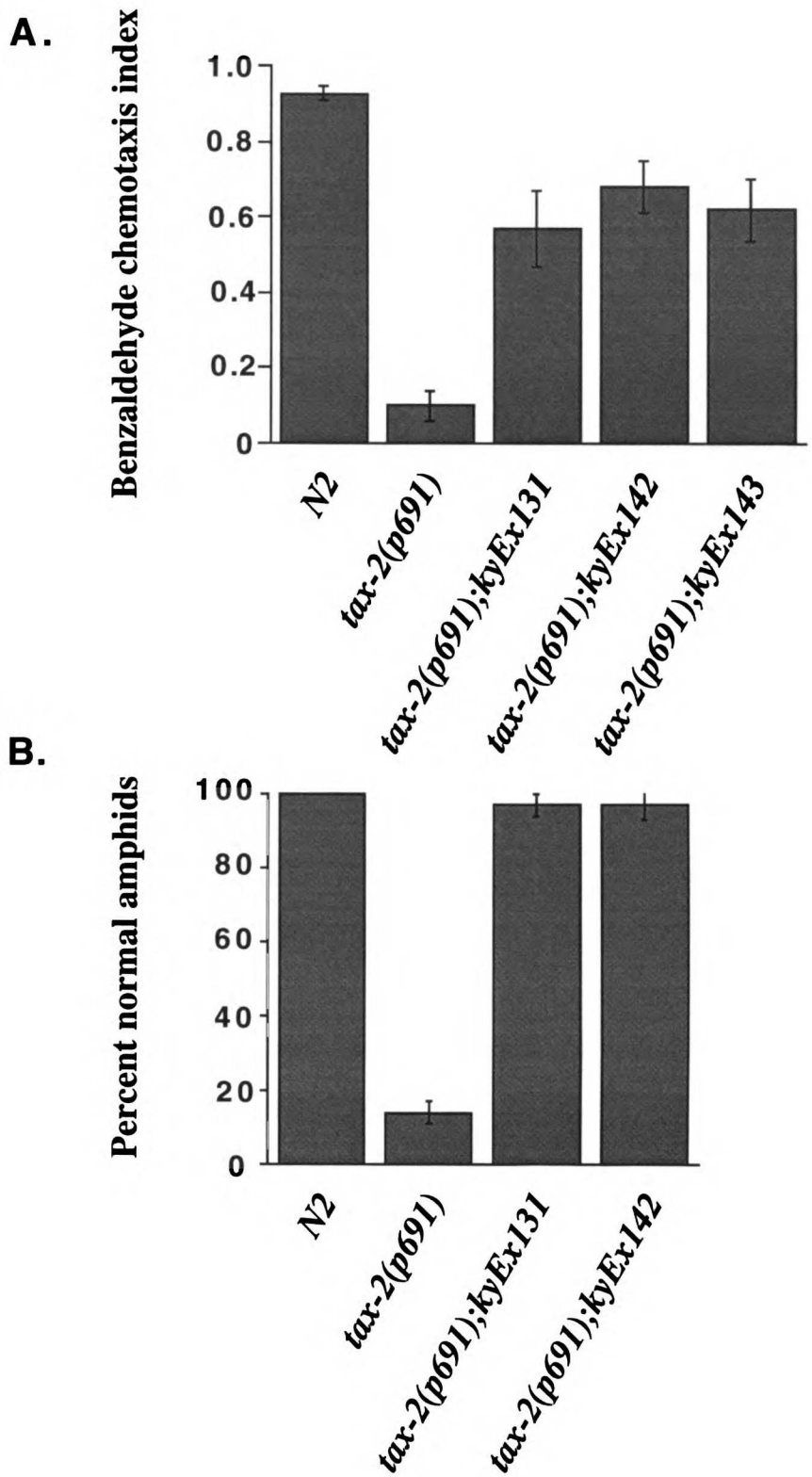
A.
Benzaldehyde chemotaxis index
1.0
0.8
0.6
0.4
0.2
0
N2
tax-2(p691)
tax-2(p691);kyEx131
tax-2(p691);kyEx142
tax-2(p691);kyEx143
B.
Percent normal amphids
100
80
60
40
20
0
N2
tax-2(p691)
tax-2(p691);kyEx131
tax-2(p691);kyEx142

Chapter Two

Multiple developmental functions of a cyclic nucleotide-gated channel in *C. elegans* sensory neurons

Ikue Mori and Y. Oshima (Kyushu University, Japan) isolated the the *ks10*, *ks15*, and *ks31* alleles of *tax-2*. All other work described in the paper is by C.M.C.

Summary

The *tax-2* and *tax-4* genes of *C. elegans* are required for normal chemosensation and thermosensation; they encode predicted beta and alpha subunits of a cyclic nucleotide-gated channel that is homologous to the channels used in vertebrate olfactory transduction and phototransduction. These sensory-specific genes are also required for normal axon outgrowth of some sensory neurons. We show here that *tax-2* and *tax-4* play a role in dauer larva formation, a developmental process controlled by sensory stimuli and four classes of sensory neurons. Dauer larva formation is regulated by two groups of genes that act partly in parallel, Group I and Group II dauer-constitutive genes. Group II genes affect a signalling pathway that uses a BMP-like secreted molecule, but the function of the Group I genes is less well understood. Depending on the genetic background, cyclic nucleotide-gated channel function can either stimulate or inhibit dauer larva formation. We suggest that these results reflect different functions of the channel in different sensory neurons. In addition, the Group I dauer formation mutants *daf-11* and *daf-21* have sensory axon guidance defects that are similar to those of *tax-2* and *tax-4*. Surprisingly, although the chemosensory neurons are of embryonic origin, the *tax-2* and *daf-11* gene products are required continuously until the adult stage to preserve normal axon morphology. These results reveal an unexpected plasticity that allows axons to be remodeled long after functional connections have been established. *tax-2*, *tax-4*, *daf-11*, and *daf-21* appear to encode genes with related functions that regulate both sensory function and development.

Introduction

C. elegans decides whether to undergo normal or dauer development mainly in response to a pheromone that reflects nematode density (Golden and Riddle, 1984). Recovery from the dauer stage is also regulated by sensory stimuli, mainly by the presence of food (Riddle, 1988). Four classes of sensory neurons that regulate dauer formation were identified by laser ablation experiments in which developmental abnormalities were observed after killing defined cell types. The amphid neurons ASG, ASI, and ADF prevent dauer formation (Bargmann and Horvitz, 1991). The ASJ neurons have two distinct functions; they promote dauer formation in the presence of dauer pheromone and promote dauer recovery in the presence of food (Bargmann and Horvitz, 1991; W. Shackwitz and J. Thomas, pers. comm.).

Over twenty *daf* (dauer formation) genes that are required for normal regulation of this developmental decision have been identified (Riddle et al., 1981). *daf* mutants may be either dauer-defective (never form dauer larvae) or dauer-constitutive (always form dauer larvae). The dauer-constitutive genes have been divided into two classes based on their genetic properties. Animals bearing mutations in either a Group I or a Group II dauer-constitutive gene form dauers efficiently at high temperature, but do not form dauers at low temperatures (Riddle et al., 1981; Thomas et al., 1993). However, animals that are mutant for both a Group I and a Group II dauer-constitutive gene form dauers at all temperatures. These results indicate that these two classes of genes have partially redundant functions in preventing dauer larva formation.

Two of the Group II genes, *daf-1* and *daf-4*, have been cloned. These two genes encode two subunits of a receptor-like protein of the TGF-ß/BMP receptor family (Estevez et al., 1993; Georgi et al., 1990). The *C. elegans daf-4* gene can bind to mammalian BMP, suggesting that receptor function is

conserved between mammals and nematodes. The other Group II genes might contribute to ligand production or response in this pathway. The site of action of these genes is unknown, although laser ablation experiments in wild-type and mutant animals suggest that the Group II genes have a function that is related to that of the ADF and ASI sensory neurons (Thomas et al., 1993; Bargmann and Horvitz, 1991). The two Group I genes *daf-11* and *daf-21* appear to promote dauer formation by causing the ASJ neurons to inappropriately stimulate dauer larva formation even in the absence of pheromone (W. Shackwitz and J.Thomas, pers. comm.). *daf-11* and *daf-21* genes are also required for some forms of olfaction and taste, implying that these genes also affect the function of other amphid sensory neurons (Vowels and Thomas, 1994).

The *C. elegans* genes *tax-2* and *tax-4* are expressed in neurons that affect dauer-formation and dauer recovery, but these genes have not been identified in screens for genes that affect dauer larva formation. *tax-2* and *tax-4* are expressed by three of the four sensory neurons that regulate dauer larva formation, the ASG, ASI, and ASJ neurons. *tax-4* and *tax-2* encode predicted alpha and beta subunits of a cyclic nucleotide-gated channel that are homologous to the channels used vertebrate olfactory and visual signal transduction. Genetic data suggests that the gene products of *tax-2* and *tax-4* form a heteromeric channel of alpha and beta subunits, as is observed in vertebrate sensory systems (This thesis ; H. Komatsu and I. Mori,pers. comm.).

tax-2 and *tax-4* are expressed in other sensory neurons in which they are required for proper sensory function and development (This thesis). *tax-2* and *tax-4*-expressing neurons include amphid sensory neurons that detect volatile and water-soluble attractants, chemical repellents and temperature

(Bargmann, 1993; Bargmann and Horvitz, 1991; Mori and Ohshima, 1995; Troemel et al., 1995). *tax-2* and *tax-4* genes are expressed in the ASE, ASK, AWC, and AFD neurons, and *tax-2* and *tax-4* mutants have defects in the chemosensory and thermosensory behaviors mediated by those neurons (This thesis; Dusenbery et al., 1975; Hedgecock and Russell, 1975; H. Komatsu and I. Mori,pers. comm.). Similarly, *tax-2* and *tax-4* are expressed in the ASJ and ASE neurons, which display highly penetrant axon outgrowth defects in *tax-2* and *tax-4* mutants (This thesis). The ASJ sensory axons fail to terminate in the proper position, instead projecting extensively into body regions where sensory axons are not usually found, while the ASE neurons sprout an extra branch (This thesis) . Within the *tax-2*- and *tax-4*-expressing neurons, the Tax-2 and Tax-4 proteins are localized in the axons and the sensory cilia, supporting the model that the channels play a role in axon development as well as in sensory transduction. The AWA and ASH neurons, which do not express *tax-2* or *tax-4*, function normally in the mutants (This thesis; H. Komatsu and I. Mori, pers. comm.).

Here we examine the role of the *tax-2* and *tax-4* genes in dauer larva formation and recovery. Genetic interactions with dauer formation genes indicate that *tax-2* and *tax-4* can either prevent or promote dauer larvae formation. We also show that mutations in the dauer-constitutive genes *daf-11* and *daf-21* affect chemosensory axon outgrowth, indicating that these genes affect neuronal development as well as neuronal function. Analysis of temperature-sensitive alleles of *tax-2* and *daf-11* reveals that these genes are required continuously for normal neuronal development and function, and that chemosensory axon morphology remains plastic throughout much of the animal's life.

Results

tax-2 and *tax-4* suppress the dauer-constitutive phenotype of Group I genes and enhance the dauer-constitutive phenotype of Group II genes

The expression of *tax-2* and *tax-4* in neurons involved in dauer larva formation suggested that the cyclic nucleotide-gated channel might function in the sensory control of dauer development. Under sparse, well-fed conditions, wild-type animals do not form any dauer larvae, but strong Group I or Group II dauer-constitutive mutants form >90% dauers (Riddle et al., 1981; Thomas et al., 1993). *tax-2* and *tax-4* mutants displayed a weak dauer-constitutive phenotype, and formed 1-5% dauer larvae at low density (Figure 2-1). At high density or in the presence of dauer pheromone, the fraction of dauer larvae increased, indicating that dauer larva formation was still regulated by pheromone in *tax-2* and *tax-4* mutants (data not shown).

The ADF, ASI, and to a lesser extent the ASG neurons, are required to regulate dauer formation (Bargmann and Horvitz, 1991). *tax-2* and *tax-4* are expressed in the ASG and ASI neurons, but not in the ADF neurons, so the normal dauer formation in *tax-2* and *tax-4* mutants might be due to ADF function. To test this hypothesis, sensory neurons were killed in *tax-2* mutants and the development of the operated animals was observed. In wild-type animals, both the ADF and ASI neurons must be killed together for dauer larvae to form in the absence of dauer pheromone. By contrast, in *tax-2* mutants dauer larvae formed when only the ADF neurons were killed (data not shown). This result indicates that the *tax-2* cyclic nucleotide-gated channel subunit is required for ASI function in dauer formation.

To examine the interactions between the genes in the dauer pathway, we constructed double mutants between *tax-2*, *tax-4* and the Group I dauer-

constitutive mutants *daf-11* and *daf-21* (Riddle et al., 1981; Vowels and Thomas, 1994). For all double mutant combinations, the strongest candidates for null mutations were used; these included *tax-4(p678)*, which is a null allele by molecular criteria (H. Komatsu and I. Mori, pers. comm.); *tax-2(p691)*, the strongest *tax-2* allele (This thesis); and the strong *daf-11(m87)* mutation. Only one *daf-21* mutation has been described. Additional double mutants were also made with other alleles of *tax-2*, *tax-4*, and *daf-11*. The *tax-2* and *tax-4* dauer formation phenotype was epistatic to the *daf-11* phenotype for all allele combinations tested: double mutants formed only a few dauer larvae in the absence of dauer pheromone, like *tax-2* or *tax-4* alone (Figure 2-1). Based on formal genetic analysis, these results indicate that *tax-2* and *tax-4* are downstream of *daf-11* in the dauer larva pathway. The temperature-sensitive mutant *tax-2(ks31ts)* (see below) was a weaker suppressor of *daf-11* dauer-constitutivity, indicating that it retains some normal *tax-2* function even at the restrictive temperature of 25°C. *tax-2(p691)* also suppressed the dauer-constitutive phenotype caused by a *daf-21* mutation. Interestingly, although they formed few dauer larvae when well-fed, the *tax-2; daf-11* and *tax-4; daf-11* double mutants formed dauer larvae efficiently under crowded conditions or in the presence of added dauer pheromone (data not shown). Thus, the *tax-2* or *tax-4* mutation restored *daf-11* mutants to almost normal regulation of dauer formation.

The Group II dauer-constitutive mutants *daf-1*, *daf-4*, *daf-7*, *daf-8*, and *daf-14* are also highly dauer constitutive in sparse, well-fed conditions. When double mutant combinations were constructed between *tax-2* or *tax-4* and *daf-1*, *daf-4*, *daf-8*, or *daf-14*, the double mutants were fully dauer-constitutive, even at low temperatures where the daf-c mutants would ordinarily form few dauers (Table 2-1). Thus, *tax-2* and *tax-4* enhanced these

daf-c mutations. In fact, because of their highly penetrant dauer-constitutivity it was impossible to isolate most of these double mutant strains as homozygotes; their phenotypes were inferred by segregation of dauers from heterozygous parents (see Methods).

tax-2 and _tax-4_ suppress the dauer recovery phenotype of Group I mutants

Like entry into the dauer stage, recovery from the dauer stage is controlled by chemical cues, particularly those provided by food. The ASJ sensory neurons are required to promote dauer recovery, and *tax-2* and *tax-4* are expressed in these neurons. Wild-type dauer larvae recover and resume normal development within 12 hours when well-fed at 15°C. *daf-11* and *daf-21* mutants have a strong recovery defect, with the exception of the unusual allele, *daf-11(m84)*, which displays normal dauer recovery (Vowels and Thomas, 1994). *tax-2* and *tax-4* animals showed a slight defect in dauer recovery (Figure 2-2).

Since *tax-2; daf-11* and *tax-4; daf-11* animals formed dauer larvae when crowded, it was possible to examine dauer larva recovery in the double mutants. The *tax-2* and *tax-4* dauer recovery phenotype was epistatic to the *daf-11* and *daf-21* phenotypes. Most double mutant dauers recovered within 48 hours at 15°, like the *tax-2* and *tax-4* single mutants (Figure 2-2). These results indicate that *tax-2* and *tax-4* act downstream of *daf-11* during dauer recovery. Interestingly, the temperature-sensitive allele, *tax-2(ks31ts)*, weakly suppressed the *daf-11* dauer recovery defect even at the permissive temperature, 15°C. This indicates that even at the permissive temperature, *tax-2* activity is decreased in this mutant. Increased suppression was observed at 20°C and 25°C (data not shown).

daf-11 and *daf-21* mutations cause amphid and phasmid axon defects

The suppression of Group I dauer-constitutivity by *tax-2* and *tax-4* is unlike previously observed suppression because animals are restored to a wild-type rather than a dauer-defective phenotype. This precise reversal of *daf-11* and *daf-21* phenotypes suggested that *tax-2* and *tax-4* might have functions related to those of *daf-11* and *daf-21*. In addition, *daf-11* and *daf-21* mutant animals have chemotaxis defects similar to those of *tax-2* and *tax-4* mutants (Vowels and Thomas, 1994), indicating that these genes affect the function of similar neurons. Since *tax-2* and *tax-4* affect axon outgrowth of the sensory neurons, we asked whether the Group I genes *daf-11* and *daf-21* affected neuronal development by examining the chemosensory axons in these mutants.

Chemosensory neurons in *daf-11* and *daf-21* mutants were observed by vital staining with the dye DiO, which stains dendrites, cell bodies, and axons of six amphid neuron pairs and two phasmid neuron pairs (Herman and Hedgecock, 1990)(Figure 2-3A). The dendrites and cell bodies of the chemosensory neurons appeared normal in the mutants, but *daf-11(m47)*, *daf-11(m87)*, *daf-11(sa195)*, *daf-11(m84)* and *daf-21(p673)* mutants had axon guidance defects similar to those of *tax-2* and *tax-4* mutants (Figure 2-3B). The most common defect was the presence of one or more inappropriate amphid axons in the ventral nerve cord due to a failure of termination of the axons in the nerve ring. This defect was observed in 40-90% of the mutant animals, depending on the allele (Figure 2-4). Like *tax-2* mutants, the *daf-11* and *daf-21* mutants also occasionally had phasmid axons that were inappropriately long, and a variety of defects in the ASJ sensory neurons (data not shown; Figure 2-

3C). By contrast, the Group II dauer-constitutive mutants *daf-1*, *daf-2*, *daf-4*, *daf-7*, *daf-8*, and *daf-14* had normal amphid and phasmid axons (data not shown).

The developmental defects in *tax-2; daf-11*and *tax-4; daf-11* double mutants were assessed to look for any suppression or enhancement of mutant phenotypes. In contrast with the suppression observed in dauer larva formation, the defects of the double mutants were similar to the defects of the single mutants (Figure 2-4). Behavioral assays for chemotaxis were also conducted on the double mutants and the chemotaxis defects in *tax-2; daf-11*, *tax-4; daf-11*, *tax-2; daf-21*, and *tax-4; daf-21* double mutants were similar to those of the single mutants (data not shown).

tax-2 and _daf-11_ function are required throughout postembryonic development for normal chemotaxis and axon morphology

The amphid chemosensory neurons are born in the embryo, and send out their axons later in embryogenesis; by the time of hatching, they can be visualized by DiO-staining and appear to have their adult morphology. The neurons also appear to be functional, since young larvae are able to chemotax to attractants. To ask when the *tax-2* gene product was required for normal chemosensory neuron development and function, we performed temperature-shift experiments on temperature-sensitive *tax-2(ks31)* mutants. *tax-2(ks31)* mutants were temperature-sensitive for both their axon outgrowth defects and their chemotaxis defects (Figure 2-5). *tax-2(ks31)* animals raised at 20°C displayed normal chemotaxis and mostly normal axons (2% defective), while *tax-2(ks31)* animals raised at 25°C had defects comparable to those of the strongest *tax-2* mutants.

To determine the time of *tax-2* gene action, animals were shifted between 20°C and 25°C at different times of development, then scored either for their chemotaxis phenotypes or for their chemosensory axon morphology as adults (Figure 2-6A). Surprisingly, the *tax-2* gene product was not required during the period of initial neural development and axon guidance in the embryo. When *ks31* mutants were raised through embryogenesis at the nonpermissive temperature and then shifted to lower temperature after hatching, the resulting adults were normal in their axon outgrowth and behavior (Figure 2-6A). Indeed, if the *tax-2* mutants were shifted to permissive temperature as late as the fourth larval stage (L4), 50% of the adults had normal axons and 60% displayed successful chemotaxis behaviors. These results indicate that the *tax-2* gene product could be supplied late in larval life and still rescue neuronal development and function. Moreover, the converse experiments revealed that the presence of the *tax-2* gene product in the embryo and young larva was not sufficient for normal axonal development. The *tax-2* gene product appeared to be required at the fourth larval stage or later for normal adult chemotaxis and axon morphology.

Additional temperature-shift experiments were conducted to ask whether *tax-2* could affect chemotaxis and axon morphology in the adult stage. Animals were raised at 20°C or 25°C until the young adult stage, shifted to the converse temperature, and chemotaxis or sensory axon morphology were scored in the adults at varying times after the temperature shift. These experiments revealed that *tax-2* was required continuously in the adult for normal chemotaxis; chemotaxis was somewhat defective 15 hours after a shift from the permissive to restrictive temperatures and was completely defective after 60 hours. Conversely, chemotaxis began recovering 6 hours after a shift from the restrictive to permissive temperature and was almost

wild-type after 45 hours (Figure 2-6B). *tax-2* was also required continuously to maintain the normal axon structure in adult animals; axon structure was slightly defective 42 hours after a shift from permissive to restrictive temperature and was completely mutant after 72 hours (Figure 2-6B). However, the normal *tax-2* gene product rescued oonly a small fraction of defective axon structure even after 72 hours in the adult stage.

daf-11(m84) is an unusual allele of *daf-11* with a strong dauer-constitutive phenotype, but a minimal defect in dauer larva recovery and chemotaxis to volatile attractants (Vowels and Thomas, 1994). We found that *daf-11(m84)* displayed a temperature-sensitive defect in amphid axon structure; all animals raised at 20°C had amphid axons that appeared to be normal, but 90% of animals raised at 25°C showed defects in amphid axon structure similar to those observed in *tax-2* animals (Figure 2-3).

To ask when the *daf-11* gene product was required for normal axon structure, temperature-shift experiments were conducted with *daf-11(m84)* or *daf-11(m84);daf-12(m20)* mutant strains. Synchronized animals were raised to the young adult stage at 20°C or 25°C, shifted to the converse temperature, and axon structure observed by DiO-staining. To perform the experiments in which animals were raised at the restrictive temperature, it was necessary to suppress the dauer-constitutivity of *daf-11* animals by including the down-stream daf-d mutation, *daf-12(m20)*. *daf-11* chemotaxis and axon outgrowth phenotypes were not suppressed in *daf-11;daf-12* double mutant strains (Figure 2-4; data not shown). As was observed with *tax-2*, *daf-11* activity was required continuously to maintain the normal axon structure in adult animals; axon structure was completely defective 62 hours after animals were shifted from permissive to restrictive temperature (Figure 2-6C). However, as

was observed in the *tax-2(ts)* mutant, defective axon morphology could only be partially corrected in the adult stage in *daf-11(m84);daf-12(m20)* mutants.

Discussion

tax-2 and *tax-4* have multiple functions in dauer larva formation

The expression of *tax-2* and *tax-4* in neurons that control dauer larva formation suggested that the cyclic nucleotide-gated channel encoded by these genes might regulate the dauer/non-dauer developmental decision. Indeed, these genes appear to play multiple roles in dauer formation. On their own, *tax-2* and *tax-4* mutants displayed a weak dauer-constitutive phenotype. In wild-type animals, the activity of the ADF and ASI neurons blocks dauer formation; cell killing experiments in *tax-2* mutants revealed a defect in this function of the ASI neurons. The ADF neurons do not express *tax-2* or *tax-4*, and they appeared to function normally.

Analysis of double mutants demonstrated a role of the channel in preventing dauer larva formation. Group II dauer-constitutive mutants do not form dauer larvae at low temperature, but double mutant combinations between *tax-2* or *tax-4* and Group II dauer-constitutive mutants formed dauers at all temperatures.

Surprisingly, *tax-2* and *tax-4* also appeared to have activities that could promote dauer larva formation. The Group I dauer-constitutive mutants *daf-11* and *daf-21* were fully suppressed by mutations in the *tax-2* and *tax-4* genes. Many dauer-defective mutations can suppress Group I dauer-constitutive mutations, resulting in a dauer-defective double mutant (Thomas et al., 1993). By contrast, the Group I/*tax-2,4* double mutants had nearly wild-type dauer formation in response to dauer pheromone. This unique true suppression

suggests a close relationship between the functions of the Group I genes and *tax-2* and *tax-4*.

The ASJ neurons promote dauer larva formation in the presence of pheromone, as well as promoting recovery from the dauer stage in the absence of pheromone (W. Shackwitz and J. Thomas, pers. comm.). In the Group I mutations, the ASJ neurons inappropriately direct dauer larva formation even in the absence of pheromone (W. Shackwitz and J. Thomas, pers. comm.) and ASJ-mediated dauer recovery is also defective. Our data suggest that the aberrant ASJ function in Group I mutants depends on the cyclic nucleotide-gated channel. The normal activation of ASJ during dauer larva formation and recovery appears to be channel-independent, since dauer formation and recovery are almost normal in *tax-2* and *tax-4* mutant strains. Thus, two different functions of the ASJ sensory neuron may use distinct cell signalling pathways.

tax-2, _tax-4_, _daf-11_, and _daf-21_ are required for normal axon guidance of a subset of sensory neurons

The Group I genes *daf-11* and *daf-21* have similar defects in axon outgrowth to those of *tax-2* and *tax-4.*, indicating that all four of these genes are required for both normal sensory neuron development and function. Three classes of axon outgrowth defects were observed in sensory neurons of these mutants: the presence of abnormal posteriorly-directed sensory processes from the nerve ring, presence of an aberrant axonal process produced by the ASJ neurons, and failure of termination of the phasmid axons in the tail. In all cases, sensory neurons in the head and tail were found in central body regions from which they are normally excluded. Since

the axons grow more extensively in the mutants, the normal function of these genes must limit or restrict axon growth.

The axon outgrowth defect in *daf-11* and *daf-21* raises the possibility that the inappropriate activation of the neuron ASJ in these mutants might arise from some defective or abnormal connection between the sensory neurons and their targets. *tax-2* and *tax-4* do not suppress the visible *daf-11* axon guidance defects, but they might alter more subtle aspects of axon guidance or connectivity.

Most previously described mutants that affect axon guidance in C. elegans affect many cell types. For example, the chemotropic factor *unc-6* affects dorsoventral axon guidance and cell migration of both neuronal and non-neuronal cell types (Hedgecock et al., 1990), and the protein kinase encoded by *unc-51* affects axon extension of virtually all axons that have been examined (Desai et al., 1988; McIntire et al., 1992). By contrast, *tax-2*, *tax-4*, *daf-11*, and *daf-21* only affected morphology of a few types of axons, consistent with the molecular evidence that these genes are only expressed in a few types of neurons.

Functional coupling of neuronal activity and neuronal development

Three general models could be proposed to explain the congruence of developmental and behavioral defects in *tax-2*, *tax-4*, *daf-11*, and *daf-21* mutants. First, the primary defect in these four mutants could be an axon guidance defect, and the behavioral defects could be consequences of mistakes in neuronal connectivity. Based on their mutant phenotypes, these gene products could generate or respond to molecules that inhibit axon growth, such as collapsin/semaphorin molecules (Luo et al., 1993; Messersmith et al.,

1995). Second, the primary defect in *tax-2, tax-4, daf-11* and *daf-21* could be a change in neuronal sensory activity or synaptic transmission, which indirectly leads to a defect in axonal guidance. In vertebrate sensory systems, normal electrical activity of the sensory neurons is required for proper connectivity in the visual, auditory, and somatosensory systems (Brainard and Knudsen, 1993; Li et al., 1994; Shatz and Stryker, 1988). Third, *tax-2, tax-4, daf-11,* and *daf-21* could have two distinct functions in neuronal development and neuronal signalling. For example, some cell types might use these gene products strictly during axon guidance, while others might use the same gene products in chemosensory signal transduction.

At this point, our data cannot rigorously distinguish between these models. However, the Tax-2 protein is expressed in both the axons and the sensory cilia, suggesting that it might function in both locations (This thesis). In addition, the temperature-shift experiments with *daf-11* and *tax-2* revealed different time courses for these genes' effects on chemotaxis and axon morphology. After 24 hours at high temperature, animals had defective chemotaxis but still maintained normal axon structure, and similarly, when animals were shifted to low temperature, their chemotaxis behaviors recovered before their axons returned to their normal morphologies. Chemotaxis appears to be more sensitive to channel function than axon defects, either because of an intrinsic difference in the functions or because different sensory neurons accumulate protein at different rates.

Late-acting neuronal plasticity in *C. elegans*

Remarkably, in the temperature shift experiments, removing the *daf-11* or *tax-2* gene products in the adult stage caused axon outgrowth. Thus, the

chemosensory axons have an unexpected ability to change their morphology at late developmental stages. Nonetheless, some part of *daf-11* and *tax-2* function appeared to be restricted to larval rather than adult stages. Full rescue of either axonal phenotype required gene expression by the fourth larval stage, suggesting that some aspects of gene function were restricted to earlier developmental stages.

The *tax-2* and *daf-11* temperature-sensitive periods reveal a process in *C. elegans* that is analogous to critical periods of vertebrate development. The chemosensory neurons are generated in the embryo, and reach their mature morphology by hatching, when chemosensory behaviors can be assayed. Yet their axonal pattern could be remodeled into the adult stage, indicating that axonal morphology is plastic during larval development. During this time, the animal is exposed to different chemosensory environments and generates different chemosensory behaviors. In principle, this late neuronal plasticity could allow activity and experience in the sensory nervous system to feed back on its connectivity.

Methods

General genetics methods. Wild-type worms were *C. elegans* variety Bristol, strain N2. General methods of *C. elegans* strain maintainance were as described (Brenner, 1974). Some strains used were provided by the *Caenorhabditis* Genetics Center. Some *daf-11* alleles were provided by J. Thomas, University of Washington, and D. Riddle, University of Missouri.

Marker mutations used were:

Linkage group(LG)I: *unc-13(e251) unc-29(e1072) lin-11(n566).*

LGIII: *dpy-17(e164) unc-32(e189).*

LGIV: *osm-3(p802)*

LGV: *him-5(e1490) unc-42(e270)*

Isolation of *tax-2* and *tax-4* mutations. The *tax-2* alleles *p694, p671,* and *p691* were previously identified based on defective chemotaxis to water-soluble attractants (Dusenbery et al., 1975). *p671* and *p691* mutants also had thermotaxis defects (Hedgecock and Russell, 1975). *tax-2* mutants *ks10, ks15,* and *ks31* were identified on the basis of thermotaxis-defective phenotypes. *tax-2(ks10)* was isolated after mutagenesis of CB1377 *daf-6(e1377)* hermaphrodites with EMS. F2 progeny were grown at 20°C and animals that migrated to high temperature (23°C-24°C) in a linear thermal gradient in multiple assays were isolated. *tax-2(ks10)* was separated from the *daf-6* mutation for further analysis. *tax-2(ks15)* was isolated in a similar screen for animals that migrated to low temperature (17°C). *tax-2(ks31)* was isolated after mutagenesis of wild-type animals with EMS. F2 progeny were grown at 25°C, and animals that migrated to the 15°C region of a linear gradient were isolated.

ks10, ks15, and *ks31* were mapped to LG1 by 3-factor linkage to *dpy-5* and *ks10* and *ks15* failed to complement *p671, p691,* or one another for behavioral defects. *ks10. ks15,* and *ks31* failed to complement *p691* for axon guidance defects.

One allele of *tax-2* and four alleles of *tax-4* were identified as suppressors of the dauer-constitutive phenotype of *daf-11. daf-11(m47)* or *daf-11(m87)* mutants were mutagenized and the F2 progeny grown at 25°C, under conditions in which virtually all *daf-11* mutants formed dauer larvae. Animals that grew to the adult stage were isolated and characterized further for their axon guidance phenotypes using DiO staining to visualized the amphid chemosensory neurons (Herman and Hedgecock, 1990). Suppressor

strains that showed an enhanced amphid axon guidance defect compared to *daf-11(m87)* were backcrossed 6-8 times by *him-5(e1490)* or wild-type animals. The suppressors were separated from *daf-11* and reisolated as single mutants based on their axon phenotypes. *tax-4(ky89)* was mapped to LGIII by 3-factor linkage to *unc-32:* from a strain of genotype *ky89/dpy-17(e164)unc-32(e189),* 0/6 Unc non-Dpy recombinants segregated *ky89* and 10/11 Dpy non-Unc recombinants segregated *ky89. ky89* also failed to complement *tax-4(p678)* for behavioral and amphid axon guidance phenotypes.

Chemotaxis assays. Population chemotaxis assays were performed as described (Bargmann, 1993). The chemotaxis index was calculated as: [Σ(worms at attractant)-Σ(worms at control)/Σ(total number of worms)]. The standard error of the mean (SEM) was calculated from the combined chemotaxis indices. Avoidance assays were performed as described (Vowels and Thomas, 1994).

DiO staining of chemosensory neurons. DiO-staining was performed essentially as described (Herman and Hedgecock, 1990), except that animals were stained for 16-18 hours on a rotator in the presence of 1 microliter of concentrated *E. coli* per ml of M9 buffer. Stained animals were viewed by fluorescence microscopy using standard FITC filters. An animal was scored as having defective amphids if any amphid neuron had abnormal axons (see Figure 3).

Dauer formation and recovery assays. Dauer formation at 25°C was tested essentially as described (Vowels and Thomas, 1992), except that animals were grown on *E. coli* strain HB101. Briefly, 5-15 adult animals raised at 20°C were

allowed to lay eggs for 1-5 hours; the eggs were transferred to 25°C and checked frequently over the next 2-3 days for the formation of L4 and dauer larvae. L4 and dauer larvae were counted each day and then removed from the plates.

Dauer recovery at 15°C was assessed as described (Vowels and Thomas, 1992) except that animals were grown on *E. coli* strain HB101. Mutants were allowed to form dauers at 25°C, then dauer larvae were selected in 2% SDS for 2 hours. Dauers were picked to 10 cm plates seeded with HB101 E. coli and placed at 15°C. After 48 hours, dauers and recovered dauers (scored by light color and pharyngeal pumping) were counted. Only larvae on the agar were scored; dauers trapped on the sides of the petri plates were ignored.

Temperature-shift experiments. Temperature-shift experiments were performed in two ways. *tax-2(ks31)* adult animals were allowed to lay eggs for 1-4 hours at 20°C or 25°C, then adults were removed from the plates. Plates were placed at 20°C or 25°C for varying times, then shifted to 25°C or 20°C, respectively. Animals were allowed to develop to the adult stage, then chemotaxis was tested and amphid axon guidance defects were observed by DiO staining. In a separate set of experiments, synchronized *tax-2(ks31)*, *daf-11(m84)* or *daf-11(m84); daf-12(m20)* animals were allowed to develop to the adult stage at either 20°C or 25°C, then were shifted to the converse temperature. Chemotaxis and axon structure were assayed at varying times after the temperature shift, for up to 3.5 days. The adult animals were transferred to fresh plates each day to free them of progeny. The *daf-12* mutation was included in some experiments to suppress the *daf-11* Daf-c phenotype. *daf-12* single mutants have wild-type amphid and phasmid neuron structure when examined by DiO-staining, and *daf-11; daf-12* double

mutants have amphid neuron axonal outgrowth defects similar to *daf-11* single mutants.

Construction of *tax-2; daf-c* and *tax-4; daf-c* double mutant strains. In general, the daf-c mutation was tracked by the Daf-c phenotype, and the *tax* mutation was tracked by balancing it in *trans* with a tightly linked marker mutation. An example is the construction of the *tax-2; daf-11* strain. *tax-2 I* males were crossed into *unc-13 lin-11 I; daf-11 V* hermaphrodites at 25°C and non-UncLin cross progeny were individually cloned onto plates at 25°C. F2 non-Unc dauers were picked into microwell dishes containing M9 buffer and E. coli, and allowed to recover and produce progeny at 15°C. Animals that segregated 1/4 Unc progeny were inferred to be of the genotype *tax-2/unc-13 lin-11; daf-11. tax-2; daf-11* homozygotes were recovered by cloning progeny to individual plates at 15°C and identifying animals that segregated no UncLin progeny. *tax-4* strain constructions followed a similar strategy, except that a different balancer chromosome, *dpy-17(e164) unc-32 (e189) III,* was used. In all cases, genotype was confirmed by complementation testing.

Because of the maternal effect phenotype of *daf-21, tax; daf-21* strains were generated by selecting F3 dauers at 25°C. Dauers were allowed to recover at 15°C, and animals that segregated 1/4 balancer mutation were inferred to be of the genotype *tax/balancer mutation; daf-21.* Homozygous animals were obtained as described above.

The linked *daf-2 tax-4* double mutant strain was constructed by mating *tax-4* males to *daf-2 unc-32* hermaphrodites, picking non-Unc cross progeny to 25°C, then selecting F2 recombinant non-Unc dauers. These were recovered in microwell plates at 15°C, then transferred to individual plates. Homozygous *daf-2 tax-4* progeny were identified by cloning progeny at 15°C

and selecting those that segregated only non-Unc progeny. The *daf-2* phenotype was confirmed by the Daf-c phenotype and the *tax-4* genotype was confirmed by complementation testing.

Constructing the *tax-2; group 2 daf-c* and *tax-4; group 2 daf-c* double mutant strains. The construction of homozygous double mutant strains between *tax-2* or *tax-4* and *daf-1, daf-4, daf-8* or *daf-14* proved impossible because the homozygous double mutants were highly dauer-constitutive. In these cases, the strain was maintained as a balanced strain in which daf-c mutant was homozygous and the *tax* mutant was balanced in *trans* to linked marker mutations. *tax-2* was balanced by *unc-13(e251) lin-11(n566) I* and *tax-4* was balanced by *dpy-17(e164) unc-32(e189) III.* Strains were constructed as described for the *tax-2; daf-11* double, except that it was impossible to isolate the homozygous double mutant strain. 30 wild-type F3 animals from *tax-2/marker; daf* F2 parents were cloned to individual plates at 15°C and allowed to lay progeny. All broods yielded 1/4 marker progeny, indicating that all adults were of the genotype *tax/marker; group2 daf-c.* In addition, these broods contained more dauers at 15°C than were observed in the *daf* mutants alone, indicating that the double homozygotes are strongly Daf-c. In all cases, the presence of *tax-2* or *tax-4* in the balanced strain was confirmed by complementation testing. The occasional apparent *tax; daf* homozygotes were all recombinants in which the marker mutation and *tax-2* had both been eliminated.

The linked double mutant strain *daf-4 tax-4* was constructed by mating *tax-4* males to *daf-4 unc-32* hermaphrodites, cloning non-Unc cross progeny at 25°C, then selecting F2 non-Unc dauer progeny. These were recovered at 15°C and maintained as the *daf-4 tax-4/daf-4 unc-32* balanced strain.

Figure legends

Figure 2-1: Percent Dauer-Constitutivity of *tax-2, tax-4, daf-11* and *daf-21* Single Mutants and Double Mutant Combinations. For each point, 200-700 animals were assayed (error bar represent the 95% confidence interval). Assays were performed as described, at 25°C.

Figure 2-2: Percent Dauer recovery of *tax-2, tax-4, daf-11* and *daf-21* Single Mutants and Double Mutant Combinations. For each point, 100-200 animals were assayed (error bar represents the 95% confidence interval). Assays were performed as described, at 15°C.

Figure 2-3: Developmental Defects of *daf-11* and *daf-21* Mutants Visualized By DiO Staining

(A) DiO staining of wildtype animal. Left-lateral view of one amphid showing DiO staining of dendrites, cell bodies and axons of 6 amphid neurons. Positions of the staining neurons are diagrammed. The normal position of the neuron ASJ is marked.

(B) DiO staining of a *daf-11* mutant animal. Left-lateral view of a DiO-stained *daf-11* mutant animal, showing an aberrant amphid neuron process projecting posteriorally from the nerve ring.

(C) DiO staining of a *daf-11* mutant animal. Left-lateral view of a DiO-stained *taf-11* mutant animal, showing an aberrant process projecting laterally from the ASJ neuron into the posterior body region. *daf-21* animals have an identical phenotype. In addition, this animals also displays an aberrant amphid axon process projecting posteriorally from the nerve ring.

(D) DiO staining of a *daf-21* mutant animal. Left-lateral view of a DiO-stained *daf-21* mutant animal, showing an aberrant amphid neuron process projecting posteriorally from the nerve ring.

Some DiO staining is observed in the gut of the animal. In all cases, anterior is to the left and dorsal is up.

Figure 2-4: Percent Defective Amphid Axons in *tax-2*, *tax-4*, *daf-11* and *daf-21* Single Mutants and Double Mutant Combinations. For each point, 200-700 DiO-stained worms were viewed (error bars denote the 95% confidence level). An amphid was scored as defective if any amphid neuron had a defect.

Figure 2-5: *tax-2(ks31ts)* is Temperature-Sensitive for Chemotaxis and Axon Guidance Defects.
(A) Response to volatile odorants of *tax-2(ks31ts)* animals raised at the permissive temperature (20°C) and the restrictive temperature (25°C). Each data point represents the average of 4-8 independent assays using approximately 100-200 animals per assay (error bars equal the SEM). The dilution of odorants in ethanol were the following: 1:200 benzaldehyde, 1:100 isoamyl alcohol, 10 mg/ml pyrazine, 1:1000 diacetyl and 1:1000 2,4,5-trimethylthiazole.
(B) Amphid axon defects of *tax-2(ks31ts)* animals raised at the permissive temperature (20°C) and the restrictive temperature (25°C). Data points refer to the percentage of normal amphid axons (error bars denote the 95% confidence level). For each point, 200-700 DiO-stained worms were viewed. An amphid was scored as defective if any amphid neuron had a defect.

Figure 2-6: *tax-2* is Continuously Required For Normal Axon Structure and Benzaldehyde Chemotaxis and *daf-11* is Continuously Required For Normal Axon Structure.

(A) *tax-2(ks31ts)* animals that were shifted from restrictive temperature (25C) to permissive temperature (20°C), or vice-versa, at various points during development. Benzaldehyde chemotaxis (top panel) and amphid axon structure (bottom panel) were assayed in the adults.

(B) *tax-2(ks31)* animals that were raised at the restrictive temperature (25°C) until adulthood, then shifted to the permissive (20°C) temperature, or vice-versa. Benzaldehyde chemotaxis (top panel) and amphid axon structure (bottom panel) were assayed at several times after the temperature shift.

(C) *daf-11(m84)* or *daf-11(m84);daf-12(m20)* animals were raised at the restrictive temperature (25°C) until adulthhood, then shifted to the permissive (20°C) temperature, or vice-versa. Amphid axon structure was assayed at several times after the termperature shift.

Chemotaxis was assayed to a 1:200 dilution of benzaldehyde in ethanol. Each data point represents the average of 4-8 independent assays using aproximately 100-200 animals per assay (error bars denote the SEM). Amphid axon structure was visualized by DiO staining. For each point, approximately 100-200 animals were viewed. Control values for chemotaxis and axon morphology are indicated in the right of each graph. An amphid was scored as defective if any amphid neuron had a defect. Abbreviations used are: e, embryo; L1, first larval stage; L2, second larval stage; L3, third larval stage; L4, fourth larval stage.

Table 2-1: Percent dauer and L4 segregants at 15 °C from single broods from *tax-2/unc-13lin-11;* group II *daf-c* and *tax-4/dpy-17unc-32;* group II *daf-c* animals.

strain	% wildtype L4	% UncLin, DpyUnc or Unc L4	% wildtype dauer	% UncLin, DpyUnc or Unc dauer	(N)
daf-1(m40)	83		17		(291)
tax-2(p691)/unc-13(e251)lin-11(n566);daf-1((m40)	49	22	27	2	(316)
tax-4(p678)/dpy-17(e163)unc-32(e189);daf-1(m40)	49	26	25	1	(610)
daf-4(e1363)	61		39		(197)
tax-2(p691)/unc-13(e251)lin-11(n566);daf-4(e1363)	31	17	49	3	(197)
daf-4(e1363)tax-4(p678)/Daf-4(e1363)unc-32(e189)	8	16	70	5	(413)
daf-8(e1393)	68		32		(344)
daf-8(e1393); tax-4(p678)/dpy-17(e164)unc-32(e189)	47	24	29	1	(913)
daf-14(m77)	47		53		(495)
tax-2(p691)/unc-13(e251)lin-11(n566);daf-14(m77)	42	14	36	9	(495)
daf14(m77);tax4(p678)/dpy-17(e164)unc-32(e189)	43	17	33	6	(520)

Figure 2-1

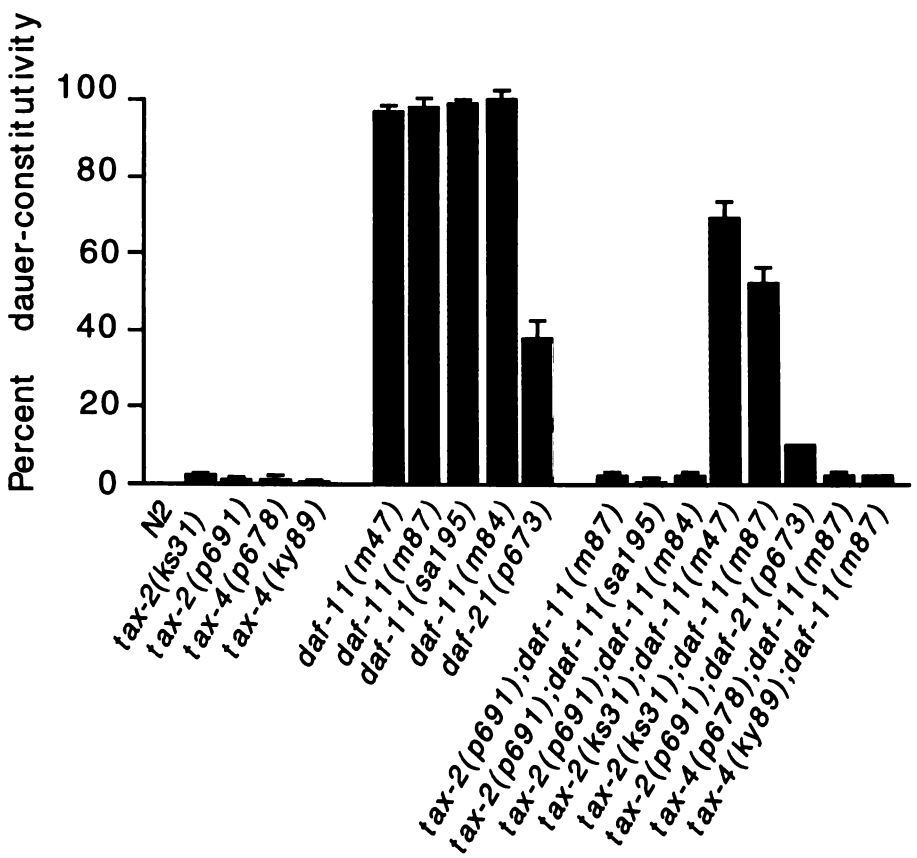
Percent dauer-constitutivity
100
80
60
40
20
0
N2
tax-2(ks31)
tax-2(p691)
tax-4(p678)
tax-4(ky89)
daf-11(m47)
daf-11(m87)
daf-11(sa195)
daf-11(m84)
daf-21(p673)
tax-2(p691);daf-11(m87)
tax-2(p691);daf-11(sa195)
tax-2(p691);daf-11(m84)
tax-2(ks31);daf-11(m47)
tax-2(ks31);daf-11(m87)
tax-2(p691);daf-21(p673)
tax-4(p678);daf-11(m87)
tax-4(ky89);daf-11(m87)

Figure 2-2

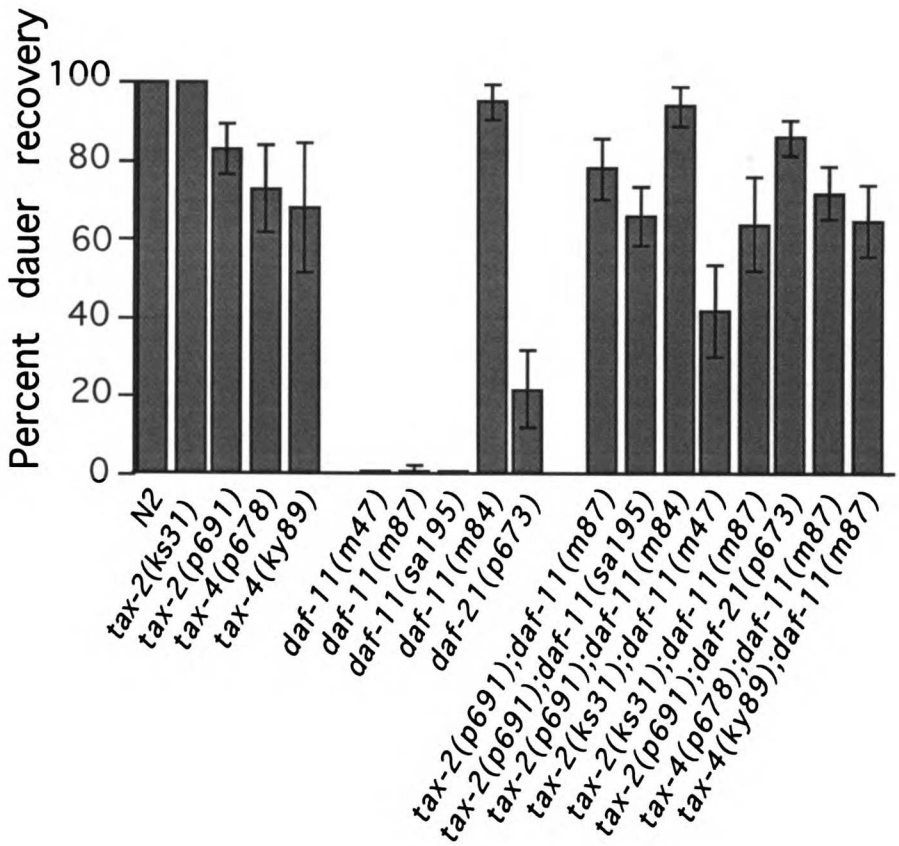
Percent dauer recovery
100
80
60
40
20
0
N2
tax-2(ks31)
tax-2(p691)
tax-4(p678)
tax-4(ky89)
daf-11(m47)
daf-11(m87)
daf-11(sa195)
daf-11(m84)
daf-21(p673)
tax-2(p691);daf-11(m87)
tax-2(p691);daf-11(sa195)
tax-2(p691);daf-11(m84)
tax-2(ks31);daf-11(m47)
tax-2(ks31);daf-11(m87)
tax-2(p691);daf-21(p673)
tax-4(p678);daf-11(m87)
tax-4(ky89);daf-11(m87)

Figure 2-3

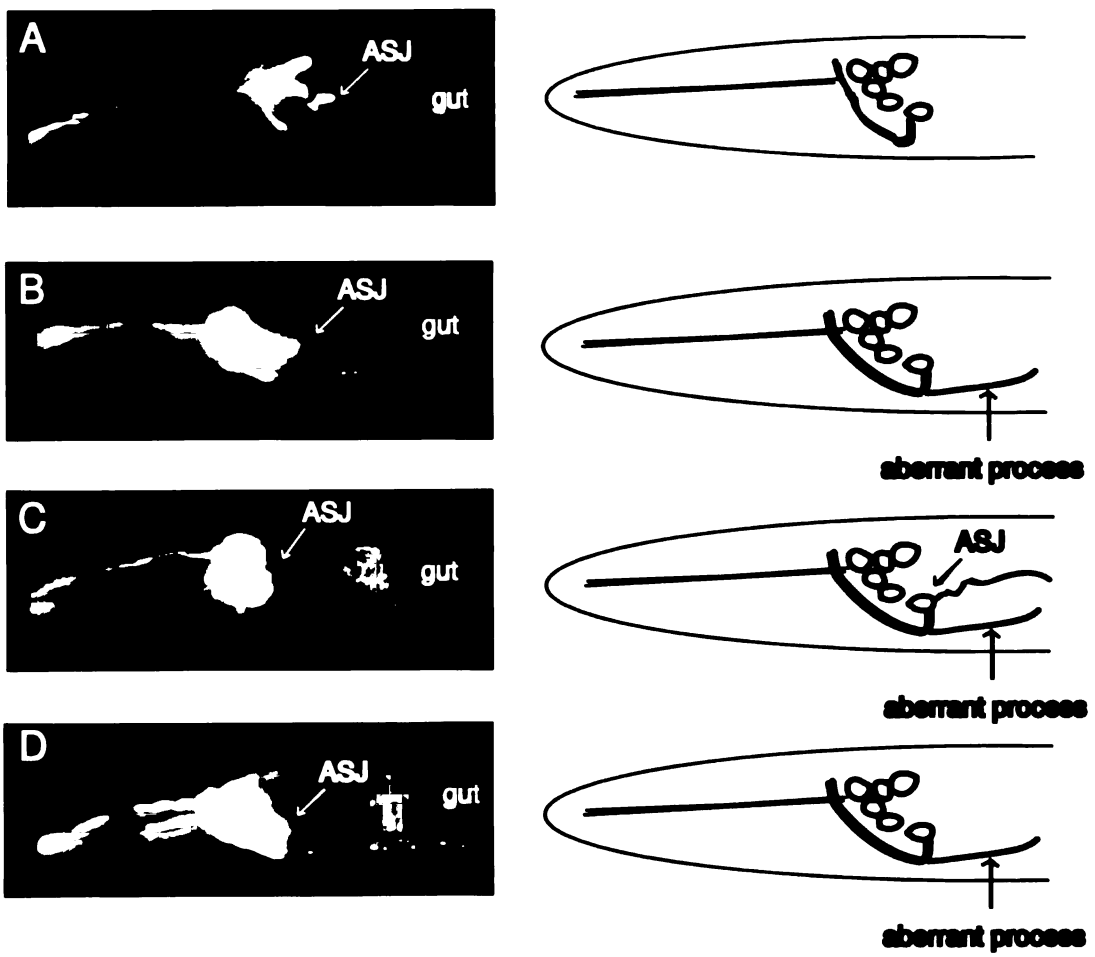
A
ASJ
gut
B
ASJ
gut
aberrant process
C
ASJ
gut
ASJ
aberrant process
D
ASJ
gut
aberrant process

Figure 2-2

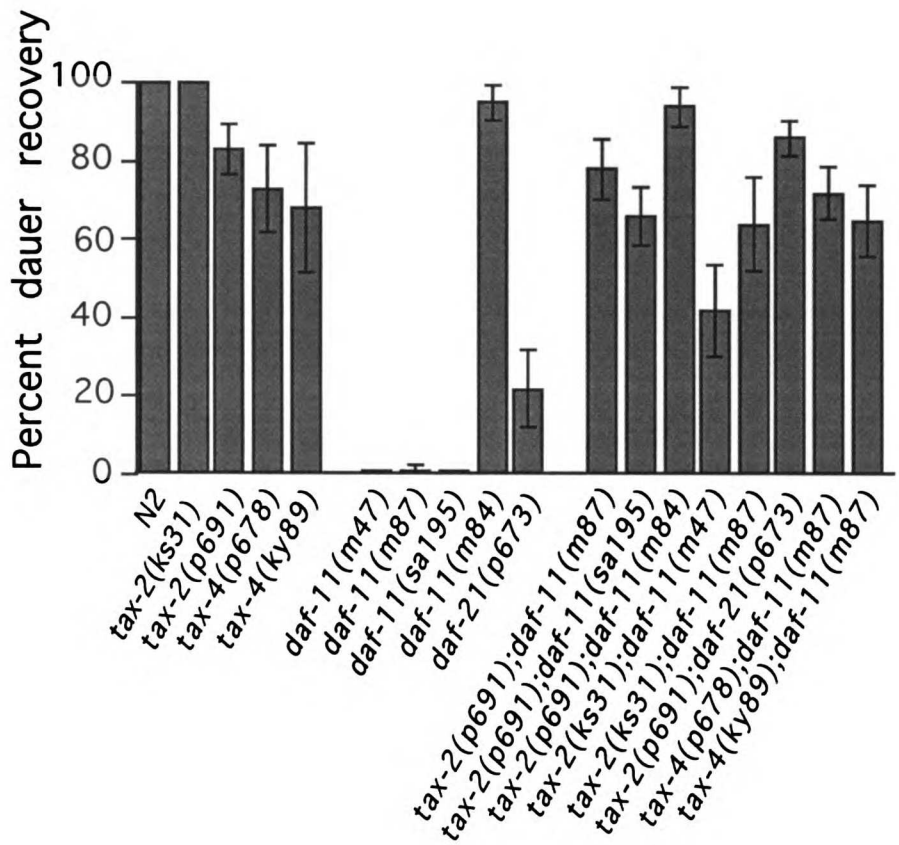
Percent dauer recovery
100
80
60
40
20
0
N2
tax-2(ks31)
tax-2(p691)
tax-4(p678)
tax-4(ky89)
daf-11(m47)
daf-11(m87)
daf-11(sa195)
daf-11(m84)
daf-21(p673)
tax-2(p691);daf-11(m87)
tax-2(p691);daf-11(sa195)
tax-2(p691);daf-11(m84)
tax-2(ks31);daf-11(m47)
tax-2(ks31);daf-11(m87)
tax-2(p691);daf-21(p673)
tax-4(p678);daf-11(m87)
tax-4(ky89);daf-11(m87)

Figure 2-5

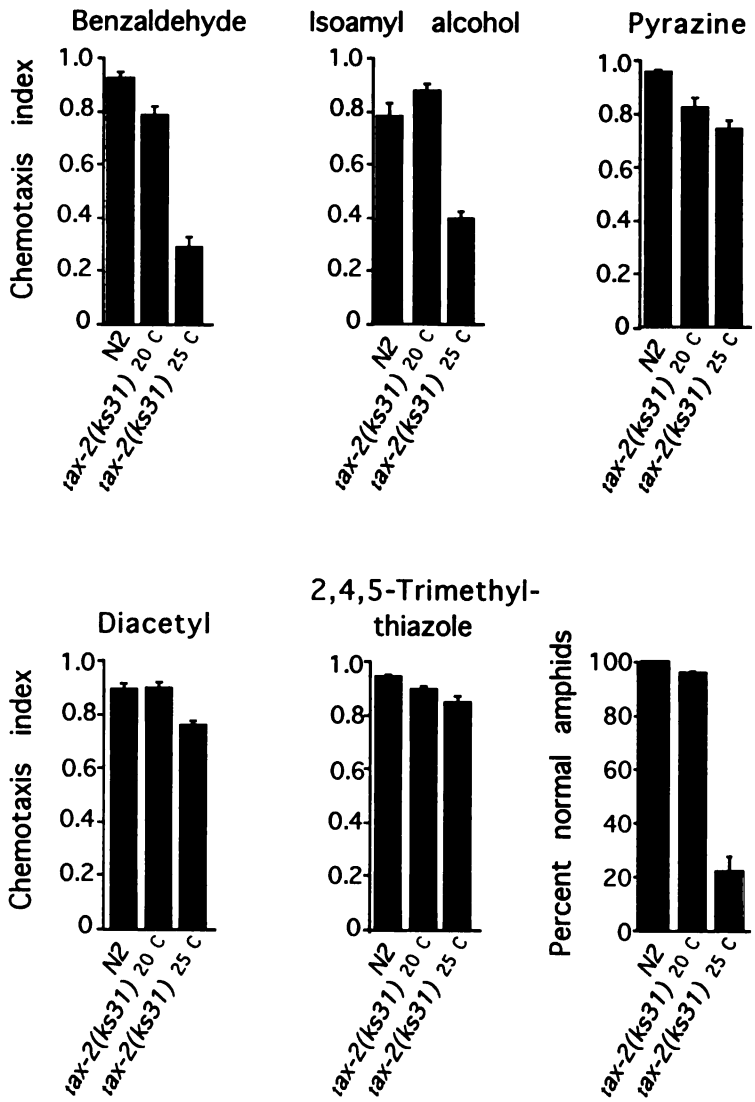
Benzaldehyde
Isoamyl alcohol
Pyrazine
Diacetyl
2,4,5-Trimethyl-thiazole
Chemotaxis index
Percent normal amphids
1.0
0.8
0.6
0.4
0.2
0
100
80
60
40
20
N2
tax-2(ks31) 20 C
tax-2(ks31) 25 C

Figure 2-6

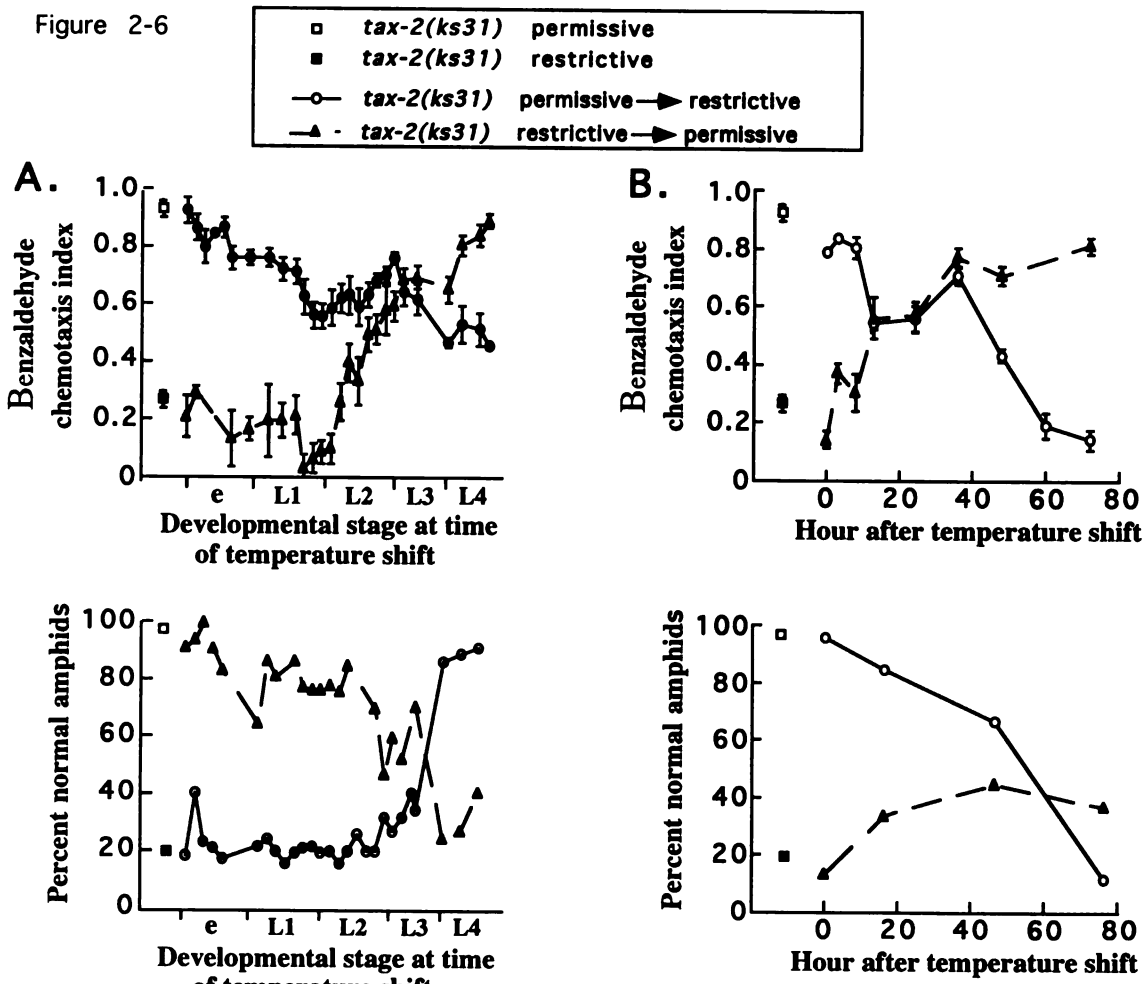
tax-2(ks31) permissive
tax-2(ks31) restrictive
tax-2(ks31) permissive → restrictive
tax-2(ks31) restrictive → permissive
A.
B.
Benzaldehyde chemotaxis index
1.0
0.8
0.6
0.4
0.2
0
e
L1
L2
L3
L4
Developmental stage at time of temperature shift
0
20
40
60
80
Hour after temperature shift
Percent normal amphids
100
80
60
40
20
0

Figure 2-6C

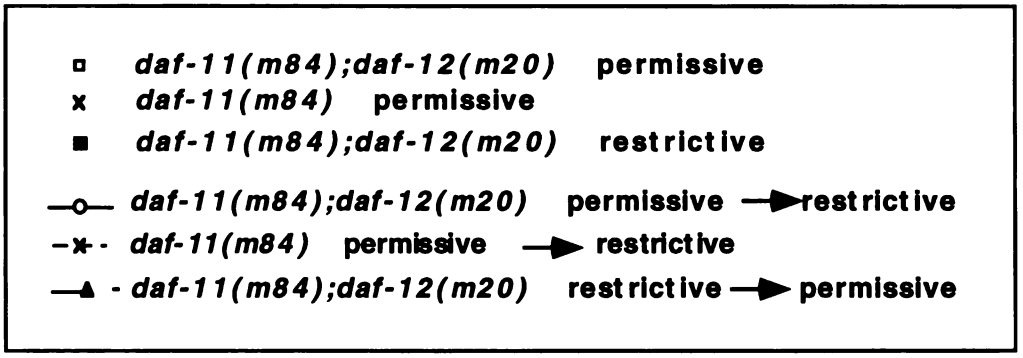
daf-11(m84);daf-12(m20) permissive
daf-11(m84) permissive
daf-11(m84);daf-12(m20) restrictive
daf-11(m84);daf-12(m20) permissive → restrictive
daf-11(m84) permissive → restrictive
daf-11(m84);daf-12(m20) restrictive → permissive

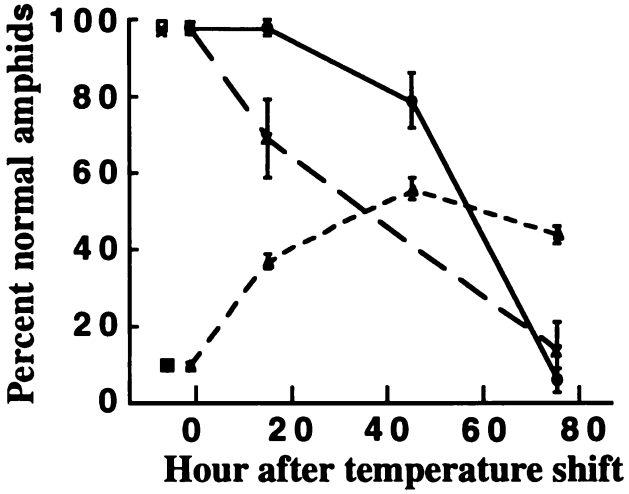
Percent normal amphids
100
80
60
40
20
0
0
20
40
60
80
Hour after temperature shift

Chapter Three

A genetic screen to identify more *tax*-2-like mutants.

Summary

The *C. elegans tax-2, tax-4, daf-11* and *daf-21* genes appear to encode genes with related function that regulate both sensory neuron development and function. *tax-4* and *tax-2*, which encode α and β subunits of a cyclic-nucleotide-gated channel, respectively, are required for chemosensation, thermosensation, normal axon guidance of some sensory axons and normal regulation of dauer larvae formation. *daf-11* and *daf-21* have similar behavioral and axon guidance phenotypes to *tax-2* and *tax-4*, and also have a strong dauer-constitutive phenotype. Mutations in *tax-2* and *tax-4* each suppress the *daf-11* and *daf-21* dauer-constitutive phenotype; however, the chemotaxis and axon guidance phenotypes in the double mutants resembled that of the strongest single mutant. We isolated 87 genetic suppressors of the *daf-11* dauer-constitutive phenotype which similarly had a stronger axon guidance defect than did the *daf-11* single mutant. The suppressors fell into three classes: four new *tax-2* and *tax-4* alleles; *ky95*, a mutant which suppresses both the *daf-11* dauer-constitutive and chemotaxis-defective phenotypes, and has an amphid neuron axon guidance defect as a single mutant; and a large group of mutants which either have amphid axon phenotypes only in the *daf-11* genetic background or are genetically linked to *daf-11*. These mutants could define new genes which act similarly to the *tax-2* and *tax-4* putative cyclic nucleotide-gated channels.

Introduction

Cyclic nucleotide-gated channels have prominent functions in vertebrate and invertebrate sensory systems. Vertebrate phototransduction, and olfactory transduction are all mediated by regulation of a cGMP or cAMP-sensitive channel (Nakamura and Gold, 1987; Stryer, 1991).

Phototransduction in some invertebrates also uses a cGMP-sensitive channel (Gomez and Nasi, 1995). In the nematode *C. elegans*, cyclic nucleotide-gated channels encoded by the *tax-2* and *tax-4* genes are required for some forms of chemosensation, thermosensation, and proper regulation of formation of the dauer larval stage. *tax-4* and *tax-2* encode predicted alpha and beta subunits of a cyclic-nucleotide-gated channel, respectively. Genetic data suggests that the gene products of *tax-2* and *tax-4* form a heteromeric channel of alpha and beta subunits, as is observed in vertebrate sensory systems (This thesis; H. Komatsu and I. Mori, pers. comm.).

In addition to these sensory functions, cyclic nucleotide-gated channels appear to have functions that are less well understood. The *tax-2* and *tax-4* genes are required for normal axon outgrowth of a subset of sensory neurons; in *tax-2* and *tax-4* mutants, some amphid and phasmid sensory axons fail to terminate in the proper position, instead projecting extensively into body regions where sensory axons are not usually found (This thesis). The *C. elegans* proteins are localized to the developing axons as well as the sensory cilia, supporting the model that the channels play a role in axon development as well as in sensory transduction (This thesis). Vertebrate cyclic nucleotide-gated channels are also found on axons of developing and mature neurons, where their function is unknown (J. Bradley and K. Zinn, pers. comm.).

Many molecules that function in sensory signal transduction with cyclic nucleotide-gated channels have been characterized in vertebrate visual and olfactory systems. Receptors (olfactory receptor or rhodopsin) activate G proteins (G_{olf} or $G_{transducin}$) which regulate downstream second messengers (adenylyl cyclase or phosphodiesterase), which indirectly regulate channel activity (Firestein and Zufall, 1994; Yau and Baylor, 1989). Ca^{2+}-calmodulin binds and regulates the activity of the channels, and other

molecules may modulate the activity of other components of the pathway (Chen and Yau, 1994; Gordon et al., 1992; Gordon et al., 1995; Hsu and Molday, 1993; Kramer and Siegelbaum, 1992). But many question remain unanswered. For example, the activity of CNG channels can be modulated by various treatments in patch experiments, but the physiological relevance of these manipulations are unknown (Gordon et al., 1992; Gordon et al., 1995). In addition, the identity and function of signal transduction components that may be acting with cyclic nucleotide-gated channels in the developing and mature sensory axons are not known.

The functions of the sensory neurons and their channels can be analyzed genetically in *C. elegans*. The entire nervous system consists of 302 neurons of 118 classes, including 16 classes of sensory neurons (White et al., 1986). The functions of eleven of these sixteen classes have been defined by cell ablation studies, in which behavioral or developmental abnormalities were observed after killing defined cell types. Two pairs of neurons recognize chemical repellents (ASH, ADL) (Bargmann et al., 1990; Troemel et al., 1995), five pairs of neurons recognize water-soluble attractants (ASE, ADF, ASG, ASI, ASK) (Bargmann and Horvitz, 1991), two pairs of neurons recognize volatile attractants (AWC, AWA) (Bargmann et al., 1993), and one pair of neurons detects temperature (AFD) (Mori and Ohshima, 1995). Three pairs of neurons that sense water-soluble attractants also regulate a developmental decision between two alternative larval states: the third-stage larva that will develop to a fertile adult, and the arrested dauer larva (ADF, ASG, ASI) (Bargmann and Horvitz, 1991). The ASJ neurons have two distinct functions in dauer development; they promote dauer formation in the presence of dauer pheromone and promote dauer recovery in the absence of pheromone (Bargmann and Horvitz, 1991; W. Shackwitz and J. Thomas, pers. comm.).

Genetic screens for behavioral mutants have identified genes that act in or on these sensory neurons. For example, both *tax-2* and *tax-4* are expressed in amphid neurons, including the ASI, ASG, and ASJ dauer-regulating neurons.

Genetic analysis has implicated *daf-11* and *daf-21* as genes which may function with the *tax-2* and *tax-4* cyclic nucleotide-gated channels (This thesis). *daf-11* encodes a retinal-class guanylyl cyclase (D. Birnby and J. Thomas, pers. comm.). Like *tax-2* and *tax-4*, *daf-11* and *daf-21* are required for some forms of chemosensation and have axon outgrowth defects in some sensory neurons that are phenotypically similar to those of *tax-2* and *tax-4* (This thesis; Vowels and Thomas, 1994). Finally, like *tax-2*, *daf-11* is required continuously throughout development for normal axon guidance (This thesis). *daf-11* and *daf-21* are also required for normal regulation of the dauer developmental pathway (Thomas et al., 1993). *daf-11* and *daf-21* mutants are strongly dauer-constitutive and dauer recovery-defective; in these mutants, the ASJ neurons appear to promote dauer larva formation even in the absence of pheromone (W. Shackwitz and J. Thomas, pers. comm.).

Double mutant analysis demonstrated genetic interactions between *daf-11* and *daf-21* and the *tax-2* and *tax-4* cyclic nucleotide-gated channels. *tax-2* and *tax-4* each strongly suppress the dauer-constitutive and dauer-recovery defects of *daf-11* and *daf-21* (This thesis). This result suggests that aberrant activation of ASJ in *daf-11* and *daf-21* mutants depends on the CNG channel, although normal ASJ function appears to be channel-independent since dauer recovery is intact in *tax-2* and *tax-4* mutants. The axon outgrowth and olfactory phenotypes of the *tax;daf*double mutants resembled those of the strongest single mutant in any given combination. Since *daf-11* and *daf-21* have less penetrant axon outgrowth defects, the double mutants always showed axon outgrowth defects with higher penetrance than that of *daf-11*

alone (This thesis). Although other sites of *daf-11* and *daf-21* action have not been determined (other than ASJ), previous work suggested that *daf-11* and *daf-21* might be acting in the amphid sensory neurons. *daf-11* and *daf-21* are suppressed by mutations in the cilia structure mutants, which have structurally abnormal chemosensory neuron cilia (Thomas et al., 1993). Also, *daf-11* and *daf-21* mutants have similar behavioral and axon outgrowth phenotypes to those of *tax-2* and *tax-4* mutants, suggesting that these genes affect similar amphid neurons (This thesis; Vowels and Thomas, 1992).

We sought to identify other genes with related functions to the *tax-2* and *tax-4* cyclic nucleotide-gated channel. A genetic screen was used to identify suppressors of the *daf-11* dauer-constitutive phenotype with an enhanced amphid axon outgrowth phenotype relative to that of *daf-11* alone. Here we describe and preliminarily characterize the three classes of suppressor identified: five new *tax-2* and *tax-4* alleles; *ky95*, a mutant which suppresses both the *daf-11* dauer-constitutive and chemotaxis-defective phenotypes, and has an amphid neuron axon guidance defect as a single mutant; and a large number of mutants which may either have amphid axon phenotypes only in the *daf-11* genetic background or are genetically linked to *daf-11*. These mutants could define new genes which act similarly to the *tax-2* and *tax-4* cyclic nucleotide-gated channels.

Results

A pilot screen for suppressors of *daf-11* dauer-constitutivity identified 7 classes of suppressors with an amphid axon guidance defect

Amy Kistler performed a pilot screen of approximately 25,000-30,000 haploid genomes in which F2 suppressors of *daf-11*(m47) or *daf-11*(m87) dauer-constitutivity were sought. 53 animals which re-tested as strong

suppressors (>60% non-dauers) were subjected to DiO staining to visualize the amphid and phasmid axon morphology. As expected, 9 of the strains did not take up DiO, a characteristic of the "cilium-structure" mutants which are already known to suppress *daf-11* (Table 3-1). Only one strain, *ky93;daf-11(m47)* showed complete suppression of *daf-11* dauer-constitutivity, benzaldehyde chemotaxis defects,and axon guidance defects, and is thus a candidate for an intragenic suppressor of *daf-11* (data not shown). All other *suppressor;daf-11* strains resembled *daf-11* in the severity of the amphid axon outgrowth defect, or showed either a novel axon guidance defect and/or an enhanced axon guidance defect similar to that of the *tax-2;daf-11* double mutant (Table 3-1).

Three novel amphid and phasmid phenotypes were observed in some of the *suppressor;daf-11* strains, and were characterized to determine the spectrum of amphid and phasmid defects that suppressor of *daf-11* dauer-constitutivity can display. The *ky81;daf-11(m87)*, *ky83;daf-11(m87)*, and *ky94;daf-11(m87)* mutant strains had highly penetrant prematurely-terminating phasmid axons, suggesting that phasmid axon extension depended on the *suppressor* and *daf-11* gene products. *ky81;daf-11* and *ky83;daf-11* also showed premature termination of the circumferential trajectory of the amphid axons. Interestingly, the short phasmid strain *ky94;daf-11(m87)* had an amphid axon phenotype similar to the *tax-2;daf-11* double mutant strains. The *ky57;daf-11(m87)*, *ky68;daf-11(m87)* and *ky105;daf-11(m47)* mutant strains showed highly penetrant long phasmid axons, suggesting that the weak *daf-11* phasmid termination defect was enhanced in these strains. Finally, four strains displayed dramatically mis-guided axons; the *ky91;daf-11(m87)*, *ky81;daf-11(m87)* and *ky56;daf-11(m87)* mutants had abberant anteriorally-projecting amphid axons at a low penetrance and

ky106;daf-11(m87) showed severe disorganization of both the amphid and phasmid axons. Some of these mutants also showed an enhanced amphid axon defect similar to that of *tax-2;daf-11* (Table 3-1). These mutants were not further characterized, unless they displayed an enhanced amphid axon defect.

The sixteen *suppressor;daf-11* strains which had an enhanced amphid axon phenotype were qualitatively tested for dauer-constitutivity under highly-inducing, crowded conditions. Under these assay conditions, *tax-2;daf-11* and *tax-4;daf-11* strains are weak suppressors of dauer formation. Most of the *suppressor;daf-11* strains were also among the weaker suppressors of the *daf-11* dauer-constitutive phenotype identified in this screen (data not shown). The strains were also tested for function of the AWC olfactory neurons. Five of the strains were able to chemotax to benzaldehyde, indicating that the *daf-11* benzaldehyde chemotaxis defect was also suppressed (Table 3-1).

The second *daf-11* suppressor screen may have enriched for mutants with a highly penetrant amphid axon phenotype

The second screen was modified to try to increase the number of suppressors that had an enhanced amphid axon phenotype similar to that of *tax-2;daf-11*. Approximately 40,000 haploid genomes of *daf-11(m47), daf-11(m87)* and *daf-11(sa195)* were screened for F2 suppressors of the dauer-constitutive phenotype. In this screen, weaker suppressors (>20% non-dauer) were selected because the interesting mutants from the first screen were among the weaker *daf-11* suppressors. *suppressor;daf-11* strains were subjected to DiO staining to examine amphid axon morphology, and all mutants that failed to fill with DiO and failed to show a stronger amphid axon guidance phenotype were discarded. 34/99 of the *suppressor;daf-11*

strains had strong amphid axon guidance defects, indicating that a higher proportion of the suppressors were in this class (Table 3-2). These mutant strains were also tested for benzaldehyde chemotaxis. 14 of the strains could chemotax to benzaldehyde, showing that the *daf-11* chemotaxis defect was also suppressed (Table 3-2).

Re-isolating suppressors as single mutants based on their amphid axon defect

Suppressor strains that showed an enhanced amphid axon phenotype compared to *daf-11* alone were back-crossed to eliminate *daf-11* (see methods). Suppressor mutants could be re-isolated as single mutants based on their amphid axon defect from only 6/50 back-crossed strains. Mapping experiments and complementation testing showed that *ky139* defined a new *tax-2* allele and *ky89, ky137, ky138,* and *ky140* defined new *tax-4* alleles. All of the mutants had highly penetrant amphid axon defects and weakly penetrant phasmid axon defects. As is observed for other *tax-2* and *tax-4* alleles, these mutants also failed to chemotax to benzaldehyde (Table 3-3). *ky89* and *ky139* also failed to chemotax to NaCl (C.M.C. and C.Bargmann, unpublished observation).

The sixth mutant, *ky95,* was recessive and had highly penetrant amphid axon defects and weakly penetrant phasmid axon defects which were identical to those observed in *tax-2* and *tax-4* (Table 3-3). *ky95* complemented *tax-2* and *tax-4* for the amphid axon phenotype. The amphid axon guidance phenotype was temperature-sensitive; animals grown at the permissive temperature (20°C) were indistinguishable from wild-type while animals grown at the restrictive temperature were strongly defective (data not shown). In addition, *ky95* had normal chemotaxis for all tested odorants at standard concentrations (Table 3-3; data not shown).

Discussion

Identifying genes with a related function to *tax-2* and *tax-4*

Mutation in the *tax-2* and *tax-4* cyclic nucleotide-gated channel each suppress the dauer-constitutive phenotype of *daf-11*, a gene with related function to the channel. To identify genes with similar functions to *tax-2* and *tax-4*, we screened for genetic suppressors of *daf-11* dauer-constitutivity which had a highly penetrant amphid sensory axon outgrowth defect similar to that of the *tax-2;daf-11* or *tax-4;daf-11* double mutant. 150 suppressors were identified, and 87/150 showed an enhanced or novel sensory axon phenotype compared to that of *daf-11* alone. No obvious differences were observed between suppressors of the three different *daf-11* alleles (Table 3-1,2). Interestingly, with the exception of several strains that failed to stain with DiO and one putative intragenic revertant with a normal axon structure, all of the *sup;pessordaf-11* strains had defective amphid axons. This suggests that mutations that can suppress both the dauer-constitutive and amphid axon outgrowth phenotypes of *daf-11* are very rare.

Some *suppressor;daf-11* strains showed no enhancement of the *daf-11* axon guidance phenotype. These suppressors could be downstream dauer-defective mutants such as *daf-3* and *daf-12* which suppress the *daf-11* dauer constitutive phenotype but do not enhance the axon outgrowth defect (Coburn et al; C.M.C. and C. Bargmann, unpublished data). Alternatively, these suppressor mutations might act in or on the dauer regulating neurons without affecting sensory axon morphology.

Alleles of *tax-2* and *tax-4* have not previously been identified in genetic screens for mutants with improper regulation of dauer formation. However one new *tax-2* allele and 4 new *tax-4* alleles were identified in this screen. All

had strong amphid axon outgrowth defects and failed to chemotax to benzaldehyde in combination with *daf-11* and as single mutants. *tax-2(ky139)* showed defects comparable to the strongest *tax-2* alleles, and molecular characterization demonstrated that the lesion was a point mutation in a conserved residue of the predicted pore region of the *tax-2* cyclic nucleotide-gated channel. Curiously, *tax-4(ky89)*, *tax-4(ky137)*, *tax-4(ky138)* and *tax-4(ky140)* all had a stronger amphid axon defect than that of the molecular null mutant, *tax-4(p678)*. The molecular lesions of these *tax-4* alleles are unknown, however the predicted pore region was sequenced and is normal in all four alleles (C.M.C. and C. Bargmann, unpublished observations).

ky95 suppressed both the *daf-11* dauer-constitutive phenotype and the benzaldehyde chemotaxis defect while enhancing its amphid axon outgrowth defect. Thus, *ky95* defines a *daf-11*-interacting gene with a new activity. As a single mutant, *ky95* showed a temperature-sensitive axon guidance defect similar to that of *daf-11* alone, and chemotaxed normally to all tested odorants. *ky95* could be acting directly or indirectly at some, but not all, *daf-11* sites of action; hence, some but not all phenotypes are suppressed. Alternatively, as was hypothesized for *tax-2* and *tax-4* suppression of *daf-11*, axon outgrowth could be an extremely sensitive system, unable to compensate or bypass the lesions caused by loss-of-function mutations. Many other models are possible; once the *daf-11* expression pattern is known, it will be easier to discern the role of *ky95*. It will also be informative to construct double mutants between *ky95* and the *tax-2* and *tax-4* cyclic nucleotide-gated channel mutants and to examine the localization of the tagged Tax-2 protein in *ky95* mutants.

daf-11 suppressor screen identified mutants which may have a synthetic phenotype

For a large number of suppressors, it proved impossible to re-isolate the suppressor as a single mutant based on the amphid axon guidance phenotype. These suppressors could be synthetic enhancers of the *daf-11* axon guidance defect, which show a phenotype only in the *daf-11* mutant background. Alternatively, the suppressors could have an amphid axon phenotype as a single mutant but be difficult to re-isolate because of a weakly penetrant phenotype or genetic linkage to the *daf-11* locus. Finally, the suppressors could be very weak alleles of the cilium structure mutants, which can appear wild-type as single mutants (C.M.C. and C. Bargmann, unpublished observations). Why are there so many mutants in this class? Since none of the suppressors have been mapped, it is possible that they represent independent isolates of the same gene or small number of genes. Alternatively, there may be many genes that can be be mutated to have this effect.

Intriguingly, 19/49 of the "synthetic" *suppressor;daf-11* strains also showed suppression of the *daf-11* benzaldehyde chemotaxis defect, suggesting that the suppressor could have some *ky95*-like activity. This observation also indicates that these strains are unlikely to contain a weak cilium-structure mutation, as such mutations do not suppress the *daf-11* benzaldehyde chemotaxis defect (C.M.C. and C. Bargmann, unpublished data).

Suppressors with a novel amphid and phasmid axon guidance defect

Ten of the suppressors isolate in the first screen showed different amphid and/or phasmid axon outgrowth phenotypes than the spectrum of defects observed in *daf-11*, *tax-2* and *tax-4*. Three of the *suppressor;daf-11*

strains had extremely long phasmid axons, suggesting that the suppressor enhanced the penetrance and expressivity of the weak *daf-11* phasmid termination defect. None of these suppressors could be re-isolated as a single mutant based on the amphid or phasmid axon phenotype (see results; C.M.C. and C. Bargmann, unpublished observations). Three strains displayed premature amphid and phasmid axon termination, suggesting that the suppressor gene product was required for the excessive axon growth observed in *daf-11*. Finally, some of the *suppressor;daf-11* strains had dramatically misguided axons. There are several possible reasons that these mutations suppress the *daf-11* dauer-constitutive phenotype. The axon outgrowth defects could inactivate the aberrant activation of the ASJ neurons thought to occur in *daf-11* mutants. This could cause suppression by a mechanism similar to that proposed for the cilium-structure mutants. Alternatively, and more speculatively, perhaps the suppressor gene products antagonize *daf-11* during normal axon outgrowth and/or guidance. *daf-11* is required for axons to terminate in the correct location; perhaps a *daf-11* antagonist would be required for axons to grow correctly to the termination point. Analysis of an engineered constitutively-active *daf-11* guanylyl cyclase might demonstrate this putative antagonism during axonal outgrowth.

Methods

Genetic methods: Genetic methods were as described in Brenner (Brenner, 1974). Some strains were provided by the *Caenorhabditis* Genetics Center. Some *daf-11* strains were provided by J. Thomas (University of Washington) and D. Riddle (University of Missouri). Marker mutations used were:
Linkage Group (LG)III: *dpy-16(e164)unc-32(e189)*
LGV: *him-5(e1490)*

***daf-11* suppressor screens:** The *daf-11* suppressor screen was described previously (This thesis). Since it is unclear whether any *daf-11* allele is a genetic null, three *daf-11* alleles were suppressed in an effort to isolate an allele-specific class of suppressors. Briefly, fourth larval stage (L4) *daf-11(m47), daf-11(m87)* and *daf-11sa195)* hermaphrodites were mutagenized with EMS and 3-5 animals were picked to 10 cm. plates at 15°C. The plates were left at 15°C until the F1 progeny had reached the L4 and young adult stages, then the plates were shifted to 25C. 3-5 days later the plates were screened for non-dauer F2 animals. Non-dauer animals that yielded non-dauer progeny at 25°C were subjected to DiO staining to visualize amphid and phasmid axon structure. Two slightly different screens were performed. In the first screen, performed by roton Amy Kistler, strong *daf-11* suppressors (defined as greater than 80% non-dauers at 25°C) were sought, and all suppressors with any amphid or phasmid phenotype were characterized. In the second screen, both weak and strong suppressors were selected, but only those with an enhanced amphid axon phenotype relative to *daf-11* alone were characterized. Approximately 70,000 genomes were screened. In both screens, suppressor strains that showed an enhanced amphid axon phenotype compared to *daf-11* alone were back-crossed by *him-5(e1490)* to eliminate *daf-11* and re-isolate the suppressor as a single mutant. Briefly, *him-5* males were crossed to *suppressor;daf-11* hermaphrodites and F1 cross-progeny were cloned. F2 broods were subjected to DiO staining and screened for animals with amphid neuron defects. Animals with amphid neuron defects which had 30% male progeny were inferred to be of the genotype *suppressor;him-5*. This was verified by complimentation testing to demonstrate that *daf-11* was indeed eliminated from the strain. In addition, the *ky89* and *ky95* mutants were back-crossed 6 more times by N2. It was impossible to re-isolate most of

the suppressors as single mutants based on an amphid axon defect, despite the enhancement of the *daf-11* amphid axon defects observed in the *suppressor;daf-11* original strain. These suppressors could be synthetic enhancers of the *daf-11* amphid axon defect which show their phenotype only in the *daf-11* mutant background. Alternatively, these suppressors could be genetically linked to *daf-11* on LGV or lack a strong amphid axon phenotype as a single mutant. These types of suppressors would be difficult to re-isolate using the *him-5* back-cross strategy.

Recessive/dominance testing: *sup;him-5* males were crossed into *dpy-5(e61)unc-32(e189)* and non-DpyUnc cross-progeny were tested for chemotaxis behavior and amphid axon phenotype.

Chemotaxis assays: Population chemotaxis assays were performed exactly as described (Bargmann et al., 1993). A 1:200 dilution of benzaldehyde was used to assay for the function of the AWC olfactory neurons. The chemotaxis index was calculated as described (Bargmann et al., 1993)

Qualitative dauer-formation assay: Animals were grown to near starvation on 100 cm. plates at 25°C, then plates were examined for the presence of large numbers of dauers. Under these conditions, *tax-2;daf-11* strains will produce large numbers of dauers because this strain is still pheromone-responsive. In contrast, *daf-11;dye-filling mutant* strains and *daf-11* strains carrying a downstream daf-d mutation (such as *daf-12)* produce very few dauers under these conditions (C.M.C. and C. Bargmann, unpublished observation).

DiO staining of chemosensory neurons: DiO staining was performed exactly as described (This thesis).

Temperature-sensitivity experiments: Animals were raised at either the permissive temperature (20°C) or the restrictive temperature (25°C), then tested as adults for chemotaxis to benzaldehyde and amphid axon structure.

Map data: The mapping of *tax-4(ky89)* and *tax-2(ky139)* has been described. *tax-4(ky137)*, *tax-4(ky138)* and *tax-4(ky140)* failed to complement *tax-4(p678)* for both the chemotaxis and amphid axon phenotypes. *ky95* was isolated in a strain which contained another mutation with a similar phenotype. The other mutation showed linkage to LGX (data not shown) and was eliminated from the *ky95* background by eliminating the original X chromosome during back-crossing. This yielded *ky95X5*. *ky95* complemented both *tax-2* and *tax-4* for chemotaxis and amphid axon phenotypes. There is presently no map position for *ky95*, however it is not linked to LGX or to *dpy-5* (LGIC), *bli-2* (LGIIC), *unc-32* (LGIIIC), *unc-5* (LGIVC), *dpy-2* (LGVC) or *lon-2* (LGXC). Mapping crosses were performed with the Bergerac strain in preparation for pcr polymorphism mapping, but the recombinants were not analyzed.

Table 3-1: The first *daf-11* suppressor screen identified 7 classes of suppressors, based on amphid and phasmid sensory neuron structure.

1. *dyf*-minus
   9/53 did not dye-fill with DiO

2. wild-type phenotype (candidate for intragenic suppression)
   ky93;daf-11(m47)

3. short phasmid sensory neurons
   ky81;daf-11(m87) (premature circumferential termination)
   ky83;daf-11(m87) (premature circumferential termination)
   *ky94;daf-11(m87)**

4. Highly penetrant very long phasmid sensory neurons
   ky57;daf-11(m87)
   *ky68;daf-11(m87)**
   *ky105;daf-11(m47)**

5. low-penetrance anteriorally-projecting amphid axon processes
   *ky91;daf-11(m87)**
   ky81;daf-11(m87)
   ky56;daf-11(m87)

6. Highly-penetrant general neuronal disorganization
   ky106;daf-11(m87) (*unc*)

7. highly-penetrant *tax*-2-like amphid axon phenotype
   ky63;daf-11(m87)
   ky64;daf-11(m87)
   ky66;daf-11(m87) (benzaldehyde chemotaxis +/-)
   ky68:daf-11(m87) (benzaldehyde chemotaxis +/-)
   ky70;daf-11(m87)
   ky79;daf-11(m47) (benzaldehyde chemotaxis +)

ky81;daf-11(m87)
ky82;daf-11(m47)
tax-4(ky89);daf-11(m87)
ky91;daf-11(m87)
ky95;daf-11(m47) (benzaldehyde chemotaxis +)
ky96;daf-11(m87) (benzaldehyde chemotaxis +)
ky97;daf-11(m87)
ky102;daf-11(m47)
ky103;daf-11(m47)

Other phenotypes observed in the strains are included in parentheses. An asterisc indicates that a *suppressor;daf-11* strain has a highly penetrant amphid axon phenotype. All of the class 7 *suppressor;daf-11* strains were also tested for supression of the *daf-11* benzaldehyde chemotaxis defect. The benzaldehyde concentration was 1:200 (diluted in ethanol). + indicates a chemotaxis index of greater than 0.6 while +/- indicates a chemotaxis index of 0.45-0.6.

Table 3-2: Benzaldehyde chemotaxis behavior of *suppressor;daf-11* strains identified in the second *daf-11* suppressor screen.

Benzaldehyde-minus *suppressor;daf-11* strains
tax-2(ky139);daf-11(m47)
tax-4(ky137);daf-11(sa195)
tax-4(ky138);daf-11(sa195)
tax-4(ky140);daf-11(m47)
16 more *suppressor;daf-11* strains that were discarded†.
Benzaldehyde-plus *suppressor;daf-11* strains
ky162;daf-11(m87)
ky163;daf-11(m47)
ky164;daf-11(m87)
ky165;daf-11(m87)
ky166;daf-11(m87)
ky167;daf-11(m87)
5A;daf-11(m47)†
25A;daf-11(m47)†
80;daf-11(sa195)†
82;daf-11(sa195)†
4 more strains that were discarded†.

Chemotaxis to a 1:200 dilution (in ethanol) of benzaldehyde was used. A strain was considered suppressed if the chemotaxis index was 0.6.
† = no *ky* allele number was assigned.

Table 3-3: Characterization of suppressors re-isolated as single mutants based on their amphid axon phenotype.

Strain	% normal amphid axons	% normal phasmid axons	Benzaldehyde chemotaxis	*sup;daf-11* benzaldehyde chemotaxis
tax-2(ky139)[a]	6	95	-	-
tax-4(ky89)[a]	5	94	-	-
tax-4(ky137)	N.D.[b]	N.D.	-	-
tax-4(ky138)	N.D.[b]	N.D.	-	-
tax-4(ky140	N.D.[b]	N.D.	-	-
ky95	23	100	+	+

[a]This thesis.
[b]Not carefully determined, but <20 % normal.

Percentage of normal amphid and phasmid axons were determined in DiO-stained animals. An amphid or phasmid was scored as defective if any axon was defective. + indicates a chemotaxis index of greater than 0.9 while - indicates a chemotaxis index of less than 0.25. Benzaldehyde chemotaxis of *suppressor;daf-11* strain is included for comparison.

Chapter 4

Conclusions and Future Directions

Summary

The *C. elegans tax-2* gene is required for some forms of olfaction, for chemosensation of salts, for thermosensation, and for proper regulation of a chemically-regulated developmental decision, the formation and recovery of the dauer larva. We show here that the *tax-2* gene encodes a putative cyclic nucleotide-gated channel that is expressed in sensory neurons, including neurons that mediate forms of olfaction, taste, thermosensation and dauer regulation that are defective in *tax-2* mutants. *tax-2* is also required for normal axon outgrowth of some sensory axons, indicating that the channel functions in sensory neuron development. Consistent with this proposed dual function, the Tax-2 protein is expressed in both sensory cilia and sensory axons.

The *tax-4*, *daf-11* and *daf-21* genes are also required for normal sensory neuron function and development in *C. elegans*. The *tax-4* mutant behavioral and axon outgrowth phenotypes are similar to those of *tax-2*, and *tax-4* encodes another predicted cyclic nucleotide-gated channel subunit (H. Komatsu and I. Mori, pers. comm.). Genetic and over-expression experiments suggest that *tax-2* and *tax-4* act together in sensory neuron development and function. The dauer-constitutive mutants *daf-11* and *daf-21* display behavioral and axon outgrowth phenotypes similar to those of *tax-2* and *tax-4*, and a genetic interaction indicates that these genes act in similar processes. Furthermore, temperature-shift experiments indicate that the *tax-2* and *daf-11* gene products are continuously required for normal sensory neuron function and axon morphology, even though the sensory neurons develop embryonically. These results demonstrate a novel late-acting plasticity of neuronal structure.

Future directions

Functional characterization

Although *tax*-2 has substantial sequence and structural homology to vertebrate CNG channels, it is important to demonstrate that it can form a channel. Since *tax*-2 appears to encode a β subunit of a CNG channel, it seems unlikely that it will form a functional homomeric channel in a heterologous expression system since all of the vertebrate β subunits fail to form channels as homomultimers. However, as is observed with the vertebrate channels, *tax*-2 may modify the kinetic and functional properties of an α subunit (perhaps *tax-4)* when reconstituted as a heteromultimeric channel in a heterologous system. Ikue Mori's group has preliminary evidence that *tax-4* forms a cGMP-gated non-specific cation conductance when expressed in 293 cells; it will be interesting to see if co-expression of *tax*-2 can modify the *tax-4* channel.

Functional characterization of the Tax-4 channel (being performed by the Mori lab) and of a possible Tax-4;Tax-2 heteromultimeric channel is critical to understanding how the channels are acting in sensory signal transduction. For example, it is essential to know if the channel is sensitive to cGMP, cAMP or both. It will also be interesting to compare the properties of a putative Tax-4;Tax-2 or Tax-4 channel expressed in heterologous cells to the native conductance recorded from the amphid sensory neurons (on the soon-to-arrive Bargmann lab rig!): if the conductances are similar, this would support the model that Tax-2 and Tax-4 could form a heteromultimer in the amphid sensory neurons. Direct physical interaction of Tax-2 and Tax-4 proteins can also be shown by immuno-precipitation experiments, either using Tax-2 and Tax-4-expressing heterologous cells, or directly from worms.

Reconstitution of a Tax-2;Tax-4 channel would also be useful for examining the effects of the *tax-2* mutations on channel function, as would direct recording from the worm amphid neurons in *tax-2* mutant animals. Four of the *tax-2* mutations are point mutations in predicted transmembrane regions, including three mutations in the predicted pore region of the channel. While all of the mutations are recessive and genetic analysis is consistent with the *p691* pore mutation being a loss-of-function mutation, it is not a foregone conclusion that the mutations eliminate or reduce channel function. For example, the mutations (especially those in the pore) could alter in the ion selectivity of the pore, as is observed in the mouse *weaver* K^+ channel mutant which is converted from a K^+ channel to Na^+ channel by a point mutation (when expressed as a homomultimer in heterologous cells). It also seems possible that channel gating or activation kinetics could be affected by pore point mutations, as is observed in engineered CNG channel mutants (see my Introduction). Finally, it should be possible to test if the *ks31ts* allele is temperature-sensitive for channel function, as opposed to channel synthesis.

Understanding the effects of the mutations will also aid the interpretation of the genetic experiments described in this thesis. It bears mention, however, that the *p694* deletion mutant is likely to be a strong loss-of-function mutant for *tax-2* in the ASE (taste) and AFD (thermosensory) neurons: the sequence deleted in the mutant appear to be required for cell-specific expression (or at least for strong expression) in ASE and AFD. The salt chemotaxis and thermotaxis phenotypes of *p694* are comparable to those observed in the other six *tax-2* alleles, although this certainly does not prove that these six alleles are also loss-of-function alleles.

Another model for the effects of the *tax-2* mutations

It seems possible that the *tax-2* mutants could cause defective CNG channel function by affecting proper assembly or membrane localization/insertion of the Tax-4 CNG channel. For example, truncated acetycholine receptor subunits dominant-negatively affect channel function by heteromultimerizing with other subunits then preventing effective membrane localization. In addition, some mutations in human rod α subunit of the cyclic nucleotide-gated channel prevented proper membrane localization when expressed in HEK cell (Dryja et al., 1995). This model seems less likely, however, again because of the mutant phenotype of the *p694* deletion mutant, which presumably does not express appreciable levels of *tax-2* in ASE and AFD. In addition, expression of several truncated *tax-2* channel fragments and of the *p691* mutant allele in wild-type worms did not cause a mutant phenotype, although it was not demonstrated that these constructs were well-expressed (unpublished data; Chapter 1). It is easy to create GFP-tagged versions of the mutant alleles, to see if expression level or sub-cellular localization of *tax-2* is affected by the mutations, and to look at the localization of a *tax-4::GFP* tag in *tax-2* mutants. I performed the converse experiment, and the subcellular localization of Tax-2::GFP protein appeared normal in the *tax-4(p678)* and *tax-4(ky89)* alleles (unpublished data). These types of experiments might also demonstrate the basis of the *ks10* and *ks15* mutant phenotypes, as no mutations in the coding region were found in these alleles.

Why does *tax-2* affect sensory neuron function and development?

This is a key question generated by my thesis work, and it is a difficult question to answer. First, I think it is extremely important to confirm the cellular and sub-cellular expression pattern observed in worms overexpressing the *tax-2::GFP* tag constructs with immunofluorescence

experiments using a *tax-2* antibody, although antibody experiments also have potential difficulties. A *tax-2* antibody could also be used to examine *tax-2* protein localization in *tax-2* and *tax-4* mutants. Next, it might be informative to express the *tax-2::GFP* tag under the control of cell-type specific promotors (especially *sre-1*, which is expressed in ASJ and ADL, and T01.1, which is expressed in ASK): perhaps *tax-2* localization is different in neurons which display axon outgrowth defects (eg: ASJ) verses neurons that have normal axons but do not function in behavior (eg:ASK). This experiment contrasts with the one we performed in Chapter 1, in which we observed the localization of Tax-2::GFP protein using the *tax-2* promotor sequences; it is not possible to say whether Tax-2::GFP protein was expressed in both the cilia and axons of every *tax-2*-expressing neuron. If an appropriate promotor is identified, it would be nice to look at ASE, which is defective for both axon structure and neuron function.

In Chapter 2, we described temperature shift experiments to ask when normal *tax-2* is required for proper behavior and normal axon development. In these experiments, the function of the AWC olfactory neuron was tested while the structure of the ASJ neuron was examined. Although we observed different temporal requirements for *tax-2* in the AWC neuron verses the ASJ neuron, it was unclear if this reflected differences between the timing of olfaction and axon outgrowth or different rates of protein accumulation in the neurons. It might be interesting to perform more temperature-shift experiments, focusing on the structure and function of a single neuron, the ASE neuron. It would be informative if it was possible to rescue ASE salt chemosensation function (by t-shifts to the permissive temperature) in adult animals that still displayed mutant ASE neuron structure. This would suggest that *tax-2* was rescuing behavioral function while the axon structure

was still defective, supporting the idea that *tax-2* has two functions in ASE. One problem with this experiment (and with all of the t-shift experiments) is that the mechanism by which *tax-2* affects axons in unknown. In particular, the change in axon morphology could lag long behind some initial *tax-2*-mediated event. For example, it is possible that in the apparently normal-looking sensory neurons that *tax-2* is subtly affecting something like synapse formation, that indirectly affects axons. Conversely, *tax-2* might function properly at the synapse (or wherever) in the adult animals that have rescued behavior but mutant long axons.

One way to ask if *tax-2* and *tax-4* act in axon development is to engineer a constitutively-open *tax-2*, *tax-4* or *tax-2;tax-4* CNG channel. There are no known mutations that produce this phenotype, unfortunately, but it might be possible to select a mutation in yeast using a method that has successfully identified constitutively-active non-specific *Shaker* potassium channels and *E. coli* mechanosensory channels (Ching Kung, pers. comm.). The *tax-2*, *tax-4*, or a tandem *tax-2;tax-4* cDNA could cloned into a GAL-regulated construct, then mutagenized *in vitro*. The construct is transformed into yeast, and transformants are selected that confer a GAL-dependent lethality. The constitutively-open channel could then be expressed in amphid neurons, and effects on axon outgrowth could be assessed. If normal *tax-2* is required to restrict or limit axon growth, it is possible that constitutively-active *tax-2* will cause very short or otherwise abnormal axons.

***daf-11* experiments**

daf-11 and *daf-21* are also required for both sensory neuron function and axon structure. Although *daf-11* has been cloned, the expression pattern and sub-cellular localization are unknown and could be informative. In addition, the molecular lesions of the many *daf-11* alleles will assist in

interpreting the genetics; although *daf-11* is recessive, the lack of a genetic deficiency of the locus has made it difficult to determine if the mutations are strong loss-of-function or even some sort of gain-of-function. The molecular identity of *daf-21* is unknown.

Since *daf-11* encodes a retinal class guanylyl cyclase (GC) (D. Birnby and J. Thomas, pers. comm.), when the clone is available, it should easy to engineer a constitutively-active GC by deleting the putative kinase domain. This engineered GC could then be expressed in amphid neurons and its effects on axon outgrowth examined. The constitutively-active *daf-11* might cause shortened or otherwise aberrant axons. In lieu of the *daf-11* clone, a heterologous constitutively-active GC could be misexpressed in the amphid neurons.

Finally, it seems slightly possible that *daf-11* might be functioning in axon guidance more directly; perhaps the ligand-binding domain of the GC is involve in sensing a guidance cue. This could be tested by misexpressing heterologous receptor GCs and their ligands in different places in the worm. For example, the GC-A receptor GC could be expressed in the amphid neurons while the ANP peptide ligand could be expressed in interneurons. Amphid axon structure could then be analyzed (after showing that neither construct affects worm neurons on their own).

Genetic experiments

A *tax-2* suppressor screen could identify molecules that act upstream and downstream of *tax-2* and, in principle, should identify genes that affect sensory function and sensory axon development. For example, this screen should identify genes that act in different sensory neurons as well as genes that act in one or a few neuron. One could identify new genes required for salt sensation, thermotaxis and olfaction, or normal axon outgrowth. *tax-2*

suppressors could be identified by screening for suppression of any behavioral phenotype (benzaldehyde olfaction is probably the most tractable) or by directly screening for suppressors of the axon phenotype (this would be easiest in an integrated *tax-2::GFP* strain). In addition, it is possible to select *tax-2* suppressors by suppressing the strong synthetic dauer-consitutivity of *tax-2;unc-31* double mutants. This screen selects for function of *tax-2* in the ASI and ASG sensory neurons. A rotation student, Jue Wang, performed a pilot of this screen and identified about 25 strong suppressors of the *tax-2;ks31);unc-31* dauer-constitutivity. A few of these were back-crossed out of the *unc-31* background by Jue and rotation student Sharif Taha, and seem to be promising suppressors of the *tax-2* benzaldehyde defect or of both the benzaldehyde and axon defects.

Activity models

It is possible that *tax-2* affects axon structure by altering membrane potential, either in the axon or in the sensory cilia. In vertebrate sensory systems, for example, neuronal activity is required in late stages of neuronal development to remodel and restrict axon arborizations to create the correct pattern of connections. It is unknown if *C. elegans* has an analogous process; however, the ASJ and ASE axons in *tax-2* and *tax-4* mutants are sometimes misrouted from the first point that the axon leaves the cell body, at a time before normal sensory stimuli are present and before synapses are made. If activity affects the development of these axons, it must occur at an earlier point in development than is observed in vertebrate sensory systems. Alternatively, it seems possible that this phenotype and the higher penetrance adult phenotype reflect errors that occur normally during amphid axon development in the worm but ae corrected in wild-type animals. Jen Zallen and Erin Peckol should answer this question by examining amphid

axon outgrowth in normal embryos. In addition, Gage Crump is starting a project in which he will look at synapse formation in neurons, including the ASJ neuron. It is possible that he will observe developmental plasticity in synapse formation or maintenance in wild-type or *tax-2/4* worms. Finally, if the *tax-2* phenotypes are due to inappropriate neuronal activity, it may be possible to phenocopy *tax-2* by mis-expressing heterologous channels in the amphid neurons. These experiment could be challenging, because it may be necesssary to modify electrical activity only in adult larval/adult animals to phenocopy *tax-2* (as opposed to during the period of axon development in the embryo). Erin Peckol is performing such experiments for her thesis project.

***tax-2* and *tax-4* prevent and promote dauer formation**

Laser ablation experiments showed that in the L1 stage, the ASJ amphid neuron is activated by pheromone and promotes dauer formation. In *daf-11* mutants, ASJ is inappropriately activated; *tax-2* and *tax-4* each suppress *daf-11* dauer-constitutivity. Are *tax-2* and *tax-4* normally required in ASJ to promote dauer-formation? This is tricky to ask, because *tax-2* and *tax-4* are required in the dauer-preventing neurons as well. It might be possible to construct *tax;daf-3* or *tax;daf-5* double mutants; *daf-3* and *daf-5* suppress the effects of the dauer-preventing neurons. Then the ASJ neuron could be killed in this strain background and the effect on dauer formation assessed. It will probably be necessary to stimulate dauer-formation with pheromone to see an effect of killing ASJ. This is not a particulary clean or easy experiment to do and it is easier to ask if *tax-2* or *tax-4* are suppressing *daf-11* by acting in the ASJ neurons. *tax-2* or *tax-4* can be expressed in *tax;daf-11* mutants under the control of the ASJ-specific promotor, *sre-1*. If the strain becomes dauer-

constitutive, this suggests that *tax-2/4* act in ASJ to suppress *daf-11* dauer-constitutivity.

tax-2/4 suppress the _daf-11_ dauer-recovery defect

The ASJ neuron is required for dauer recovery. *daf-11* and *daf-21* mutants are strongly dauer-recovery defective; *tax-2* and *tax-4* each suppress the *daf-11/21* dauer-recovery defect. Based on the laser ablation analysis of the *daf-11* role in dauer formation, *daf-11* mutations seemed to activate the ASJ neuron in dauer formation, yet *daf-11* mutations seemed to inhibit the ASJ function in dauer recovery. In addition, *tax-2/4* mutants have fairly normal dauer recovery, yet they also strongly suppress the *daf-11/21* dauer recovery defects. What is going on?

To understand these experiments, it is necesssary to show that the ASJ neuron is required for dauer recovery in *tax-2/4* mutants by killing ASJ in dauers and asking if they recover. In addition, it has never been shown that *daf-11/21* are actually acting in the ASJ neuron during dauer recovery. For example, it seems possible that another amphid neuron is inappropriately activated by the *daf-11*mutation and is affecting dauer recovery. Laser ablation experiments of all other amphid neurons but ASJ should indicate if inappropriate activation of a non-ASJ neuron is causing the *daf-11* recovery defect. Finally, if *sre-1::tax-2/4* can suppress the suppression of the dauer-recovery defects seen in *tax-2/4;daf-11* strains, this would also suggest that *tax-2/4* was required in ASJ to suppress the *daf-11* defect. If *tax-2/4* and *daf-11*are all acting in ASJ, this would be very interesting, because it would imply that different activities of the ASJ neuron are required for its roles in dauer-formation and dauer-recovery. Perhaps a developmental change occurs in the ASJ neuron.

tax-2/4 each suppress the _daf-11/21_ dauer formation and recovery defects but not the olfaction and axon outgrowth defects

It is easy to hypothesize that *tax-2/4* suppress *daf-11* dauer-formation defects because *daf-11* is a negative regulator of *tax-2/4* in the dauer -regulating neurons (see model A for a few possible pathways). By contrast, *tax-2*, *tax-4* and *daf-11* are all required for normal behavior, so it is not surprising that the double mutant combinations also display defective behavior. In these neurons, one hypothesizes that *daf-11* is a positive regulator of *tax-2/4* function (see model B).

What about the axon outgrowth defects of the *tax;daf* double mutants? In Chapter two, we showed that the axon outgrowth defects of the double mutants were no more defective than those of the single mutants, however, we did not show that the amphid axons affected in the *tax;daf* double mutants are the same as are affected in the single mutants. If the same axons are affected in the single and double mutants, that shows that the gene are acting in a similar process; *daf-11* may positively regulate *tax-2* (model B). If different axons are affected (which seems unlikely), that would be really interesting because it would simultaneously show suppression of the single mutant phenotypes and a synthetic phenotype in the double mutant strain.

How can *daf-11* be both a positive and negative regulator of *tax-2/4* function? It is possible that the signalling pathways are different in the different amphid neurons. Further genetic and molecular analysis of sensory signal transduction should clarify the situation. For example, 58 genetic suppressors of *daf-11* which enhance the *daf-11* amphid axon defects are described in Chapter Three. Interestingly, a large number of the suppressor mutants suppressed the *daf-11* dauer-constitutivity, and the benzaldehyde olfactory defect. These mutants, exemplified by the very interesting *ky95*

Figure legend

Figure 4-1: Models of possible *tax-2*, *tax-4* and *daf-11* interactions.

Figure 4-1

A. *daf-11* is a negative regulator of *tax-2* and *tax-4*.

daf-11 ⊣ *tax-2/tax-4*

daf-11 → X ⊣ *tax-2/tax-4*

eg A1:

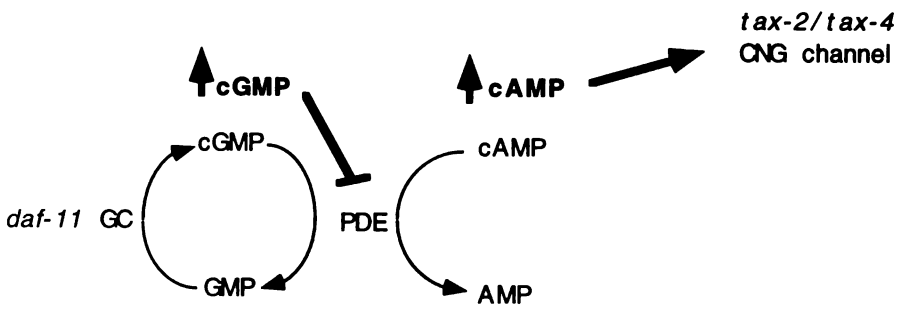

eg A2:

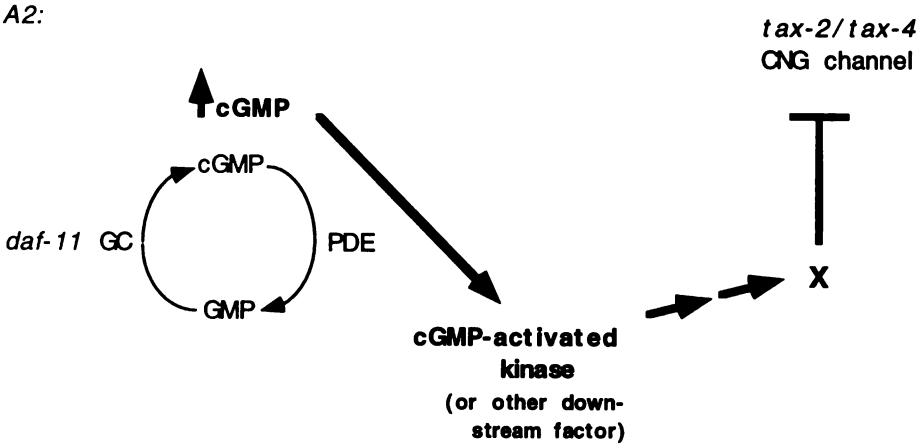

B. *daf-11* is a positive regulator of *tax-2/tax-4*

daf-11 ⟶ *tax-2/tax-4*

daf-11 ⊣ X ⊣ *tax-2/tax-4*

eg B1:

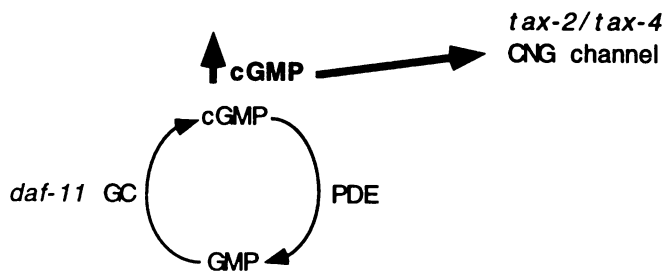

eg B2:

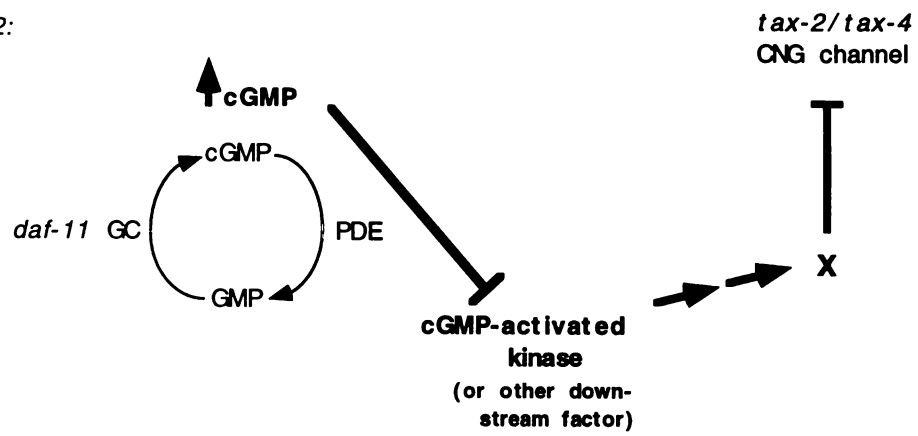

Bibliography

Ahmad, I., Leinders-Zufall, T., Kocsis, J. D., Shepherd, G. M., Zufall, F., and Barnstable, C. J. (1994). Retinal ganglion cells express a cGMP-gated cation conductance activatable by nitric oxide donors. Neuron *12*, 155-165.

Altenhofen, W., Ludwig, J., Eismann, E., Kraus, W., Bonigk, W., and Kaupp, U. (1991). Control of ligand specificity in cyclic nucleotide-gated channels from rod photoreceptors and olfactory epithelium. Proc. Natl.Acad.Sci.USA *88*, 9868-9872.

Altschul, S. F., Gish, W., Miller, W., Myers, E. W., and Lipman, D. J. (1990). Basic local alignment search tool. J. Mol. Biol. *215*, 403-410.

Arancio, O., Kandel, E. R., and Hawkins, R. D. (1995). Activity-dependent long-term enhancement of transmitter release by presynaptic 3',5'-cyclic GMP in cultured hippocampal neurons. Nature *376*, 74-80.

Avenet, P., and Lindemann, B. (1988). Amiloride-blockable sodium currents in isolated taste receptor cells. J. Memb. Biol. *105*, 245-255.

Bargmann, C. I. (1993). Genetic and cellular analysis of behavior in *C. elegans*. Ann.Rev.Neurosci. *16*, 47-71.

Bargmann, C. I., Hartwieg, E., and Horvitz, H. R. (1993). Odorant-selective genes and neurons mediate olfaction in *C. elegans*. Cell *74*, 515-527.

Bargmann, C. I., and Horvitz, H. R. (1991). Chemosensory neurons with overlapping functions direct chemotaxis to multiple chemicals in *C. elegans*. Neuron *7*, 729-742.

Bargmann, C. I., and Horvitz, H. R. (1991). Control of larval development by chemosensory neurons in *Caenorhabditis elegans*. Science *251*, 1243-1246.

Bargmann, C. I., Thomas, J. H., and Horvitz, H. R. (1990). Chemosensory cell function in the behavior and development of *Caenorhabditis elegans*. Cold Spring Harbor Symp. Quant. Biol. *LV*, 529-538.

Barstead, R. J., and Waterston, R. H. (1989). The basal component of the nematode dense-body is vinculin. J. Biol. Chem. *264*.

Baumann, A., Frings, S., Godde, M., Seifert, R., and Kaupp, U. B. (1994). Primary structure and functional expression of a Drosophila cyclic nucleotide-gated channel present in eyes and antennae. EMBO J. *13*, 5040-5050.

Baylor, D., Lamb, T., and Yau, K.-W. (1979). Responses of retinal rods to single photons. J. Physiol. *288*, 613-619.

Bedlack, R., Wei, M., and Loew, L. (1992). Localized membrane depolarizations and localized calcium influx during electric field-guided neurite growth. Neuron *9*, 393-403.

Berghard, A., and Buck, L. B. (1996). Sensory transduction in vomeronasal neurons: evidence for G alpha o, G alpha i2, and adenylyl cyclase II as major components of a pheromone signalling cascade. J. Neurosci. *16*, 909-918.

Biel, M., Zong, X., Distler, M., Bosse, E., Klugbauer, N., Murakami, M., Flockerzi, V., and Hofmann, F. (1994). Another member of the cyclic nucleotide-gated channel family, expressed in testis, kidney, and heart. Proc. Natl. Acad. Sci. USA *91*, 3505-3509.

Bonigk, W., Altenhofen, W., Muller, F., Dose, A., Illing, M., Molday, R. S., and Kaupp, U. B. (1993). Rod and cone photoreceptor cells express distinct genes for cGMP-gated channels. Neuron *10*, 865-877.

Bradley, J., Li, J., Davidson, N., Lester, H. A., and Zinn, K. (1994). Heteromeric olfactory cyclic nucleotide-gated channels: a new subunit that confers increased sensitivity to cAMP. Proc.Natl.Acad.Sci.USA *91*, 8890-8894.

Brainard, M. S., and Knudsen, E. I. (1993). Experience-dependent plasticity in the inferior colliculus: a site for visual calibration of the neural representation of auditory space in the barn owl. J. Neurosci. *13*, 4589-4608.

Brenner, S. (1974). The genetics of Caenorhabditis elegans. Genetics *77*, 71-94.

Broillet, M.-C., and Firestein, S. (1996). Direct activation of the olfactory cyclic nucleotide-gated channel through modification of sulfhydryl groups by NO compounds. Neuron *16*, 377-385.

Bruggemann, A., Pardo, L. A., Stuhmer, W., and Pongs, O. (1993). Ether-a-go-go encodes a volatage-gated channel permeable to K+ and Ca2+ and modulated by cAMP. Nature *365*, 445-448.

Budnik, V., Zhong, Y., and Wu, C. F. (1990). Morphological plasticity of motor axons in *Drosophila* mutants with altered excitability. J. Neurosci. *10*, 3754-3768.

Catterall, W. (1995). Structure and function of voltage-gated ion channels. Ann.Rev.Biochem. *64*, 493-531.

Chen, T., and Yau, K. (1994). Direct modulation by Ca(2+)-calmodulin of cyclic nucleotide-activated channel of rat olfactory receptor neurons. Nature *368*, 545-548.

Chen, T.-Y., Illing, M., Molday, L., Hsu, Y.-T., Yau, K.-W., and Molday, R. (1994). Subunit 2 (or β) of retinal rod cGMP-gated channel is a component of the 240--kDa channel-associated protein and mediates Ca2+-calmodulin modulation. Proc. Natl. Acad. Sci. USA *91*, 11757-11761.

Chen, T.-Y., Peng, Y.-W., Dhallen, R., Ahamedi, B., Reed, R., and Yau, K.-W. (1993). A new subunit of the cyclic nucleotide-gated cation channel in retinal rods. Nature *362*, 764-767.

Colbert, H. A., and Bargmann, C. I. (1995). Odorant-specific adaptation pathways generate olfactory plasticity in *C. elegans*. Neuron *14*, 803-812.

Constantine-Paton, M., Cline, H., and Debski, E. (1990). Patterned activity, synaptic convergence, and the NMDA receptor in developing visual pathways. Ann. Rev. Neurosci. *13*, 129-154.

Cook, S., and Babcock, D. (1993). Selective modulation by cGMP of the K+ channel activated by speract. J.Biol.Chem *268*, 22402-22407.

Culotti, J. G., and Russell, R. L. (1978). Osmotic avoidance defective mutants of the nematode Caenorhabditis elegans. Genetics *90*, 243-256.

Desai, C., Garriga, G., McIntire, S. L., and Horvitz, H. R. (1988). A genetic pathway for the development of the Caenorhabditis elegans HSN motor neurons. Nature *336*, 638-646.

Dhallan, R. S., Yau, K.-W., Schrader, K. A., and Reed, R. R. (1990). Primary structure and functional expression of a cyclic nucleotide-activated channel from olfactory neurons. Nature *347*, 184-187.

Dhallen, R., Macke, J., Eddy, R., Shows, T., Reed, R., et al. (1992). Human rod photoreceptor cGMP-gated channel: amino acid sequence, gene structure, and functional expression. J.Neurosci *12*, 3248-3256.

Dryja, T. P., Finn, J. T., Peng, Y. W., McGee, T. L., Berson, E. L., and Yau, K-W. (1995). Mutations in the gene encoding the alpha subunit of the rod cGMP-gated channel in autosomal recessive retinitis pigmentosum. Proc. Nat. Acad. Sci. USA *92*:10177-10181.

Dubin, A. E., and Dionne, V. E. (1994). Action potentials and chemosensitive conductances in the dendrites of olfactory neurons suggest new features for odor transduction. J. Gen. Physiol. *103*, 181-201.

Dusenbery, D. B. (1974). Analysis of chemotaxis in the nematode Caenorhabditis elegans by countercurrent separation. J. Exp. Zool. *188*, 41-7.

Dusenbery, D. B., Sheridan, R. E., and Russell, R. L. (1975). Chemotaxis-defective mutants of the nematode Caenorhabditis elegans. Genetics *80*, 297-309.

Eismann, E., Muller, F., Heinemann, S., and Kaupp, U. (1994). A single negative residue within the pore region of a cGMP-gated channel controls rectification, Ca2+ blockage, and ionic selectivity. Proc.Natl.Acad.Sci.USA *91*, 1109-1113.

El-Husseini, A., Bladen, C., and Vincent, S. (1995). Expression of the olfactory cyclic nucleotide-gated channel (CNG1) in the rat brain. Neuroreport *6*, 1459-1463.

Estevez, M., Attisano, L., Wrana, J. L., Albert, P. S., Massague, J., and Riddle, D. L. (1993). The daf-4 gene encodes a bone morphogenetic protein receptor controlling C. elegans dauer larva development. Nature *365*, 644-649.

Felsenfeld, J. (1989). PHYLIP--Phylogeny Inference Program (Version 3.2). Cladistics *5*, 164-166.

Fesenko, E., Kolesnikov, S., and Lyubarsky, A. (1985). Induction by cGMP of cationic conductance in plasma membrane of retinal rod outer segment. Nature *313*, 310-313.

Fesenko, E. E., Novoselov, V. I., and Krapivinskaya, L. D. (1979). Molecular mechanisms of olfactory reception. IV. Some biochemical characteristics of the camphor receptor from rat olfactory epithelium. Bioch. Biophys. Acta *587*, 424-433.

Firestein, F., and Zufall, F. (1994). The cyclic nucleotide gated channel of olfactory receptor neurons. Sem. Cell Biol. *5*, 39-46.

Firestein, S., Zufall, F., and Shepherd, G. M. (1991). Single odor-sensitive channels in olfactory receptor neurons are also gated by cyclic nucleotides. J. Neurosci. *11*, 3565-3572.

Fox, K., Schlaggar, B., Glazewski, S., and O'Leary, D. (1996). Glutamate receptor blockade at cortical synapses disrupts development of thalamocortical and columnar organization in somatosensory cortex. Proc. Nat. Acad. Sci. USA *93*, 5584-5589.

Frings, S., Lynch, J., and Lindemann, B. (1992). Properties of cyclic nucleotide-gated channels mediating olfactory transduction: activation, selectivity and blockage. J. Gen. Physiol *100*, 45-67.

Frings, S., Seifert, R., Godde, M., and Kaupp, U. B. (1995). Profoundly different calcium permeation and blockage determine the specific function of distinct cyclic nucleotide-gated channels. Neuron *15*, 169-179.

Georgi, L. K., Albert, P. S., and Riddle, D. L. (1990). *daf-1*, a *C. elegans* gene controlling dauer larva development, encodes a novel receptor protein kinase. Cell *61*, 635-645.

Golden, J. W., and Riddle, D. L. (1984). The Caenorhabditis elegans dauer larva: developmental effects of pheromone, food, and temperature. Dev. Biol. *102*, 368-78.

Gomez, M., and Nasi, E. (1995). Activation of light-dependent K+ channels in ciliary invertebrate photoreceptors involves cGMP but not the IP3/Ca2+ cascade. Neuron *15*, 607-618.

Goodman, C., and Shatz, C. (1993). Developmental mechanisms of neuronal connectivity. Cell/Neuron *10*, 77-98.

Gordon, S., Brautigan, D., and Zimmerman, A. (1992). Protein phosphatases modulate the apparent affinity of the light-regulated ion channel in retinal rods. Neuron *9*, 739-748.

Gordon, S., Downing-Park, J., Tam, B., and Zimmerman, A. (1995). Diacylglycerol analogs inhibit the rof cGMP-gated channel by a phosphorylation-independent mechanism. Biophys. J. *69*, 409-417.

Gordon, S., Downing-Park, J., and Zimmerman, A. (1995). Modulation of the cGMP-gated ion channel in frog rods by calmodulin and an endogenous inhibitory factor. J.Phys. *486*, 533-546.

Gordon, S., and Zagotta, W. (1995). A histidine residue associated with the gate of the cyclic nucleotide-activated channel in rod photoreceptors. Neuron *14*, 177-183.

Gordon, S. E., and Zagotta, W. N. (1995). Localization of regions affecting an allosteric transition in cyclic nucleotide-activated channels. Neuron *14*, 857-864.

Gordon, S. E., and Zagotta, W. N. (1995). Subunit interactions in coordination of Ni2+ in cyclic nucleotide-gated channels. Proc. Natl. Acad. Sci.USA *92*, 10222-10226.

Goulding, E., Ngai, J., Kramer, R., Colicos, S., Axel, R., Siegelbaum, S., and Chess, A. (1992). Molecular cloning and single-channel properties of the cylic nucleotide-gated channel from catfish olfactory neurons. Neuron *8*, 45-58.

Goulding, E., Tibbs, G., Liu, D., and Siegelbaum, S. (1993). Role of H5 domain in determining pore diameter and ion permeation through cyclic nucleotide-gated channels. Nature *372*, 61-64.

Goulding, E. H., Tibbs, G. R., and Siegelbaum, S. A. (1994). Molecular mechanism of cyclic nucleotide-gated channel activation. Nature *372*, 369-374.

Hatt, H., and Ache, B. (1994). Cyclic nucleotide- and inositol phosphate-gated ion channels in lobster olfactory receptor neurons. Proc. Natl. Acad. Sci. USA *91*, 6264-6268.

Hedgecock, E. M., Culotti, J. G., and Hall, D. H. (1990). The unc-5, unc-6, and unc-40 genes guide circumferential migrations of pioneer axons and mesodermal cells on the epidermis in C. elegans. Neuron *4*, 61-85.

Hedgecock, E. M., and Russell, R. L. (1975). Normal and mutant thermotaxis in the nematode Caenorhabditis elegans. Proc. Natl. Acad. Sci. USA *72*, 4061-5.

Heginbotham, L., Abramson, T., and MacKinnon, R. (1992). A functional connection between the pores of distantly related ion channels as revealed by mutant K+ channels. Science *258*, 1152-1155.

Henderson, C. E., Huchet, M., and Changeux, J. P. (1983). Denervation increases a neurite-promoting activity in extracts of skeletal muscle. Nature *302*, 609-611.

Henn, D., Baumann, A., and Kaupp, U. (1995). Probing the transmembrane topology of cyclic nucleotide-gated ion channels with a gene fusion approach. Proc. Natl.Acad.Sci.USA *92*, 7425-7429.

Henn, D. K., Baumann, A., and Kaupp, U. B. (1995). Probing the transmembrane topology of cyclic nucleotide-gated ion channels with a gene fusion approach. Proc.Natl.Acad.Sci.USA *92*, 7425-7429.

Herman, R., and Hedgecock, E. (1990). Limitation of the size of the vulval primordium of Caenorhabditis elegans by lin-15 expression in surrounding hypodermis. Nature *348*, 169-171.

Hess, E. (1996). Identification of the weaver mouse mutation: the end of the beginning. Neuron *16*, 1073-1076.

Hiraoka, Y., Sedat, J. W., and Agard, D. A. (1990). Determination of three-dimensional imaging properties of a light microscope system. Partial confocal behavior in epifluorescence microscopy. Biophys. J. *57*, 325-333.

Hsu, Y.-T., and Molday, R. (1993). Modulation of the cGMP-gated channel of rod photoreceptor cells by calmodulin. Nature *361*, 76-79.

Huang, L. S., Tzou, P., and Sternberg, P. W. (1994). The lin-15 locus encodes two negative regulators of Caenorhabditis elegans vulval development. Mol. Biol. Cell *5*, 395-412.

Huang, X. Y., and Hirsh, D. (1989). A second trans-spliced RNA leader sequence in the nematode Caenorhabditis elegans. Proc. Natl. Acad. Sci. USA *86*, 8640-8644.

Jan, L., and Jan, Y. (1992). Tracing the roots of ion channels. Cell *69*, 715-718.

Jarecki, J., and Keshishian, H. (1995). Role of neural activity during synaptogenesis in Drosophila. J. Neurosci. *15*, 8177-8190.

Kaplan, J., and Horvitz, H. (1993). A dual mechanosensory and chemosensory neuron in *Caenorhabditis elegans*. Proc. Natl. Acad. Sci. USA *90*, 2227-2231.

Karpen, J., Brown, R., Stryer, L., and Baylor, D. (1993). Interactions between divalent cations and the gating machinery of cyclic-GMP-activated channels in salamander retinal rods. J.Gen.Physiol. *101*, 1-25.

Kater, S., and Mills, L. (1991). Regulation of growth cone behavior by calcium. J. Neurosci. *11*, 891-899.

Kaupp, U., Nudome, T., Tanabe, T., Terada, S., Bonigk, W., Stuhmer, W., Cook, N., Kangawa, K., Matsuo, H., Hirose, T., Miyata, T., and Numa, S. (1989). Primary structure and functional expression of complementary DNA of the rod photoreceptor cyclic GMP-gated channel. Nature *342*, 762-766.

Kleene, S. J. (1993). Origin of the chloride current in olfactory transduction. Neuron *11*, 123-132.

Klein, R. D., and Meyer, B. J. (1993). Independent domains of the Sdc-3 protein control sex determination and dosage compensation in C. elegans. Cell *72*, 349-364.

Kleinschmidt, A., Bear, M., and Singer, W. (1987). Blockade of NMDA receptors disrupts experience-dependent modifications in kitten striate cortex. Science *238*, 355-358.

Kofuji, P., Hofer, M., Millen, K., Millonig, J., Davidson, N., Lester, H., and Hatten, M. (1996). Functional analysis of the weaver mutant GIRK2 K+ channel and rescue of weaver granule cells. Neuron *16*, 941-952.

Korschen, H. G., Illing, M., Seifert, R., Sesti, F., Williams, A., Gotzes, S., Colville, C., Muller, F., Dose, A., Godde, M., Molday, L., Kaupp, U. B., and Molday, R. S. (1995). A 240 kDa protein represents the complete beta subunit of the cyclic nucleotide-gated channel from rod photoreceptor. Neuron *15*, 627-636.

Kountalos, Y., and Yau, K.-W. (1996). Regulation of the sensitivity in vertebrate rod photoreceptors by calcium. TINS *19*, 73-81.

Kramer, R., Goulding, E., and Siegelbaum, S. (1994). Potassium channel inactivation peptide blocks cyclic nucleotide-gated channels by binding to the conserved pore domain. Neuron *12*, 655-662.

Kramer, R., and Siegelbaum, S. (1992). Intracellular Ca2+ regulates the sensitivity of cyclic nucleotide-gated channels in olfactory receptor neurons. Neuron *9*, 897-906.

Kumar, V., and Webr, I. (1992). Molecular model of the cyclic nucleotide-binding domain of the cGMP-gated ion channel. Biochemistry *31*, 4643-4649.

Leiders-Zufall, T., Rosenbloom, H., Barnstable, C., Shepherd, G., and Zufall, F. (1995). A calcium-permeable cGMP-activated conductance in hippocampal neurons. Neuroreport *6*, 1761-1765.

Lewis, J. A., and Hodgkin, J. A. (1977). Specific neuroanatomical changes in chemosensory mutants of the nematode Caenorhabditis elegans. J. Comp. Neurol. *172*, 489-510.

Li, Y., Erzurumlu, R. S., Chen, C., Jhaveri, S., and Tonegawa, S. (1994). Whisker-related neuronal patterns fail to develop in the trigeminal brainstem nuclei of NMDAR1 knockout mice. Cell *76*, 427-437.

Liman, E. R., and Buck, L. B. (1994). A second subunit of the olfactory cyclic nucleotide-gated channel confers high sensitivity to cAMP. Neuron *13*, 611-621.

Liu, D., Tibbs, G., and Siegelbaum, S. (1996). Subunit stoichiometry of cyclic nucleotide-gated channels and effects of subunit order. Neuron *16*, 983-990.

Liu, M., Chen, T.-Y., Ahamed, B., Li, J., and Yau, K.-W. (1994). Calcium-calmodulin modulation of the olfactory cyclic nucleotide-gated cation channel. Science *266*, 1348-1354.

Lowe, G., and Gold, G. H. (1993). Nonlinear amplification by calcium-dependent chloride channels in olfactory receptor cells. Nature *366*, 283-286.

Luo, Y., Raible, D., and Raper, J. A. (1993). Collapsin: a protein in brain that induces the collapse and paralysis of neuronal growth cones. Cell *75*, 217-227.

Maricq, A. V., Peckol, E., Driscoll, M., and Bargmann, C. I. (1995). Mechanosensory signalling in *C. elegans* mediated by the GLR-1 glutamate receptor. Nature *378*, 78-81.

Mattson, M., and Kater, S. (1987). Calcium regulation of neurite elongation and growth cone motility. J. Neurosci *7*, 4034-4043.

McCaig, C. (1989). Nerve growth in the absence of growth cone filopodia and the effects of an applied electric field. J.Cell Sci. *93*, 715-721.

McIntire, S. L., Garriga, G., White, J. G., Jacobson, D., and Horvitz, H. R. (1992). Genes necessary for directed axonal elongation or fasciculation in *Caenorhabditis elegans*. Neuron *8*; 307-329.

Mello, C. C., Kramer, J. M., Stinchcomb, D., and Ambros, V. (1991). Efficient gene transfer in C. elegans: Extrachromosomal maintenance and integration of transforming sequences. EMBO J. *10*, 3959-3970.

Messersmith, E. K., Leonardo, E. D., Shatz, C. J., Tessier-Lavigne, M., Goodman, C. S., and Kolodkin, A. L. (1995). Semaphorin III can function as a selective chemorepellent to pattern sensory projections in the spinal cord. Neuron *14*, 949-959.

Molday, R., Molday, L., Dose, A., Clark, L., Illing, M., et al. (1991). The cGMP channel of the rod photoreceptor cell: characterization and orientation of the amino terminus. J.Biol.Chem. *219*, 21917-21922.

Mori, I., and Ohshima, Y. (1995). Neural regulation of thermotaxis in Caenorhabditis elegans. Nature *376*, 344-348.

Nakamura, T., and Gold, G. H. (1987). A cyclic nucleotide-gated conductance in olfactory receptor cilia. Nature *325*, 442-444.

Neeley, M., and Nicholls, J. (1995). Electrical activity, growth cone motility and the cytoskeleton. J. Exp. Biol. *198*, 1433-1446.

Patil, N., Cox, D. R., Bhat, D., Faham, M., Myers, R. M., and Peterson, A. S. (1995). A potassium channel mutation in weaver mice implicates membrane excitability in granule cell differentiation. Nature Genetics *11*, 126-129.

Riddle, D. L. (1988). The dauer larva. In *The Nematode* Caenorhabditis elegans, W. B. Wood, ed. (New York: Cold Spring Harbor Laboratory), pp. 393-412.

Riddle, D. L., Swanson, M. M., and Albert, P. S. (1981). Interacting genes in nematode dauer larva formation. Nature *290*, 668-671.

Rieke, F., and Schwartz, E. A. (1994). A cGMP-gated current can control exocytosis at cone synapses. Neuron *13*, 863-873.

Root, M., and MacKinnon, R. (1993). Identification of an external divalent-cation binding site in the pore of a cyclic nucleotide-gated channel. Neuron *11*, 459-466.

Root, M., and MacKinnon, R. (1994). Two identical noninteracting sites in an ion channel revealed by proton transfer. Science *256*, 1852-1856.

Sambrook, J., Fritsch, E. F., and Maniatis, T. (1989). Molecular Cloning: A Laboratory Manual, 2nd Edition (Cold Spring Harbor, NY: Cold Spring Harbor Press).

Schacher, S., Kandel, E. R., and Montarolo, P. (1993). cAMP and arachidonic acid simulate long-term structural and functional changes produced by neurotransmitters in Aplysia sensory neurons. Neuron *10*, 1079-1088.

Sengupta, P., Chou, J. C., and Bargmann, C. I. (1996). *odr-10* encodes a seven transmembrane domain olfactory receptor required for responses to the odorant diacetyl. Cell *84*, 899-909.

Shatz, C. (1996). Emergence of order in visual system development. Proc. Nat. Acad. Sci. USA *93*, 602-608.

Shatz, C. (1990). Impulse activity and the patterning of connections during CNS development. Neuron *5*, 745-756.

Shatz, C., and Stryker, M. (1988). Prenatal tetrodotoxin infusion blocks segregation of retinogeniculate afferents. Science *242*, 87-89.

Sklar, P. B., Anholt, R. R. H., and Snyder, S. H. (1986). The odorant-sensitive adenylate cyclase of olfactory receptor cells: differential stimulation by distinct classes of odorants. J. Biol. Chem. *261*, 25538-25543.

Slesinger, P., Patil, N., Liso, N., Jan, Y., Jan, L., and Cox, D. (1996). Functional effects of the mouse weaver mutation on G protein-gated inwardly rectifying K+ channels. Neuron *16*, 321-331.

Stryer, L. (1991). Visual excitation and recovery. J.Biol. Chem. *266*, 10711-10714.

Stryker, M., and Harris, W. (1986). Binolcular impulse blockade prevents the formation of dominance columns in the cat visual cortex. J. Neurosci. *6*, 2117-2133.

Stryker, M., and Strickland, S. (1984). Physiological segregation of ocular dominance columns depends on the pattern of afferent electrical activity. Invest. Ophthalmol.Vis.Sci *25*, 278-291.

Sudlow, L., Huang, R.-C., Green, D., and Gillette, R. (1993). cAMP-activated Na+current of molluscan neurons is resistant to kinase inhibitors and is gated by cAMP in the isolated patch. J.Neurosci. *13*, 5188-5193.

Sulston, J. E., and Horvitz, H. R. (1977). Post-embryonic cell lineages of the nematode, Caenorhabditis elegans. Dev. Biol. *56*, 110-56.

Sulston, J. E., Schierenberg, E., White, J. G., and Thomson, J. N. (1983). The embryonic cell lineage of the nematode Caenorhabditis elegans. Dev. Biol. *100*, 64-119.

Sun, Z.-P., Akabas, M., Goulding, E., Karlin, A., and Siegelbaum, S. (1996). Exposure of residues in the cyclic nucleotide-gated channel pore: P region structure and function in gating. Neuron *16*, 141-149.

Thomas, J., Birnby, D., and Vowels, J. (1993). Evidence for parallel processing of sensory information controlling dauer formation in Caenorhabditis elegans. Genetics *134*, 1105-1117.

Thompson, J. D., Higgins, D. G., and Gibson, T. J. (1994). CLUSTAL W: improving the sensitivity of progressive multiple sequence alignment through sequence weighting, position-specific gap penalties and weight matrix choice. Nuc. Acids Res. *22*, 4673-4680.

Troemel, E. R., Chou, J. H., Dwyer, N. D., Colbert, H. A., and Bargmann, C. I. (1995). Divergent seven transmembrane receptors are candidate chemosensory receptors in C. elegans. Cell *83*, 207-218.

Varnum, M. D., Black, K. D., and Zagotta, W. N. (1995). Molecular mechanism for ligand discrimination of cyclic nucleotide-gated channels. Neuron *15*, 619-625.

Vowels, J., and Thomas, J. (1994). Multiple chemosensory defects in daf-11 and daf-21 mutants of Caenorhabditis elegans. Genetics *138*, 303-316.

Vowels, J. J., and Thomas, J. H. (1992). Genetic analysis of chemosensory control of dauer formation in *Caenorhabditis elegans*. Genetics *130*, 105-123.

Wang, B. B., Muller-Immergluck, M. M., Austin, J. Robinson, N. T., Chisholm, A. and Kenyon, C. (1993). A homeotic gene cluster patterns the anteroposterior body axis of C. elegans. Cell *74*, 29-42.

Wang, T., Xie, Z., and Lu, B. (1995). Nitric oxide mediates activity-dependent synaptic suppression at developing neuromuscular synapses. Nature *374*, 262-266.

Ward, S. (1973). Chemotaxis by the nematode Caenorhabditis elegans: identification of attractants and analysis of the response by use of mutants. Proc. Natl. Acad. Sci. USA *70*, 817-21.

Ward, S., Thomson, N., White, J. G., and Brenner, S. (1975). Electron microscopical reconstruction of the anterior sensory anatomy of the nematode Caenorhabditis elegans. J. Comp. Neurol. *160*, 313-337.

Ware, R. W., Clark, D., Crossland, K., and Russell, R. L. (1975). The nerve ring of the nematode *Caenorhabditis elegans*: sensory input and motor output. J. Comp. Neur. *162*, 71-110.

Watanabe, S.-I., and Matthews, G. (1988). Regional distribution of cGMP-activated ion channels in the plasma membrane of the rod photoreceptor. J.Neurosci. *8*, 2334-2337.

Weber, I., and Steitz, T. (1987). Structure of a complex of catabolite gene activator protein and cyclic AMP refined at 2.5 A resolution. J.Mol.Biol. *198*, 311-326.

Weyand, I., Godde, M., Frings, S., Weiner, J., Muller, F., Altenhofen, W., Hatt, H., and Kaupp, U. B. (1994). Cloning and functional expression of a cyclic-nucleotide-gated channel from mammalian sperm. Nature *368*, 859-863.

White, J. G., Southgate, E., Thomson, J. N., and Brenner, S. (1986). The structure of the nervous system of the nematode *Caenorhabditis elegans*. Phil. Transact. R. Soc. Lond. B *314*, 1-340.

Williams, E., Doherty, P., Turner, G., Reid, R., Hemperly, J., and Walsh, F. (1992). Calcium influx into neurons can solely account for cell-contact-dependent neurite outgrowth stimulated by transfected L1. J.Cell Biol. *119*, 883-892.

Wohlfart, P., Haase, M., Molday, R., and Cook, N. (1992). Antibodies against the synthetic peptides used to determine the topology and site of glycosylation of the cGMP-gated channel from bovine photoreceptors. J.Biol.Chem. *267*, 644-648.

Yao, X., Segal, A. S., Welling, P., Zhang, X., McNicholas, C. M., Engel, D., Boulpaep, E. L., and Desir, G. V. (1995). Primary structure and functional expression of a cGMP-gated potassium channel. Proc. Natl. Acad. Sci.USA *92*, 11711-11715.

Yau, K.-W., and Baylor, D. (1989). Cyclic GMP-activated conductance of retinal photoreceptor cells. Ann. Rev. Neurosci. *12*, 289-327.

Zagotta, W., and Siegelbaum, S. (1996). Structure and Function of cyclic nucleotide-gated channels. Ann.Rev.Neurosci *19*, 235-263.

Zhong, Y., Budnik, V., and Wu, C. (1992). Synaptic plasticity in Drosophila memory and hyperexcitable mutants: role of cAMP cascade. J. Neurosci *12*, 644-651.

Zhuo, M., Hu, Y., Schultz, C., Kandel, E. R., and Hawkins, R. D. (1994). Role of guanylyl cyclase and cGMP-dependent protein kinase in long-term potentiation. Nature *368*, 635-639.

Zufall, F., Firestein, S., and Shepherd, G. (1994). Cyclic nucleotide-gated ion channels and sensory transduction in olfactory receptor neurons. Ann. Rev. Biophys. Biomol. Struct. *23*, 577-607.

Appendix A: A *tax-2* homolog identified by the *C. elegans* Genome Sequencing project is expressed in amphid sensory neurons.

We were interested in knowing if *C. elegans* possessed any other cyclic nucleotide-gated channels, and if so, where they were expressed. We searched the databases generated by the Genome Sequencing project and found a predicted cyclic nucleotide-gated channel on cosmid F38E11.8 (BLAST probability = 2.0e-10). This cosmid is located on chromosome IV, between *daf-10* and *elt-1*. Inspection of the protein sequence (predicted by GeneFinder and prepared by the *C. elegans* Genome Project) revealed that F38E11.8 contains sequences that are characteristic of CNG channels (Figure 1). There are 6 predicted transmembrane domains, including a region similar to the S4 voltage-sensor domain of potassium channels, and a predicted cyclic nucleotide-binding domain. In addition, the predicted pore region is very similar to the cyclic nucleotide-gated cation channels (as opposed to the cyclic nucleotide-gated potassium channels).

Sequence alignments and BLAST searches indicated that F38E11.8 is most like the alpha subunits of the bovine and human rod and rat olfactory cyclic nuceotide-gated channels. When only the more conserved transmembrane and cyclic nucleotide-binding domains are aligned, F38E11 is 26% and 25% identical with the human rod alpha subunit and the rat olfactory alpha subunits, respectively (data not shown). We also aligned F38E11.8 with the TAX-2 and TAX-4 protein sequences, and found that F38E11.8 is 22% and 24% identical over the transmembrane domains and cyclic nucleotide-binding domains, respectively (Figure 1).

To determine where F38E11.8 was expressed, we fused the upstream sequences of F38E11.8 to the green fluorescent protein (F38E11.8::GFP) and

examined GFP expression in transgenic worms. This construct drove GFP expression in the amphid sensory neurons AWC, AFD, ASE, AWB and ASI. Therefore, F38E11.8::GFP is expressed in a subset of the TAX-2 and TAX-4-expressing neurons (this thesis; H. Komatsu and I. Mori, pers. comm.). Like *tax-2p:GFP* (Chapter 1), expression of F38E11.8::GFP was observed starting in young embryos and persisting through all larval stages and in the adult. To determine if F38E11.8 could complement the *tax-2* or *tax-4* mutants, the complete F38E11 cosmid was injected into *tax-2* and *tax-4* animals, and the chemotaxis behavior of transgenic progeny was assayed. Overexpression of the F38E11 cosmid could not rescue the *tax-2* or *tax-4* benzaldehyde chemotaxis defects.

Comments

A putative cyclic nucleotide-gated channel, F38E11.8, is expressed in a subset of the amphid sensory neurons which express the TAX-2 and TAX-4 cyclic nucleotide-gated channels. It would be interesting to examine the subcellular localization of a tagged F38E11.8 protein to determine if it is localized to the sensory cilia, the axons or both. The localization pattern could then be examined in *tax-2* and *tax-4* mutant background to determine if mutations in other predicted CNG channel subunits affect the localization of the F38E11.8 CNG. The expression pattern of the tagged protein would also indicate if F38E11.8 is expressed in any other neurons; inclusion of other sequences, especially the first intron, may drive reporter gene expression in more cell types as is observed with other genes (eg: *tax-2*; this thesis).

If F38E11.8 is another CNG channel subunit expressed in some of the same amphid sensory neurons as TAX-2 and TAX-4, this is quite interesting since a third CNG channel subunit has not been described in any other system (of course electrophysiology is necessary to determine if any of the putative *C.*

elegans CNG channels actually form channels, and to characterize the channels). F38E11.8 could function as a third subunit in a heteromultimeric channel also possibly consisting of TAX-2 and TAX-4. Alternatively, as is observed with the GIRK family of K+ channels, F38E11.8 could increase the combinational diversity of CNG channels expressed in the amphid neurons by heteromultimerizing with either TAX-2 or TAX-4. In this capacity, F38E11.8 could modulate or even reduce TAX-2 or TAX-4 function. Further experiments could explore these possibilities. The F38E11.8 rescue experiments should be repeated using a smaller clone instead of the entire cosmid. The TAX-4 rescue of *tax-2* mutant phenotypes were only successful when a smaller TAX-4 genomic clone was used (C.M.C., unpublished data); this effect could be due to higher levels of overexpression from the smaller clone verses the cosmid. In addition, it would be interesting to see if F38E11.8 overexpression can enhance or otherwise modulate TAX-4 rescue of *tax-2* mutants. Finally, the chemotaxis phenotype of wild-type animals overexpressing F38E11.8 should be determined; this could reveal a negative modulatory role of F38E11.8.

Methods

To construct F38E11.8::GFP, primer CC101 (5'-GATCTTCCTctgcagCGCCAGAAGATTCCCACAGAC-3'; lower case letters indicate an inserted restriction site) and CC102 (5'-GCTTCTGTGggatccGTGTGCTCATTTTCTCCC) were used to amplify 850 bp of the upstream sequences F38E11.8 plus the first two amino acids of the coding region (because F38E11.8 is at the end of the cosmid contig, only 850 bp of upstream region was in the database). PCR condition were the following: 35 cycles of 95°C for 30 sec, 52°C for 1 min, 72°C for 2 min, followed by 10 min at 72°C. After digesting with BamH1 and Pst1, the pcr product was ligated into

the GFP expression vector pPD95.79. Primers (CC110 and CC111) were synthesized to create a GFP-tagged version of F38E11.8, however the experiment was not performed. Injection experiments were performed exactly as described (This thesis). For the rescue experiments, cosmid F38E11 was injected at 20 ng/ul with the co-injection marker, as described. Transgenic progeny were assayed for benzaldehyde chemotaxis (1:200 dilution).

Figure legend.

Figure A-1: Sequence comparison of the predicted transmembrane and cyclic nucleotide-binding domains of the predicted amino acid sequences of the F38E11.8, the *tax*-2 cDNA, and the predicted amino acid sequence of TAX-4. The amino and carboxy termini are completely unconconserved, and were not included in this comparison. Identical residues are shaded. Amino acids are numbered beginning approximately at S1. Predicted transmembrane domains and the cyclic nucleotide-binding domain are underlined.

Figure A-1

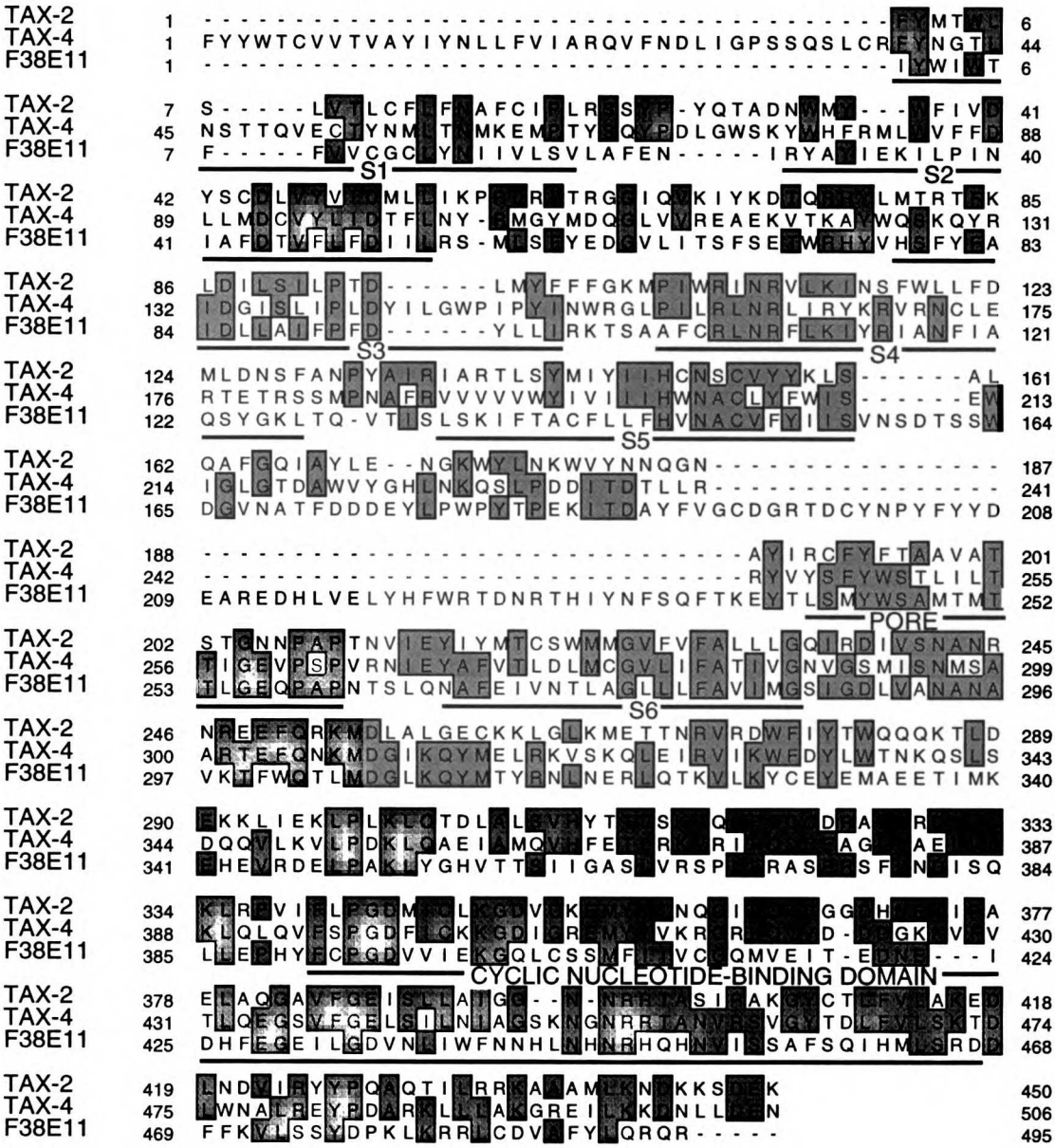
TAX-2
TAX-4
F38E11
S1
S2
S3
S4
S5
PORE
S6
CYCLIC NUCLEOTIDE-BINDING DOMAIN

Appendix B: *tax-2* has genetic interactions with other mutants which affect amphid and phasmid axon structure.

Double mutant combinations between *tax-2* and other genes that affect the development of chemosensory axons were constructed to determine if *tax-2* showed genetic interactions with other genes required for normal axon structure of sensory neurons. DiO staining was used to examine the structure of 6 pairs of amphid sensory neurons and the two pairs of phasmid sensory neurons.

The *unc-69* gene is required for normal structure of the amphid commisure, the ventrally-directed process bundle that the amphid axons enter as they leave the cell bodies. In *unc-69* mutants animals, the amphid commisure does not form. Most of the amphid axons still project anteriorally to the nerve ring by novel, often circuitous trajectories (M.O. Hengartner, C.C. and C.I.B., unpublished observations). *tax-2;unc-69* double mutants had more severe amphid defects than either single mutant, indicating that the *tax-2* and *unc-69* genes are genetically redundant. The amphid axons failed to join the amphid commisure, and many of them also failed to project to the nerve ring. Instead, the abberant axons projected into the posterior body region, as is seen in the affected axons in the *tax-2* single mutant. In *tax-2* single mutants, however, only two amphid neurons show defective axons while all of the amphid neurons produced defective axons in the *tax-2;unc-69* double mutants. Due to the disruption of the amphid commissure, the misdirected axons were seen to emerge directly from the amphid cell bodies. This observation verified that *tax-2* can cause defects in the amphid axons and excluded the possibility that the *tax-2* mutations were allowing dye transfer to other non-chemosensory axons.

The *unc-69*, *unc-34* and *unc-76* genes are required for normal development of the phasmid axons. Mutations in *unc-69*, *unc-34* and *unc-76* cause premature termination of the phasmid axons in the ventral nerve cord (M.O.Hengartner, C.C., and C.I.B., unpublished observations). In *tax-2;unc-69* and *tax-2;unc-34* double mutants, the phasmid processes terminated prematurely at a similar penetrance to that of the *unc-69* and *unc-34* single mutants (Figure 1). Thus, the excessive phasmid axon extension observed in *tax-2* mutants depended on the genes that are required for normal phasmid development. *tax-2* weakly suppressed the *unc-76* phasmid defects. In *tax-2;unc-76* double mutants, 24% of the phasmid axons were full length, compared to 3% full-length axons in the *unc-76* single mutant (Figure 1). Thus, the *tax-2* gene is required for the premature phasmid axon termination observed in the *unc-76* mutants. Interestingly, about 1/4 of the phasmid axons were normal length in the *tax-2;unc-76* double mutants, while only 5-8 % of phasmid axons are affected in *tax-2* single mutants (see Chapter 1).

Figure legend

Figure B-1. Percent normal phasmid axons in double mutant combinations between *tax*-2 and other genes required for normal phasmid axon development.

Phasmid axon structure was examined by DiO staining. For each point, 100-300 DiO-stained worms were viewed (error bars denote the 95% confidence level). An phasmid was scored as defective if any phasmid neuron had a defect.

Figure B-1

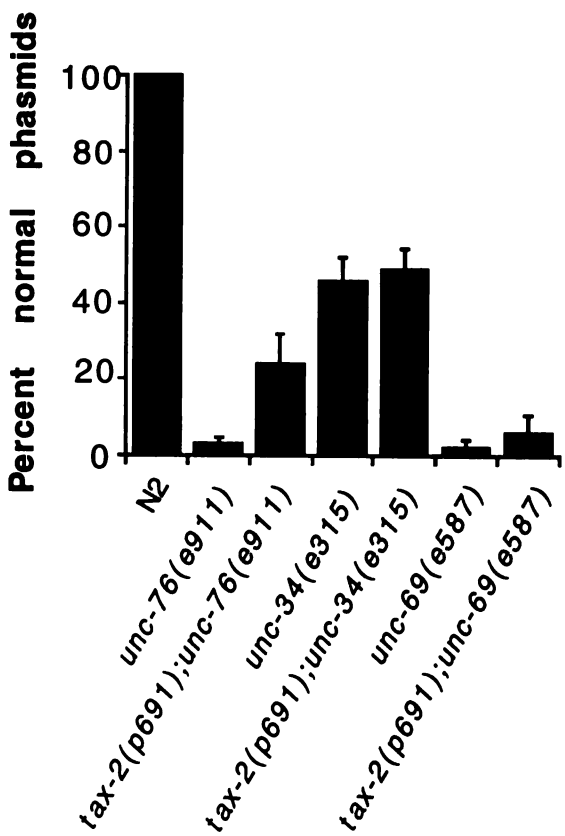
Percent normal phasmids
100
80
60
40
20
0
N2
unc-76(e911)
tax-2(p691);unc-76(e911)
unc-34(e315)
tax-2(p691);unc-34(e315)
unc-69(e587)
tax-2(p691);unc-69(e587)

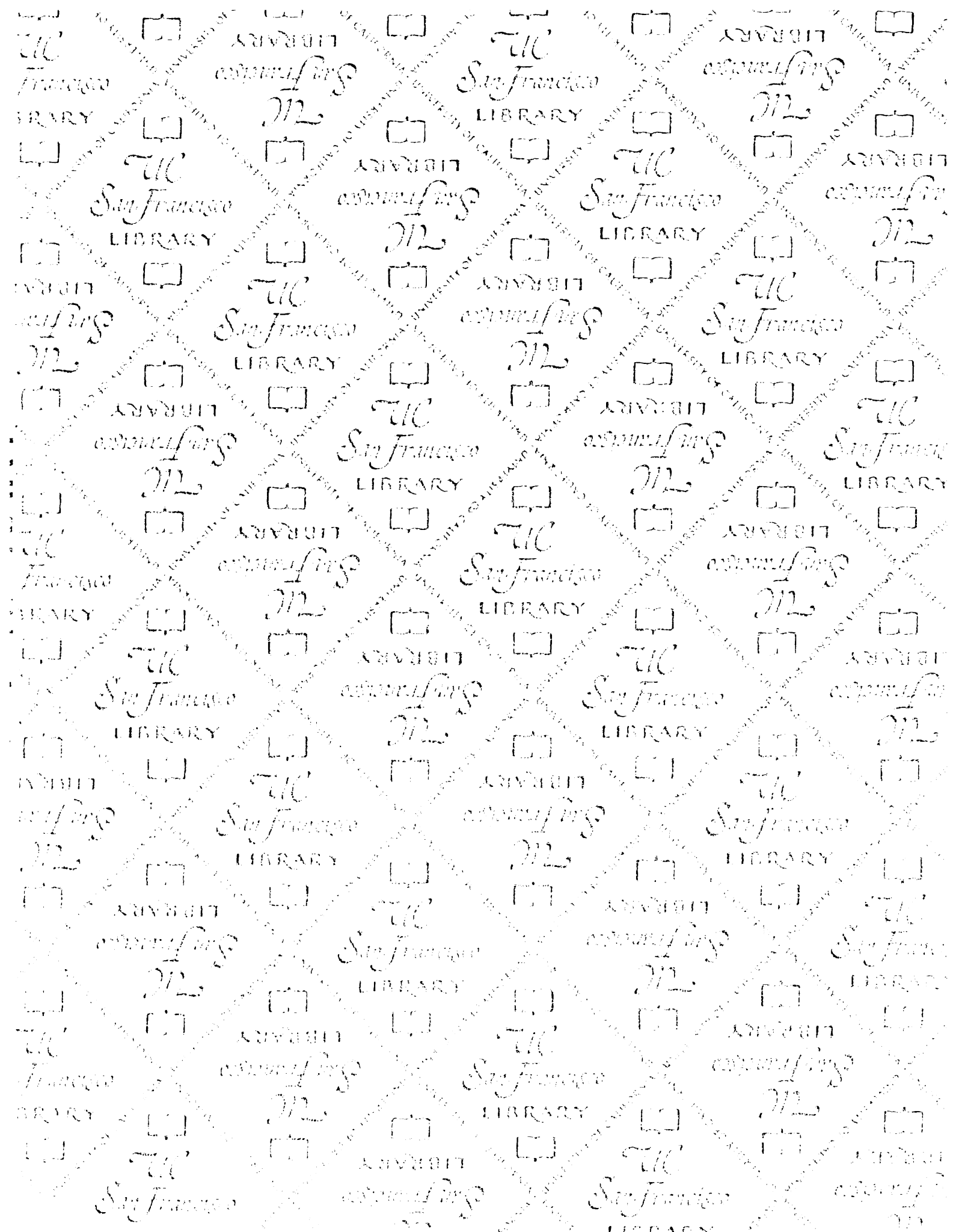
UC
San Francisco
LIBRARY

For reference

Not to be taken from the room.